Asymptotic Modeling of the Electromagnetic Scattering by Small Spheres Perfectly Conducting

Justine Labat, Victor Péron, Sébastien Tordeux

Asymptotic modeling of the electromagnetic scattering by small spheres perfectly conducting

Justine Labat, Victor Péron , Sébastien Tordeux

RESEARCH REPORT

N° 9169

November 2018

Project-Team Magique 3D, Inria Bordeaux Sud-Ouest, UPPA-E2S, LMAP UMR 5142

ISSN 0249-6399 ISRN INRIA/RR--9169--FR+ENG

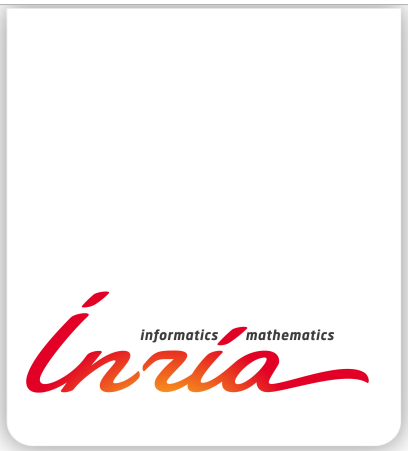

Asymptotic modeling of the electromagnetic scattering by small spheres perfectly conducting

Justine Labat*, Victor Péron *, Sébastien Tordeux*

Project-Team Magique 3D, Inria Bordeaux Sud-Ouest, UPPA-E2S, LMAP UMR 5142

Research Report n° 9169 — November 2018 — 58 pages

Abstract: In this report, we use the method of matched asymptotic expansions to approximate the solution of the time-harmonic electromagnetic scattering problem by a small perfectly conducting sphere. This method consists in defining two local approximations using multi-scale expansions over far and near fields, related in a matching area. We make explicit the asymptotics up to the second order of approximation for the near-field expansion and up to the fifth order for the far-field expansion. We illustrate these results with numerical experiments making evident the performance of the asymptotic models.

Key-words: Asymptotic expansions, Maxwell's equations, Reduced models

* Team-Project Magique 3D, University of Pau and Pays de l'Adour, Inria Bordeaux Sud-Ouest, LMAP UMR CNRS 5142

RESEARCH CENTRE
BORDEAUX – SUD-OUEST

200 avenue de la Vieille Tour
33405 Talence Cedex

Modélisation asymptotique de la diffraction des ondes électromagnétiques par de petites sphères parfaitement conductrices

Résumé : Dans ce rapport, nous utilisons la méthode des développements asymptotiques raccordés afin d'approcher la solution du problème de diffraction d'ondes électromagnétiques par une petite sphère parfaitement conductrice. Cette méthode consiste à définir deux approximations locales de la solution en utilisant des développements multi-échelles, dîts de champ proche et de champ lointain. Ces développements sont raccordés dans une zone de transition. Nous effectuons les développements jusqu'au deuxième ordre pour le champ proche et jusqu'au cinquième ordre pour le champ lointain. Nous illustrons ces résultats avec des expériences numériques qui mettent en évidence la performance des développements en fonction de la taille de l'obstacle.

Mots-clés : Développements asymptotiques, Équations de Maxwell, Modèles réduits

1 Introduction

Many physical phenomena involve multiple electromagnetic scattering by small obstacles [7, 22, 40, 43]. All exact theories and numerical techniques for computing the electromagnetic fields are based on solving Maxwell equations either analytically or numerically. For scatterers of arbitrary shape, the use of numerical methods is required. Classical numerical approaches like finite element and boundary element methods, developed for example in [5, 18, 32] for solving the scattering problem for Maxwell equations, are very efficient when the size of the scatterers is larger than the incident wavelength. However, these methods become very expensive both in terms of computation time and memory capacity when the scatterers are significantly small in comparison with the wavelength and when we deal with large three-dimensional domains. That is partly due to the necessity of refining meshes as finer as the obstacles are small. An other method for the multiple electromagnetic scattering problem by large obstacles has been developed by Ganesh and Hawkins in [23]. This is a meshless method based on the Galerkin discretization of the corresponding integral equation into local spectral basis depending on the center of the obstacles. But, according to the authors, this method is unstable when the obstacles tend to be small. In the same philosophy, the multiple acoustic scattering by small obstacles is treated in [4, 37] where the discretization of the integral equation in a Fourier basis is discussed in two-dimensional domains. These *spectral* methods allow to get analytical formulations when the obstacles have particular shapes like spheres [29, 44].

Several methods can be considered to overcome difficulties related to the small size of the obstacles. For instance, techniques of local mesh refinement can be considered but remain limited and expensive when we have a lot of inhomogeneities. The asymptotic analysis [15, 19, 24, 31] is therefore a good approach. The asymptotic theory in singularly perturbed domains has turned out to be very efficient in numerical techniques. Dependence of the solution on a small parameter is taken into consideration and the initial problem can be decomposed into a collection of elementary problems. Different methods bring out of this branch of analysis like the method of multiscale expansions [8, 26, 34, 41] or the method of matched asymptotic expansions [12, 13, 30, 38]. Although these methods lead to different iteration procedures for the construction of the asymptotics, the approximations coincide locally [16]. Problems dealing with multiple electromagnetic scattering by small obstacles have already given rise to numerous works [1, 3, 11, 20, 26]. In [26], Korikov and Plamenevskii used the method of compound solutions, that is a multiscale expansion method, to approximate the solution of the interior Maxwell problem with a small hole, both for the time-harmonic and the time-dependent Maxwell equations. They set up a rigourous functional framework to express asymptotic expansions of the solution, including elliptic regularization, at any order. Error estimates are proved in a dissipative framework. In [3, 42], asymptotic formulas for perturbations in the tangential trace of the magnetic field caused by the presence of heterogeneities have been derived and rigorously justified. Nevertheless, only the first term of the volumical asymptotic expansion for the electromagnetic fields is given. The asymptotic formulas are used in the theory of inverse problems through boundary integral methods in order to determine physical properties, location and size of the small obstacles [1, 2].

The method of matched asymptotic expansions consists in constructing distinct expansions of the solution in different regions of the domain of propagation with appropriate scales, and matching them in intermediate regions also called matching areas [39]. The justification of matching rules can be obtained from the hypothesis of structure of a uniform expansion into the whole domain [21]. This approach allows to define local approximations of the solution at any order, relatively to the obstacle size but is difficult to justify rigorously [38]. It is typically used to study the single scattering problem and in this case, involves two different expansions. The tran-

sition to the multiple scattering can be performed thanks to an appropriate model like Born or Foldy-Lax model [6, 10]. The Born theory is based on a superposition principle and the solution of the multiple scattering problem is approximated by the sum of the scattered fields generated in the presence of isolated obstacles. This approximation is quite accurate when the distance between the obstacles is sufficiently large. On the contrary, if interactions between obstacles cannot be neglected, the Foldy theory improves the previous one [20]. Some intermediate models between Born and Foldy are compared in [11] for the multiple electromagnetic scattering by finitely many point-like obstacles.

In this report, we develop the method of matched asymptotic expansions to approximate the solution of the electromagnetic scattering problem by a small perfectly conducting sphere. We derive explicitly the first terms of the asymptotics, up to the second order for the near-field expansion and up to the fifth order for the far-field expansion. Moreover, we give a physical interpretation of these first terms through the idealistic notion of electric and magnetic multipoles. In contrast with [26], this work is concerned essentially with numerical and applicable objectives. By the way, we illustrate our results thanks to numerical experiments making evident the performance of the asymptotic models.

This paper is organized as follows. In Section 2, we describe the problem that we consider and we present the main results that we have established. These results characterize the first terms of the asymptotic expansions for the electromagnetic scattering problem by a small sphere perfectly conducting. In Section 3, we display some numerical results to make evident the performance of the asymptotic expansions. From these local expansions, we construct a global approximation by truncating suitably the whole domain. In Section 4, we present the full method of matched asymptotic expansions applied on the electromagnetic scattering by a small perfectly conducting sphere. We make explicit the matching conditions thanks to the use of modal decompositions for the near-field and far-field terms introduced in Appendix C. Then, we pursue the construction of the first terms of the far-field and near-field expansions based on their modal decomposition in spherical geometries. In Section 5, we apply our results to define a collected model which consists in gathering the terms, not with respect to the δ-powers, but with respect to their nature, in terms of multipoles. Finally, we illustrate a multiple scattering model in electromagnetism based on the Born approximation and we discuss about the Foldy-Lax model.

2 Problem description and main results

In this section, we describe the electromagnetic wave scattering problem by a finite number of small spheres and we introduce the asymptotic expansions for the single scattering problem.

2.1 Normalization of the equations

The propagation of time-harmonic electromagnetic waves of angular frequency ω in a homogeneous and isotropic dielectric with electric permittivity $\varepsilon > 0$ and magnetic permeability $\mu > 0$ is described by an incident wave $\mathfrak{Re}\big[\big(\boldsymbol{\mathcal{E}}^{\text{inc}}(\mathbf{x}), \boldsymbol{\mathcal{H}}^{\text{inc}}(\mathbf{x})\big)\exp(-i\omega t)\big]$. The incident field $(\boldsymbol{\mathcal{E}}^{\text{inc}}, \boldsymbol{\mathcal{H}}^{\text{inc}})$ satisfies the time-harmonic Maxwell equations

$$\begin{cases} \mathbf{curl}\, \boldsymbol{\mathcal{E}}^{\text{inc}} - i\omega\mu\boldsymbol{\mathcal{H}}^{\text{inc}} = 0 & \text{in } \mathbb{R}^3, \\ \mathbf{curl}\, \boldsymbol{\mathcal{H}}^{\text{inc}} + i\omega\varepsilon\boldsymbol{\mathcal{E}}^{\text{inc}} = \boldsymbol{\mathcal{J}} & \text{in } \mathbb{R}^3, \end{cases}$$

where the electric current density $\boldsymbol{\mathcal{J}}$ is a smooth vector field with compact support in $\mathbb{R}^3$ that is related to the electric charge density ρ through the charge conservation principle

$$-i\omega\rho + \operatorname{div} \boldsymbol{\mathcal{J}} = 0 \qquad \text{in } \mathbb{R}^3.$$

Remark 1. When $\boldsymbol{\mathcal{J}}$ is of class $\boldsymbol{\mathscr{C}}^\infty$, the incident fields $\boldsymbol{\mathcal{E}}^{\text{inc}}$ and $\boldsymbol{\mathcal{H}}^{\text{inc}}$ are also of class $\boldsymbol{\mathscr{C}}^\infty$ into any bounded sub-domain of $\mathbb{R}^3$.

In Table 1, we introduce the classical electromagnetic fields, densities and potentials, with *calligraphic* symbols. Afterwards, we define a normalization and we denote the normalized quantities with *straight* symbols.

	Usual convention		Normalized quantities		
Electric field	$\boldsymbol{\mathcal{E}}$	[Vm^{-1}]	E	$=$	$\varepsilon\mu^{\frac{1}{2}}\boldsymbol{\mathcal{E}}$
Magnetic field	$\boldsymbol{\mathcal{H}}$	[Am^{-1}]	H	$=$	$\varepsilon^{\frac{1}{2}}\mu\boldsymbol{\mathcal{H}}$
Electric charge density	ρ	[Cm^{-3}]	ϱ	$=$	$\mu^{\frac{1}{2}}\rho$
Electric current density	$\boldsymbol{\mathcal{J}}$	[Am^{-2}]	j	$=$	$\mu^{\frac{1}{2}}\boldsymbol{\mathcal{J}}$
Electric potential	$\mathcal{V}$	[V]	V	$=$	$\varepsilon\mu^{\frac{1}{2}}\mathcal{V}$
Magnetic potential	$\boldsymbol{\mathcal{A}}$	[Vsm^{-1}]	A	$=$	$\varepsilon^{\frac{1}{2}}\boldsymbol{\mathcal{A}}$

Table 1: Normalization of the electromagnetic quantities

Taking in account this normalization, the incident field $(\mathsf{E}^{\text{inc}}, \mathsf{H}^{\text{inc}})$, that is of class $\boldsymbol{\mathscr{C}}^\infty$ into any bounded domain of $\mathbb{R}^3$, satisfies the time-harmonic Maxwell equations

$$\begin{cases} \mathbf{curl}\, \mathsf{E}^{\text{inc}} - i\kappa \mathsf{H}^{\text{inc}} = 0 & \text{in } \mathbb{R}^3, \\ \mathbf{curl}\, \mathsf{H}^{\text{inc}} + i\kappa \mathsf{E}^{\text{inc}} = \dfrac{\mathsf{j}}{c} & \text{in } \mathbb{R}^3. \end{cases}$$

The wave-number κ satisfies the dispersion relation

$$\kappa = \frac{\omega}{c},$$

with the wave-speed $c = (\mu\varepsilon)^{-\frac{1}{2}}$.

Remark 2. The charge conservation principle remains unchanged and we have $-i\omega\varrho + \operatorname{div} \mathsf{j} = 0$.

Remark 3. For example, the incident field $(\mathsf{E}^{\text{inc}}, \mathsf{H}^{\text{inc}})$ can be an electromagnetic plane wave,

$$\mathsf{E}^{\text{inc}}(\mathbf{x}) = \mathbf{p}\exp(i\mathbf{k}\cdot\mathbf{x})\,; \qquad \mathsf{H}^{\text{inc}}(\mathbf{x}) = \frac{1}{\kappa}(\mathbf{k}\times\mathbf{p})\exp(i\mathbf{k}\cdot\mathbf{x})\,, \qquad \text{with } \mathbf{k}\cdot\mathbf{p} = 0, \tag{2.1}$$

where the wave-vector $\mathbf{k}$ that is proportional to the wave-number κ sets the angle of propagation and $\mathbf{p}$ denotes the polarization vector.

2.2 Description of the scattering problem

In the presence of small obstacles with characteristic length δ, the incident field $(\mathsf{E}^{\text{inc}}, \mathsf{H}^{\text{inc}})$ is scattered and gives birth to a new field $(\mathsf{E}_\delta^{\text{tot}}, \mathsf{H}_\delta^{\text{tot}})$ which can be decomposed into the incident field and a scattered field $(\mathsf{E}_\delta, \mathsf{H}_\delta)$

$$\mathsf{E}_\delta^{\text{tot}} = \mathsf{E}^{\text{inc}} + \mathsf{E}_\delta\,; \qquad \mathsf{H}_\delta^{\text{tot}} = \mathsf{H}^{\text{inc}} + \mathsf{H}_\delta.$$

Both the total field $(\mathbf{E}_\delta^{\text{tot}}, \mathbf{H}_\delta^{\text{tot}})$ and the scattered field $(\mathbf{E}_\delta, \mathbf{H}_\delta)$ have to satisfy Maxwell equations in the exterior domain of the obstacles with the same wave-number κ. The scattered field also needs to satisfy the outgoing Silver-Müller radiation condition at infinity

$$\lim_{r\to\infty} r\big(\mathbf{H}_\delta \times \widehat{x} - \mathbf{E}_\delta\big) = 0, \qquad r = |\mathbf{x}|\,,\ \widehat{x} = \frac{\mathbf{x}}{r}.$$

The created fields strongly depend on geometry and physical properties of the obstacles. In this paper, we consider the multiple electromagnetic scattering by K spherical obstacles $\mathcal{B}(c_k, \delta)$, $k = 1, \dots, K$, perfectly conducting, each one being centered at c_k with small radius $\delta > 0$, see Figure 1. We assume that any distance $\mathbf{d}_{jk}$ between two obstacles is not small in comparison

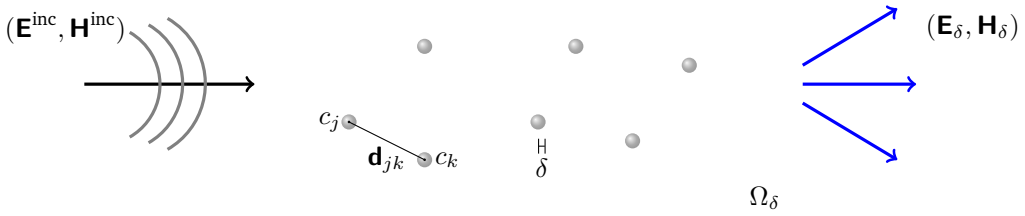

Figure 1: Domain of propagation

with λ. The domain of propagation Ω_δ is defined by

$$\Omega_\delta = \mathbb{R}^3 \setminus \bigcup_{k=1}^{K} \overline{\mathcal{B}(c_k, \delta)}.$$

The scattering problem reads as

$$\begin{cases} \mathbf{curl}\,\mathbf{E}_\delta - i\kappa\mathbf{H}_\delta = 0 & \text{in } \Omega_\delta, \\ \mathbf{curl}\,\mathbf{H}_\delta + i\kappa\mathbf{E}_\delta = 0 & \text{in } \Omega_\delta, \\ \mathbf{n}\times\mathbf{E}_\delta = -\mathbf{n}\times\mathbf{E}^{\text{inc}} & \text{on } \partial\Omega_\delta, \\ \mathbf{n}\cdot\mathbf{H}_\delta = -\mathbf{n}\cdot\mathbf{H}^{\text{inc}} & \text{on } \partial\Omega_\delta, \\ \lim\limits_{r\to\infty} r\big(\mathbf{H}_\delta\times\widehat{x} - \mathbf{E}_\delta\big) = 0 & \text{uniformly in } \widehat{x}, \end{cases} \tag{2.2}$$

where $\mathbf{n}$ denotes the outward-pointing normal unit vector of $\partial\Omega_\delta$. It is well-known that the electromagnetic scattering problem by a finite number of spheres is well-posed, see for instance [32, 33]. Moreover, the solution $(\mathbf{E}_\delta, \mathbf{H}_\delta)$ have an analytical decomposition into Ω_δ. In Appendix D, we recall some properties about its decomposition.

Remark 4. For lipschitz obstacles, the exterior Maxwell problem (2.2) has a unique solution $(\mathbf{E}_\delta, \mathbf{H}_\delta)$ in $\mathbf{H}_{\text{loc}}(\mathbf{curl}\,, \Omega_\delta)$ if the tangential trace of the electric field $\mathbf{n}\times\mathbf{E}_\delta$ on $\partial\Omega_\delta$ belongs to the Sobolev space

$$\mathbf{H}_{\text{t}}^{-\frac{1}{2}}(\text{div}_{\partial\Omega_\delta}, \partial\Omega_\delta) = \Big\{\mathbf{u}\in\mathbf{H}^{-\frac{1}{2}}(\partial\Omega_\delta),\ \text{div}_{\partial\Omega_\delta}\mathbf{u}\in H^{-\frac{1}{2}}(\partial\Omega_\delta) \text{ and } \mathbf{u}\cdot\mathbf{n} = 0 \text{ on } \partial\Omega_\delta\Big\}.$$

A characterization of this space for lipschitz domains is established in [9]. Moreover, this condition ensures that the normal trace of the magnetic field $\mathbf{n}\cdot\mathbf{H}_\delta$ on $\partial\Omega_\delta$ belongs to $H^{-\frac{1}{2}}(\partial\Omega_\delta)$. Then, well-posedness in $\mathbf{H}_{\text{loc}}(\mathbf{curl}\,, \Omega_\delta)$ derives from the Fredholm theory and can be proved thanks to a boundary integral equation posed on $\partial\Omega_\delta$ and the use of integral representation

given by the Stratton-Chu formulas, see [14], or with an equivalent interior problem by equipping the fictive boundary with a transparent condition. These formulations are also equivalent to prove well-posedness of this problem into Sobolev weighted spaces for **curl** and div, see [33], that allows to precise the behavior of the fields at infinity.

Remark 5. The numerical simulation of scattering by small obstacles, using finite element methods (FEM, DG, HDG, ...), can become very expensive or not affordable in terms of computation time and memory capacity even in the context of mesh refinement and parallel computation. This is mainly due to the size of the linear system which should be inverted.

Afterwards, we introduce the results that we have established for $K = 1$ and $c_1 = 0$, *i.e.* for the scattering problem by one small sphere $\mathcal{B}(0,\delta)$ centered at the origin with small radius δ. We come back to the multiple scattering problem in Section 5. This is driven by the fact that the numerical validation confirms these results only for one small sphere. For any smooth vector field $\mathbf{u}$ we denote by $\gamma_n\mathbf{u}$ its normal trace on the unit sphere $\mathcal{S}^2$ in $\mathbb{R}^3$ and $\gamma_t\mathbf{u}$ and $\gamma_\times\mathbf{u}$ its tangential traces on $\mathcal{S}^2$, defined by

$$\gamma_n\mathbf{u} = (\mathbf{e}_r\cdot\mathbf{u})_{|\mathcal{S}^2}\,, \qquad \gamma_\times\mathbf{u} = (\mathbf{e}_r\times\mathbf{u})_{|\mathcal{S}^2}\,, \qquad \gamma_t\mathbf{u} = (\gamma_\times\mathbf{u})\times\mathbf{e}_r, \tag{2.3}$$

where $\mathbf{e}_r$ denotes the outward-pointing normal unit vector of $\mathcal{S}^2$.

2.3 Main results

In this section, we present the local approximations in far and near fields of the solution to problem (2.2). The asymptotic expansions introduced in paragraphs 2.3.1 and 2.3.2 have been derived thanks to the method of matched asymptotic expansions. In the last paragraph, we give a physical interpretation for the first terms of the asymptotics in terms of equivalent sources that are electromagnetic multipoles.

2.3.1 Far-field approximation

Far from the obstacle, we prove that the exact solution possesses the following formal asymptotic expansion

$$\mathbf{E}_\delta = \delta^3\widetilde{\mathbf{E}}_3 + \delta^5\widetilde{\mathbf{E}}_5 + \ldots\,; \qquad \mathbf{H}_\delta = \delta^3\widetilde{\mathbf{H}}_3 + \delta^5\widetilde{\mathbf{H}}_5 + \ldots.$$

For any positive integer p, the far-field terms $(\widetilde{\mathbf{E}}_p, \widetilde{\mathbf{H}}_p)$ are defined in the asymptotic domain

$$\Omega^\star = \mathbb{R}^3\setminus\{0\}\,.$$

From this point of view, the scatterer is replaced by a point-like obstacle. Moreover, the third-order far-field terms $(\widetilde{\mathbf{E}}_3, \widetilde{\mathbf{H}}_3)$ are given by

$$\widetilde{\mathbf{E}}_3(\mathbf{x}) = -\frac{\kappa^3}{2}h_1^{(1)}(\kappa r)\gamma_\times\big(\mathbf{H}^{\mathrm{inc}}(0)\big) - \kappa^3\frac{h_1^{(1)}(\kappa r)+\kappa r h_1^{(1)'}(\kappa r)}{i\kappa r}\gamma_t\big(\mathbf{E}^{\mathrm{inc}}(0)\big) - 2\kappa^3\frac{h_1^{(1)}(\kappa r)}{i\kappa r}\gamma_n\big(\mathbf{E}^{\mathrm{inc}}(0)\big)\widehat{x} \tag{2.4}$$

and

$$\widetilde{\mathbf{H}}_3(\mathbf{x}) = -\kappa^3 h_1^{(1)}(\kappa r)\gamma_\times\big(\mathbf{E}^{\mathrm{inc}}(0)\big) + \frac{\kappa^3}{2}\frac{h_1^{(1)}(\kappa r)+\kappa r h_1^{(1)'}(\kappa r)}{i\kappa r}\gamma_t\big(\mathbf{H}^{\mathrm{inc}}(0)\big) + \kappa^3\frac{h_1^{(1)}(\kappa r)}{i\kappa r}\gamma_n\big(\mathbf{H}^{\mathrm{inc}}(0)\big)\widehat{x}, \tag{2.5}$$

with $\mathbf{x} = r\widehat{x}$, $h_n^{(1)}$ denotes the n-order spherical Hankel function of the first kind and γ_n, $\gamma_\times$ and γ_t are the trace operators defined in (2.3). The fifth-order far-field terms $(\widetilde{\mathbf{E}}_5, \widetilde{\mathbf{H}}_5)$ are given by

$$\begin{aligned}\widetilde{\mathbf{E}}_5(\mathbf{x}) = \frac{3\kappa^5}{10} h_1^{(1)}(\kappa r)\gamma_\times\big(\mathbf{H}^{\text{inc}}(0)\big) - \frac{3\kappa^5}{10}\frac{h_1^{(1)}(\kappa r) + \kappa r h_1^{(1)'}(\kappa r)}{i\kappa r}\gamma_t\big(\mathbf{E}^{\text{inc}}(0)\big)\\ - \frac{3\kappa^5}{5}\frac{h_1^{(1)}(\kappa r)}{i\kappa r}\gamma_n\big(\mathbf{E}^{\text{inc}}(0)\big)\widehat{x} - \frac{\kappa^4}{9}h_2^{(1)}(\kappa r)\gamma_\times\Big(\mathbb{J}^{\text{sym}}_{\mathbf{H}^{\text{inc}}}(0)\widehat{x}\Big)\\ - \frac{\kappa^4}{6}\frac{h_2^{(1)}(\kappa r) + \kappa r h_2^{(1)'}(\kappa r)}{i\kappa r}\gamma_t\Big(\mathbb{J}^{\text{sym}}_{\mathbf{E}^{\text{inc}}}(0)\widehat{x}\Big) - \frac{\kappa^4}{2}\frac{h_2^{(1)}(\kappa r)}{i\kappa r}\gamma_n\Big(\mathbb{J}_{\mathbf{E}^{\text{inc}}}(0)\widehat{x}\Big)\widehat{x}\end{aligned} \tag{2.6}$$

and

$$\begin{aligned}\widetilde{\mathbf{H}}_5(\mathbf{x}) = -\frac{3\kappa^5}{10} h_1^{(1)}(\kappa r)\gamma_\times\big(\mathbf{E}^{\text{inc}}(0)\big) - \frac{3\kappa^5}{10}\frac{h_1^{(1)}(\kappa r) + \kappa r h_1^{(1)'}(\kappa r)}{i\kappa r}\gamma_t\big(\mathbf{H}^{\text{inc}}(0)\big)\\ - \frac{3\kappa^5}{5}\frac{h_1^{(1)}(\kappa r)}{i\kappa r}\gamma_n\big(\mathbf{H}^{\text{inc}}(0)\big)\widehat{x} - \frac{\kappa^4}{6}h_2^{(1)}(\kappa r)\gamma_\times\Big(\mathbb{J}^{\text{sym}}_{\mathbf{E}^{\text{inc}}}(0)\widehat{x}\Big)\\ + \frac{\kappa^4}{9}\frac{h_2^{(1)}(\kappa r) + \kappa r h_2^{(1)'}(\kappa r)}{i\kappa r}\gamma_t\Big(\mathbb{J}^{\text{sym}}_{\mathbf{H}^{\text{inc}}}(0)\widehat{x}\Big) + \frac{\kappa^4}{3}\frac{h_2^{(1)}(\kappa r)}{i\kappa r}\gamma_n\Big(\mathbb{J}_{\mathbf{H}^{\text{inc}}}(0)\widehat{x}\Big)\widehat{x},\end{aligned} \tag{2.7}$$

where $\mathbb{J}_\diamond$ denotes the Jacobian matrix of $\diamond$ and $\mathbb{J}^{\text{sym}}_\diamond = \frac{1}{2}\big(\mathbb{J}_\diamond + \mathbb{J}_\diamond^\top\big)$ the symmetric Jacobian of $\diamond$.

Remark 6. The fourth-order far-field terms $(\widetilde{\mathbf{E}}_4, \widetilde{\mathbf{H}}_4)$ are reduced to null-field.

2.3.2 Near-field approximation

Close to the obstacle, we prove that the exact solution possesses the formal asymptotic expansion

$$\mathbf{E}_\delta(\delta\,\cdot) = \widehat{\mathbf{E}}_0 + \delta\widehat{\mathbf{E}}_1 + \delta^2\widehat{\mathbf{E}}_2 + \dots\,, \qquad \mathbf{H}_\delta(\delta\,\cdot) = \widehat{\mathbf{H}}_0 + \delta\widehat{\mathbf{H}}_1 + \delta^2\widehat{\mathbf{H}}_2 + \dots.$$

Here, for any non-negative integer p, the near-field terms $(\widehat{\mathbf{E}}_p, \widehat{\mathbf{H}}_p)$ are defined in fast variable $\mathbf{X} = \frac{\mathbf{x}}{\delta}$ in the dimensionless domain $\widehat{\Omega}$ given by

$$\widehat{\Omega} = \mathbb{R}^3 \setminus \overline{\mathcal{B}(0,1)}.$$

The zeroth-order near-field terms $(\widehat{\mathbf{E}}_0, \widehat{\mathbf{H}}_0)$ are given by

$$\widehat{\mathbf{E}}_0(\mathbf{X}) = \frac{1}{\mathrm{R}^3}\Big\{3\gamma_n\big(\mathbf{E}^{\text{inc}}(0)\big)\widehat{x} - \mathbf{E}^{\text{inc}}(0)\Big\}; \qquad \widehat{\mathbf{H}}_0(\mathbf{X}) = -\frac{1}{2\mathrm{R}^3}\Big\{3\gamma_n\big(\mathbf{H}^{\text{inc}}(0)\big)\widehat{x} - \mathbf{H}^{\text{inc}}(0)\Big\}, \tag{2.8}$$

with $\mathbf{X} = \mathrm{R}\widehat{x}$ and $\mathrm{R} = \frac{r}{\delta}$. The first-order near-field terms $(\widehat{\mathbf{E}}_1, \widehat{\mathbf{H}}_1)$ are given by

$$\begin{aligned}\widehat{\mathbf{E}}_1(\mathbf{X}) &= \frac{1}{\mathrm{R}^4}\Big\{-\gamma_t\big(\mathbb{J}^{\text{sym}}_{\mathbf{E}^{\text{inc}}}(0)\,\widehat{x}\big) + \frac{3}{2}\gamma_n\big(\mathbb{J}_{\mathbf{E}^{\text{inc}}}(0)\,\widehat{x}\big)\widehat{x}\Big\} + \frac{i\kappa}{2\mathrm{R}^2}\,\gamma_\times\big(\mathbf{H}^{\text{inc}}(0)\big),\\ \widehat{\mathbf{H}}_1(\mathbf{X}) &= \frac{1}{\mathrm{R}^4}\Big\{\frac{2}{3}\gamma_t\big(\mathbb{J}^{\text{sym}}_{\mathbf{H}^{\text{inc}}}(0)\,\widehat{x}\big) - \gamma_n\big(\mathbb{J}_{\mathbf{H}^{\text{inc}}}(0)\,\widehat{x}\big)\widehat{x}\Big\} + \frac{i\kappa}{\mathrm{R}^2}\,\gamma_\times\big(\mathbf{E}^{\text{inc}}(0)\big).\end{aligned} \tag{2.9}$$

The second-order near-field terms $(\widehat{\mathbf{E}}_2, \widehat{\mathbf{H}}_2)$ are given by

$$\widehat{\mathbf{E}}_2(\mathbf{X}) = \frac{1}{\mathrm{R}^5}\Big\{\frac{2}{3}\gamma_n\big(\widehat{x}^\top \mathbb{H}_{\mathbf{E}^{\mathrm{inc}}}(0)\,\widehat{x}\big)\widehat{x} + \frac{2\kappa^2}{15}\gamma_n\big(\mathbf{E}^{\mathrm{inc}}(0)\big)\widehat{x} - \frac{1}{2}\gamma_t\big(\widehat{x}^\top \mathbb{H}_{\mathbf{E}^{\mathrm{inc}}}(0)\,\widehat{x}\big) - \frac{i\kappa}{3}\gamma_\times\big(\mathbb{J}^{\mathrm{sym}}_{\mathbf{H}^{\mathrm{inc}}}(0)\,\widehat{x}\big) - \frac{\kappa^2}{5}\gamma_t\big(\mathbf{E}^{\mathrm{inc}}(0)\big)\Big\} + \frac{i\kappa}{3\mathrm{R}^3}\gamma_\times\big(\mathbb{J}^{\mathrm{sym}}_{\mathbf{H}^{\mathrm{inc}}}(0)\,\widehat{x}\big) - \frac{3\kappa^2}{10\mathrm{R}^3}\Big\{\mathbf{E}^{\mathrm{inc}}(0) - 3\gamma_n\big(\mathbf{E}^{\mathrm{inc}}(0)\big)\widehat{x}\Big\} + \frac{\kappa^2}{2\mathrm{R}}\Big\{\mathbf{E}^{\mathrm{inc}}(0) + \gamma_n\big(\mathbf{E}^{\mathrm{inc}}(0)\big)\widehat{x}\Big\}$$

and

$$\widehat{\mathbf{H}}_2(\mathbf{X}) = \frac{1}{\mathrm{R}^5}\Big\{ -\frac{1}{2}\gamma_n\big(\widehat{x}^\top\, \mathbb{H}_{\mathbf{H}^{\mathrm{inc}}}(0)\,\widehat{x}\big)\widehat{x} - \frac{\kappa^2}{10}\gamma_n\big(\mathbf{H}^{\mathrm{inc}}(0)\big)\widehat{x} + \frac{3}{8}\gamma_t\big(\widehat{x}^\top \mathbb{H}_{\mathbf{H}^{\mathrm{inc}}}(0)\widehat{x}\big) - \frac{i\kappa}{4}\gamma_\times\big(\mathbb{J}^{\mathrm{sym}}_{\mathbf{E}^{\mathrm{inc}}}(0)\widehat{x}\big) + \frac{3\kappa^2}{20}\gamma_t\big(\mathbf{H}^{\mathrm{inc}}(0)\big)\Big\} + \frac{i\kappa}{2\mathrm{R}^3}\gamma_\times\big(\mathbb{J}^{\mathrm{sym}}_{\mathbf{E}^{\mathrm{inc}}}(0)\,\widehat{x}\big) + \frac{3\kappa^2}{10\mathrm{R}^3}\Big\{3\gamma_n\big(\mathbf{H}^{\mathrm{inc}}(0)\big)\widehat{x} - \mathbf{H}^{\mathrm{inc}}(0)\Big\} - \frac{\kappa^2}{4\mathrm{R}}\Big\{\mathbf{H}^{\mathrm{inc}}(0) + \gamma_n\big(\mathbf{H}^{\mathrm{inc}}(0)\big)\widehat{x}\Big\},$$

where $\mathbb{H}_\diamond$ denotes the third-order Hessian tensor of $\diamond$.

Remark 7. The Hessian tensor of a vector field $\mathbf{f} = (f_1, f_2, f_3)^\top$ evaluated at 0, is defined by

$$(\mathbb{H}_{\mathbf{f}}(0))_{ijk} = \partial_k\partial_j f_i(0)$$

and for $\mathbf{x} = (x, y, z)$, we define the product $\mathbf{x}^\top\mathbb{H}_{\mathbf{f}}(0)\mathbf{x}$ as

$$\big(\mathbf{x}^\top\mathbb{H}_{\mathbf{f}}(0)\mathbf{x}\big)_i = (\mathbb{H}_{\mathbf{f}}(0))_{i11}x^2 + (\mathbb{H}_{\mathbf{f}}(0))_{i22}y^2 + (\mathbb{H}_{\mathbf{f}}(0))_{i33}z^2 + ((\mathbb{H}_{\mathbf{f}}(0))_{i12} + (\mathbb{H}_{\mathbf{f}}(0))_{i21})xy + ((\mathbb{H}_{\mathbf{f}}(0))_{i13} + (\mathbb{H}_{\mathbf{f}}(0))_{i31})xz + ((\mathbb{H}_{\mathbf{f}}(0))_{i23} + (\mathbb{H}_{\mathbf{f}}(0))_{i32})yz.$$

Remark 8. In the context of the multiple scattering by K spheres, the method of matched asymptotic expansions involves $K+1$ expansions. Firstly, the far-field expansion is defined in the punctured domain $\mathbb{R}^3 \setminus \bigcup\{c_k\}$ and read as the superposition of K scattered fields. The formulas (2.4)-(2.5) and (2.6)-(2.7) have to be translated to deduce the scattered field generated by an obstacle centered at c_k. In the other hand, the K near-field expansions, that are defined in the k-th fast variable $\mathbf{X}^{(k)} = \frac{\mathbf{x}-c_k}{\delta}$, are living in $\widehat{\Omega}$ again.

2.4 Physical interpretation

This section is based on results of classical multipole theory in electromagnetism, see for instance [28, 35]. In Appendix B, we introduce the notion of electric and magnetic multipoles and we develop expressions of electromagnetic fields created in the presence of such kind of sources in static and time-harmonic regime. That allows to describe the first terms of the asymptotics in terms of multipoles.

2.4.1 First near-field terms

The zeroth-order electric near-field term $\widehat{\mathbf{E}}_0$, given by (2.8), can be represented as an electric field created in the presence of an electric dipole of direction $4\pi\mathbf{E}^{\mathrm{inc}}(0)$, in static regime and

the zeroth-order magnetic near-field term $\widehat{\mathbf{H}}_0$ as a magnetic field created in the presence of a magnetic dipole of direction $-2\pi\mathbf{H}^{\text{inc}}(0)$ in static regime again. According to (B.4)-(B.10), the zeroth-order near-field terms can be put in the compact form

$$\widehat{\mathbf{E}}_0 = \mathbf{E}^{\text{elec}}_{\text{dip}}[4\pi\mathbf{E}^{\text{inc}}(0), \kappa = 0]\,, \qquad \widehat{\mathbf{H}}_0 = \mathbf{H}^{\text{mag}}_{\text{dip}}[-2\pi\mathbf{H}^{\text{inc}}(0), \kappa = 0].$$

The first-order electric near-field term $\widehat{\mathbf{E}}_1$ given by (2.9) is represented as the superposition of

- an electric field created in the presence of a filiform magnetic current in a magnetic dipole configuration in static regime, along the direction $-2\pi c\,\mathbf{curl}\,\mathbf{E}^{\text{inc}}(0) = -2\pi i\omega\mathbf{H}^{\text{inc}}(0)$, where ω denotes the angular frequency of the incident wave,
- an electric field created in the presence of an electric quadrupole along directions $(\mathbf{u}^{\text{E}}, \mathbf{v}^{\text{E}})$, in static regime, satisfying the following system of equations

$$\begin{cases} u^{\text{E}}_i v^{\text{E}}_i - u^{\text{E}}_j v^{\text{E}}_j = -\dfrac{8\pi}{3}\big(\partial_i E^{\text{inc}}_i(0) - \partial_j E^{\text{inc}}_j(0)\big) & (i,j) \in \{(1,2),(2,3)\}\,, \\ u^{\text{E}}_i v^{\text{E}}_j + u^{\text{E}}_j v^{\text{E}}_i = -\dfrac{8\pi}{3}\big(\partial_i E^{\text{inc}}_j(0) + \partial_j E^{\text{inc}}_i(0)\big) & (i,j) \in \{(1,2),(2,3),(3,1)\}\,, \end{cases} \tag{2.10}$$

  where $\mathbf{u}^{\text{E}} = (u^{\text{E}}_1, u^{\text{E}}_2, u^{\text{E}}_3)$, $\mathbf{v}^{\text{E}} = (v^{\text{E}}_1, v^{\text{E}}_2, v^{\text{E}}_3)$ and $\partial_i E^{\text{inc}}_j$ denotes the i-th partial derivative of the j-th coordinate of $\mathbf{E}^{\text{inc}}$ for $i, j = 1, 2, 3$.

The first-order magnetic near-field term $\widehat{\mathbf{H}}_1$ given by (2.9) is represented as the superposition of

- a magnetic field created in the presence of a filiform electric current in an electric dipole configuration in static regime, along the direction $-4\pi c\,\mathbf{curl}\,\mathbf{H}^{\text{inc}}(0) = 4\pi i\omega\mathbf{E}^{\text{inc}}(0)$,
- a magnetic field created in the presence of a magnetic quadrupole along directions $(\mathbf{u}^{\text{H}}, \mathbf{v}^{\text{H}})$, in static regime satisfying the following systems of equations

$$\begin{cases} u^{\text{H}}_i v^{\text{H}}_i - u^{\text{H}}_j v^{\text{H}}_j = \dfrac{16\pi}{9}\big(\partial_i H^{\text{inc}}_i(0) - \partial_j H^{\text{inc}}_j(0)\big) & (i,j) \in \{(1,2),(2,3)\}\,, \\ u^{\text{H}}_i v^{\text{H}}_j + u^{\text{H}}_j v^{\text{H}}_i = \dfrac{16\pi}{9}\big(\partial_i H^{\text{inc}}_j(0) + \partial_j H^{\text{inc}}_i(0)\big) & (i,j) \in \{(1,2),(2,3),(3,1)\}\,. \end{cases} \tag{2.11}$$

  where $\partial_i H^{\text{inc}}_j$ denotes the i-th partial derivative of the j-th coordinate of $\mathbf{H}^{\text{inc}}$ for $i, j = 1, 2, 3$.

Remark 9. The systems of equations (2.10) and (2.11) have an infinity of complex solutions. Indeed, if $(\mathbf{u}, \mathbf{v})$ is solution of one of them, then $(\mathbf{v}, \mathbf{u})$ or $(c\mathbf{u}, \frac{1}{c}\mathbf{v})$ for $c \neq 0$ is also solution. Actually, this formulation is only a physical interpretation and we have not the uniqueness for the quadrupole configuration.

According to (B.5)-(B.12) and (B.11)-(B.7), the first-order near-field terms $\widehat{\mathbf{E}}_1$ and $\widehat{\mathbf{H}}_1$ can be put in the compact form

$$\widehat{\mathbf{E}}_1 = \mathbf{E}^{\text{elec}}_{\text{quad}}\big[\mathbf{u}^{\text{E}}, \mathbf{v}^{\text{E}}, \kappa = 0\big] + \mathbf{E}^{\text{mag}}_{\text{dip}}\big[-2\pi i\omega\mathbf{H}^{\text{inc}}(0), \kappa = 0\big],$$
$$\widehat{\mathbf{H}}_1 = \mathbf{H}^{\text{mag}}_{\text{quad}}\big[\mathbf{u}^{\text{H}}, \mathbf{v}^{\text{H}}, \kappa = 0\big] + \mathbf{H}^{\text{elec}}_{\text{dip}}\big[4\pi i\omega\mathbf{E}^{\text{inc}}(0), \kappa = 0\big].$$

Remark 10. The second-order near-field terms $\widehat{\mathbf{E}}_2$ and $\widehat{\mathbf{H}}_2$ appear like the superposition of octupoles, quadrupoles and dipoles, but we have not performed the whole computation in this document.

2.4.2 First far-field terms

The third-order electric far-field term $\widetilde{\mathbf{E}}_3$ can be represented like the superposition of

- an electric field created in the presence of a time-harmonic electric dipole along direction $4\pi\mathbf{E}^{\text{inc}}(0)$,
- an electric field created in the presence of a time-harmonic magnetic dipole along direction $-2\pi\mathbf{H}^{\text{inc}}(0)$.

The third-order magnetic far-field term $\widetilde{\mathbf{H}}_3$ can be represented like the superposition of

- a magnetic field created in the presence of a time-harmonic magnetic dipole along direction $-2\pi\mathbf{H}^{\text{inc}}(0)$,
- a magnetic field created in the presence of a time-harmonic electric dipole along direction $4\pi\mathbf{E}^{\text{inc}}(0)$.

According to (B.8)-(B.14) and (B.13)-(B.9), the third-order far-field terms can be put in the compact form

$$\begin{aligned}\widetilde{\mathbf{E}}_3 &= \mathbf{E}_{\text{dip}}^{\text{elec}}\big[4\pi\mathbf{E}^{\text{inc}}(0),\kappa\big] + \mathbf{E}_{\text{dip}}^{\text{mag}}\big[-2\pi\mathbf{H}^{\text{inc}}(0),\kappa\big]\\ \widetilde{\mathbf{H}}_3 &= \mathbf{H}_{\text{dip}}^{\text{elec}}\big[4\pi\mathbf{E}^{\text{inc}}(0),\kappa\big] + \mathbf{H}_{\text{dip}}^{\text{mag}}\big[-2\pi\mathbf{H}^{\text{inc}}(0),\kappa\big].\end{aligned} \tag{2.12}$$

Remark 11. In a same way, we can prove that the fifth-order far-field terms $\widetilde{\mathbf{E}}_5$ and $\widetilde{\mathbf{H}}_5$ can be represented like a superposition of dipoles and quadrupoles.

3 Numerical experiments

Numerical experiments allow to make evident the orders of convergence associated to the different levels of near-field and far-field approximations that we have postulated in Theorems 1 and 2 in Section A.3. To illustrate our results, we propose two test-cases: the first one consists in considering an incident plane wave involving an analytical solution; in the second one, we consider an incident gaussian beam [36] involving the numerical approximation of the reference solution. We compare the local approximations into sub-domains that are independent of δ in the suitable system of coordinates. Moreover, we construct a global approximation of the solution thanks to the near-field and far-field approximations. However, the numerical order of convergence that we obtained in the comparisons for the global approximation is non-optimal.

3.1 The reference solution

Test 1: Incident plane wave. The spherical obstacle is enlighted by an electromagnetic plane wave $(\mathbf{E}^{\text{inc}}, \mathbf{H}^{\text{inc}})$ of wavelength λ defined in (2.1). The wave vector $\mathbf{k}$ and the polarization vector $\mathbf{p}$ are chosen such that

$$\mathbf{k} = \begin{pmatrix} 0 \\ 0 \\ -\kappa \end{pmatrix} \; ; \qquad \mathbf{p} = \begin{pmatrix} 1 \\ 0 \\ 0 \end{pmatrix} \; ; \qquad \kappa = \frac{2\pi}{\lambda}. \tag{3.1}$$

On Figure 2, we represent cross-sections of the x-coordinates of the real part of the incident electric field with $\lambda = 1$.

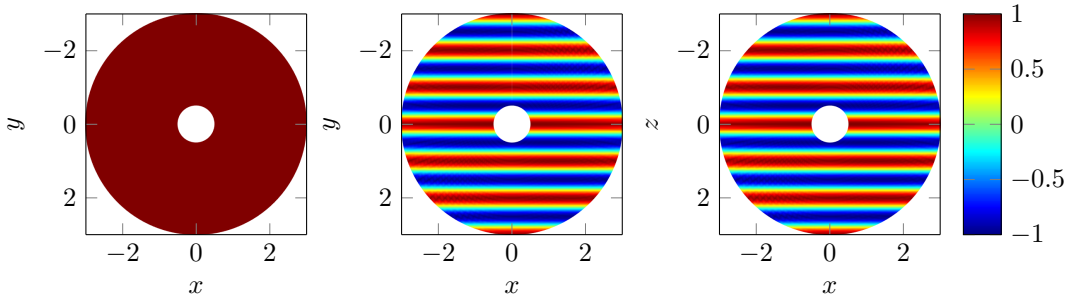

(a) $z = 0$ (b) $x = 0$ (c) $y = 0$

Figure 2: Cross sections of the x-coordinates of the real part of the incident electric field associated to Test 1 with $\lambda = 1$

Test 2: Incident gaussian beam. For the same physical parameters given by (3.1), an electromagnetic gaussian beam of waist w polarized by the vector $\mathbf{p}$ and directed along the z-axis, is given by

$$\mathbf{E}^{\text{inc}}(\mathbf{x}) = \frac{z_0 \exp(i\kappa z)}{z_0 + iz} \exp\left(-\frac{1}{2}\frac{\kappa(x^2+y^2)}{z_0+iz}\right)\mathbf{p},$$

$$\mathbf{H}^{\text{inc}}(\mathbf{x}) = \frac{z_0 \exp(i\kappa z)}{z_0 + iz} \exp\left(-\frac{1}{2}\frac{\kappa(x^2+y^2)}{z_0+iz}\right) \begin{pmatrix} \dfrac{ix}{z_0+iz} \\ \dfrac{iy}{z_0+iz} \\ 1 - \dfrac{1}{\kappa(z_0+iz)} + \dfrac{1}{2}\dfrac{x^2+y^2}{(z_0+iz)^2} \end{pmatrix} \times \mathbf{p},$$

for any $\mathbf{x} = (x, y, z)$, where $z_0 = \frac{\kappa w^2}{2}$ denotes the Rayleigh range. This is an approximate solution of the time-harmonic Maxwell equations assuming that $w \geq \frac{2\lambda}{\pi}$. On Figure 3, we represent cross-sections of the x-coordinates of the real part of the incident electric field with $\lambda = 5$ and $w = 5$.

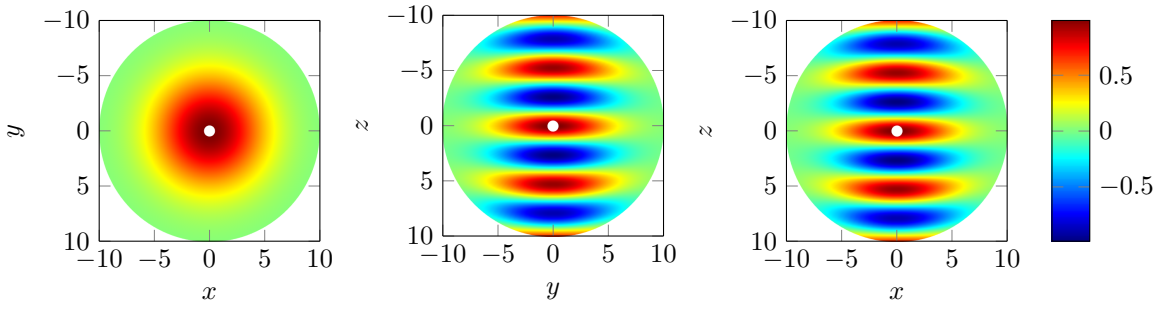

(a) $z = 0$ (b) $x = 0$ (c) $y = 0$

Figure 3: Cross sections of the x-coordinates of the real part of the incident electric field associated to Test 2 with $\lambda = 5$ and $w = 5$

Thereafter, we investigate the numerical order of convergence of the far-field and near-field

approximations. The norm used in the comparison is the Sobolev $\mathbf{L}^2$-norm of the difference between the reference solution and our approximations, into some domains of interest. To obtain the data, we calculate

- the reference solution $(\mathbf{E}_\delta^{\text{ref}}, \mathbf{H}_\delta^{\text{ref}})$, based on the computation of the Mie series representation with analytical coefficients for the first test and approximated coefficients, calculated from projections of the incident field, for the second one (see Remark 12 below for more details),
- the near-field approximation $(\widehat{\mathbf{E}}_{\delta,P}, \widehat{\mathbf{H}}_{\delta,P})$ or the far-field approximation $(\widetilde{\mathbf{E}}_{\delta,P+3}, \widetilde{\mathbf{H}}_{\delta,P+3})$ for $P = 0, 1$ or 2, defined by (A.10) and (A.9),
- the absolute errors $\|\mathbf{E}_\delta^{\text{ref}} - \diamond^{\text{E}}\|$ and $\|\mathbf{H}_\delta^{\text{ref}} - \diamond^{\text{H}}\|$ or the relative errors $\|\mathbf{E}_\delta^{\text{ref}} - \diamond^{\text{E}}\|/\|\mathbf{E}_\delta^{\text{ref}}\|$ and $\|\mathbf{H}_\delta^{\text{ref}} - \diamond^{\text{H}}\|/\|\mathbf{H}_\delta^{\text{ref}}\|$, replacing $(\diamond^{\text{E}}, \diamond^{\text{H}})$ either by $(\widehat{\mathbf{E}}_{\delta,P}, \widehat{\mathbf{H}}_{\delta,P})$ or $(\widetilde{\mathbf{E}}_{\delta,P+3}, \widetilde{\mathbf{H}}_{\delta,P+3})$, in spherical coordinates by using a Riemann sum for angles θ and φ and a trapezoidal rule for radius r into domains of interest,

for a range of δ between 10^0 and 10^{-4}.

Remark 12. The reference solution $(\mathbf{E}_\delta^{\text{ref}}, \mathbf{H}_\delta^{\text{ref}})$ is calculated from the Mie series representation (D.6)-(D.7) truncated at $n = 5$. For Test 1, the incident wave is a plane wave and possesses analytical coefficients according to its Jacobi-Anger decomposition (D.4). For gaussian beams, we approximate numerically the projections (D.8) with a quadrature formula based on Simpson's rule.

On Figures 4 and 5, we draw cross sections of the x-coordinates of the modulus of the scattered electric fields $\mathbf{E}_\delta^{\text{ref}}$ induced by the two different tests with $\delta = 0.5$.

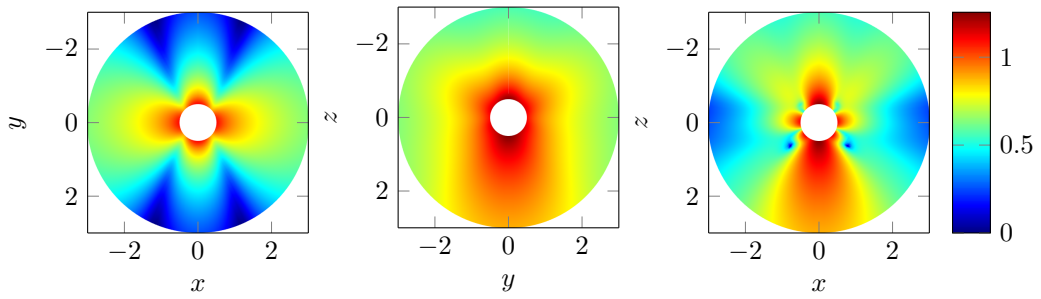

(a) $z = 0$ (b) $x = 0$ (c) $y = 0$

Figure 4: Cross sections of the x-coordinates of the scattered electric field modulus in logarithmic scale associated to Test 1 with $\lambda = 1$

3.2 Near-field approximation

To illustrate the convergence results for the near-field approximations, we introduce a subdomain of $\widehat{\Omega}$ independent of δ in the fast variable $\mathbf{X}$,

$$\Omega_\delta^{2\delta} = \mathcal{B}(0, 2\delta) \setminus \overline{\mathcal{B}(0, \delta)}.$$

For the results on Figures 6 and 7, we investigate the numerical order of convergence for the $\mathbf{L}^2$-norm of the near-field approximations into the domain $\Omega_\delta^{2\delta}$ with respect to the size of the

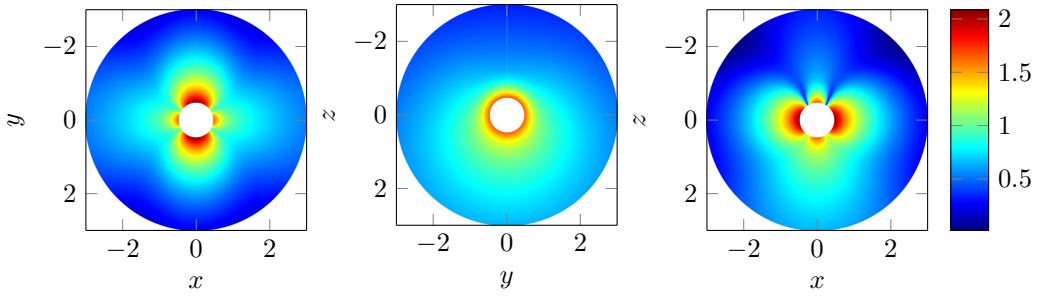

(a) $z = 0$ (b) $x = 0$ (c) $y = 0$

Figure 5: Cross sections of the x-coordinates of the scattered electric field modulus in logarithmic scale associated to Test 2 with $\lambda = 5$ and $w = 5$

obstacles δ such that

$$\delta \in \left\{ \frac{1}{10^p},\ p = 1 : 0.1 : 4 \right\}.$$

Figure 6 makes evident the different orders of convergence for the near-field approximations $(\widehat{\mathbf{E}}_{\delta,0}, \widehat{\mathbf{H}}_{\delta,0})$, $(\widehat{\mathbf{E}}_{\delta,1}, \widehat{\mathbf{H}}_{\delta,1})$ and $(\widehat{\mathbf{E}}_{\delta,2}, \widehat{\mathbf{H}}_{\delta,2})$ induced by Test 1, using the $\mathbf{L}^2$-norm into the domain $\Omega_\delta^{2\delta}$, see Theorem 2 in Section A.3.

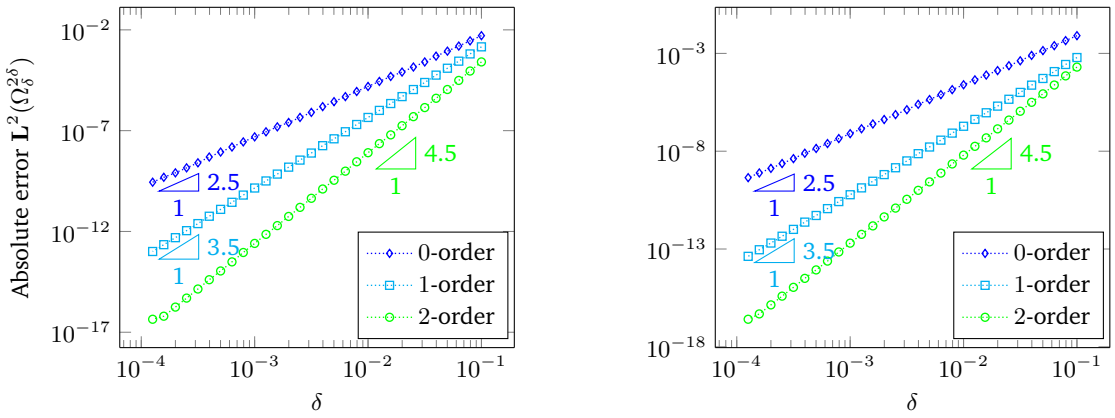

(a) Electric field (b) Magnetic field

Figure 6: Absolute $\mathbf{L}^2$-errors for near-field approximations associated to Test 1 with $\lambda = 5$

Figure 7 shows the same analysis for Test 2.
We observe that the different levels of approximation follow the rule

P-order approximation	$\Longleftrightarrow$	Convergence rate : $\frac{3}{2} + P + 1.$ (absolute $\mathbf{L}^2$-error)

The power $\frac{3}{2}$ is due to the behavior of the exact solution $\mathbf{E}_\delta^{\text{ref}}(\delta\,\cdot)$ close to the obstacle. Convergence of the near-field asymptotics is numerically validated regarding error estimates provided

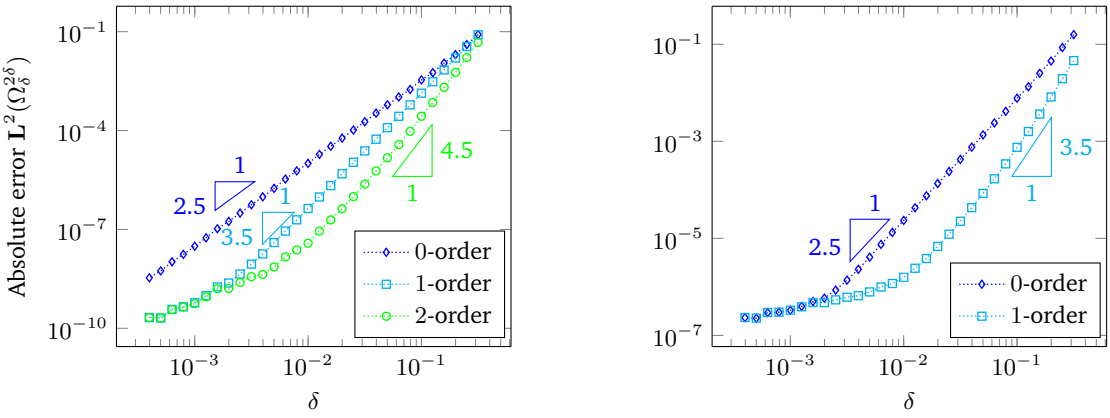

(a) Electric field

(b) Magnetic field

Figure 7: Absolute $\mathbf{L}^2$-errors for near-field approximations associated to Test 2 with $\lambda = 5$ and $w = 5$

by Theorem 2. For the results stemed from Test 1, the different orders of convergence are satisfying. For the results from Test 2, the loss of convergence in asymptotic regime can be explained by the consideration of an approximate incident wave. However, there exists a range of obstacle sizes for which the convergence is valid.

3.3 Far-field approximation

To illustrate the convergence results for the far-field approximations, we introduce a subdomain independent of δ,

$$\Omega_\lambda^{2\lambda} = \mathcal{B}(0, 2\lambda) \setminus \overline{\mathcal{B}(0, \lambda)}.$$

For the results on Figures 8 and 9, we investigate the numerical order of convergence for the $\mathbf{L}^2$-norm of the far-field approximations into the domain $\Omega_\lambda^{2\lambda}$ with respect to the size δ of the obstacles such that

$$\delta \in \left\{ \frac{1}{10^p},\ p = 0.5 : 0.1 : 2.9 \right\}.$$

Figure 8 makes evident the different orders of convergence for the far-field approximations $(\widetilde{\mathbf{E}}_{\delta,3}, \widetilde{\mathbf{H}}_{\delta,3})$ and $(\widetilde{\mathbf{E}}_{\delta,5}, \widetilde{\mathbf{H}}_{\delta,5})$ induced by Test 1, using the $\mathbf{L}^2$-norm into the domain $\Omega_\lambda^{2\lambda}$, see Theorem 1 in Section A.3.

Figure 9 shows the same analysis for Test 2.

Noting that the fourth-order far-field term is equal to null-field, we observe that the different levels of approximation follow the rule

P-order approximation	$\Longleftrightarrow$	Convergence rate : $P+1$. (absolute $\mathbf{L}^2$-error)

Convergence of the far-field asymptotics is numerically validated regarding error estimates provided by Theorem 1. For the results stemed from Test 1, the different orders of convergence are made evident. Moreover, we observe a stagnation in asymptotic regime due to the numerical

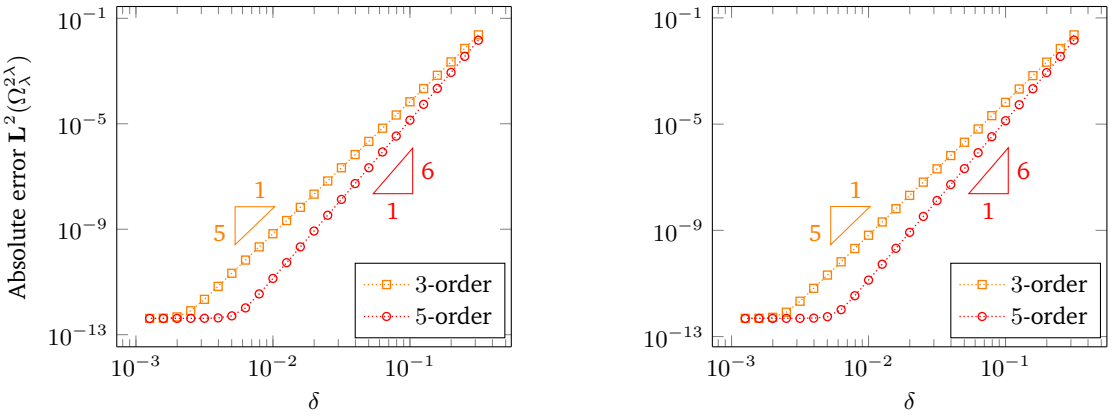

(a) Electric field

(b) Magnetic field

Figure 8: Absolute $\mathbf{L}^2$-errors for the far-field approximations associated to Test 1 with $\lambda = 5$

precision. For the results from Test 2, the loss of convergence in asymptotic regime can be explained by the consideration of an approximate incident wave. However, there exists a range of obstacle sizes for which the convergence is valid.

3.4 Toward a global approximation

To link the different levels of approximation of near and far fields, we investigate the relative error with respect to the reference solution. For the results on Figures 10 and 11, we make evident the numerical order of convergence for the different levels of approximation induced by Test 1 with respect to the size δ of the obstacle. Figure 10 shows the different relative orders of convergence with respect to the reference solution of the different levels of near-field approximations associated to Test 1.

Figure 11 shows the same analysis for the different levels of far-field approximations associated to Test 1.

We observe that a near-field approximation of order P is related to a far-field expansion of order $P+3$. Hence, from the local approximations $(\widetilde{\mathbf{E}}_{\delta,P+3}, \widetilde{\mathbf{H}}_{\delta,P+3})$ and $(\widehat{\mathbf{E}}_{\delta,P}, \widehat{\mathbf{H}}_{\delta,P})$ given by Equations (A.9) and (A.10) for $P = 0, 1$ and 2, the derivation of a global approximation into the whole bounded domain

$$\Omega_\delta^\lambda = \left\{\mathbf{x} \in \mathbb{R}^3,\ \delta < |\mathbf{x}| < \lambda\right\},$$

goes through a combination of these both data. We introduce the sub-domains $\Omega_{\delta,\lambda}^{\mathrm{F}}$ and $\Omega_\delta^{\mathrm{N}}$ of Ω_δ^λ, related to the validity of the far-field and near-field expansions, see Remarks 15 and 18 in Sections 4.2 and 4.3,

$$\Omega_{\delta,\lambda}^{\mathrm{F}} = \left\{\mathbf{x} \in \mathbb{R}^3,\ 2\sqrt{\lambda\delta} < |\mathbf{x}| < \lambda\right\};\qquad \Omega_\delta^{\mathrm{N}} = \left\{\mathbf{x} \in \mathbb{R}^3,\ \delta < |\mathbf{x}| < \sqrt{\lambda\delta}\right\}.$$

A global approximation $(\mathbf{E}_{\delta,P}, \mathbf{H}_{\delta,P})$ for $P = 0, 1$ or 2 is then given by

- $(\mathbf{E}_{\delta,P}, \mathbf{H}_{\delta,P}) = (\widehat{\mathbf{E}}_{\delta,P}, \widehat{\mathbf{H}}_{\delta,P})$ in $\Omega_\delta^{\mathrm{N}}$,
- $(\mathbf{E}_{\delta,P}, \mathbf{H}_{\delta,P}) = (\widetilde{\mathbf{E}}_{\delta,P+3}, \widetilde{\mathbf{H}}_{\delta,P+3})$ in $\Omega_{\delta,\lambda}^{\mathrm{F}}$,

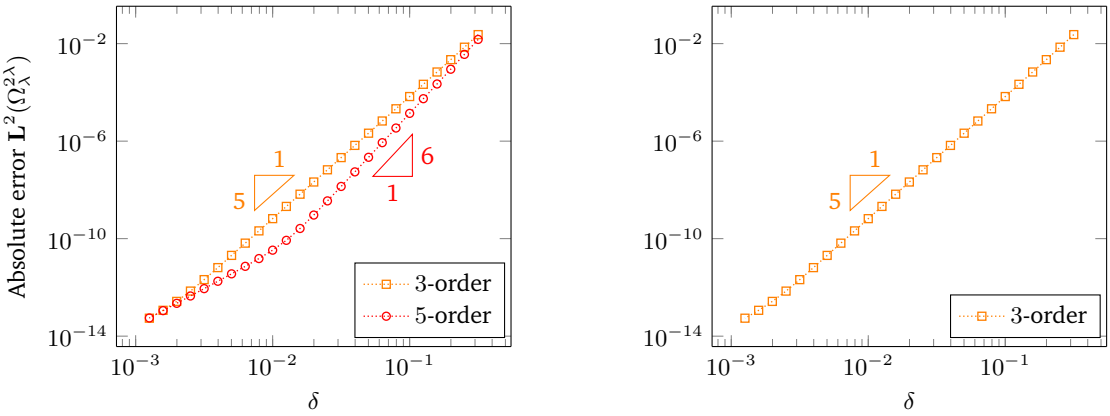

(a) Electric field

(b) Magnetic field

Figure 9: Absolute $\mathbf{L}^2$-errors for the far-field approximations associated to Test 2 with $\lambda = 5$ and $w = 5$

- a combination of the two data in the matching area $\left\{\mathbf{x} \in \mathbb{R}^3,\ \sqrt{\lambda\delta} < |\mathbf{x}| < 2\sqrt{\lambda\delta}\right\}$.

We consider a cut-off function $\chi_\delta : \mathbb{R}^+ \longmapsto [0,1]$ which is equal to 1 in a neighborhood of the obstacle and equal to 0 far from the obstacle, in terms of distance. For the numerical experiments we choose $\chi_\delta = \chi(\frac{\cdot}{\sqrt{\lambda\delta}})$ where χ is such that

$$\chi \in \mathscr{C}^\infty(\mathbb{R})\,; \qquad \chi(r) = \begin{cases} 1 & \text{if } r \leq 1 \\ 0 & \text{if } r \geq 2 \end{cases}\,; \qquad \chi'(r) \leq 0 \text{ for any } r \geq 0.$$

A global approximation $(\mathbf{E}_{\delta,P}, \mathbf{H}_{\delta,P})$ of order $P = 0, 1$ and 2 is then defined for $\mathbf{x} \in \Omega_\delta^\lambda$ by

$$\mathbf{E}_{\delta,P}(\mathbf{x}) = \chi_\delta(|\mathbf{x}|)\widehat{\mathbf{E}}_{\delta,P}(\frac{\mathbf{x}}{\delta}) + \Big(1 - \chi_\delta(|\mathbf{x}|)\Big)\widetilde{\mathbf{E}}_{\delta,P+3}(\mathbf{x}),$$
$$\mathbf{H}_{\delta,P}(\mathbf{x}) = \chi_\delta(|\mathbf{x}|)\widehat{\mathbf{H}}_{\delta,P}(\frac{\mathbf{x}}{\delta}) + \Big(1 - \chi_\delta(|\mathbf{x}|)\Big)\widetilde{\mathbf{H}}_{\delta,P+3}(\mathbf{x}).$$

Remark 13. The choice of the sub-domains $\Omega_\delta^{\mathrm{N}}$ and $\Omega_{\delta,\lambda}^{\mathrm{F}}$ is non-optimal to make evident the order of convergence of the global approximation in the whole bounded domain Ω_δ^λ. Actually, the dependence on $\sqrt{\delta}$ in the sub-domains creates a scale factor in the error computation. Error estimates would enable to quantify this dependence.

For the results on Figure 12, we investigate the numerical order of convergence for the $\mathbf{L}^2$-norm in the whole bounded domain Ω_δ^λ with respect to the size of the obstacles δ such that

$$\delta \in \left\{\frac{1}{10^p},\ p = 1 : 0.1 : 4\right\}.$$

Figure 12 makes evident the different orders of convergence for the global approximations $(\mathbf{E}_{\delta,0}, \mathbf{H}_{\delta,0})$, $(\mathbf{E}_{\delta,1}, \mathbf{H}_{\delta,1})$ and $(\mathbf{E}_{\delta,2}, \mathbf{H}_{\delta,2})$, using the $\mathbf{L}^2$ norm in the whole bounded domain Ω_δ^λ for the electric and magnetic fields.

Remark 14. By virtue of Remark 13, the order of convergence is non-optimal for $(\mathbf{E}_{\delta,1}, \mathbf{H}_{\delta,1})$ and $(\mathbf{E}_{\delta,2}, \mathbf{H}_{\delta,2})$. We observe that the order is degrading between the first and the second order of approximations.

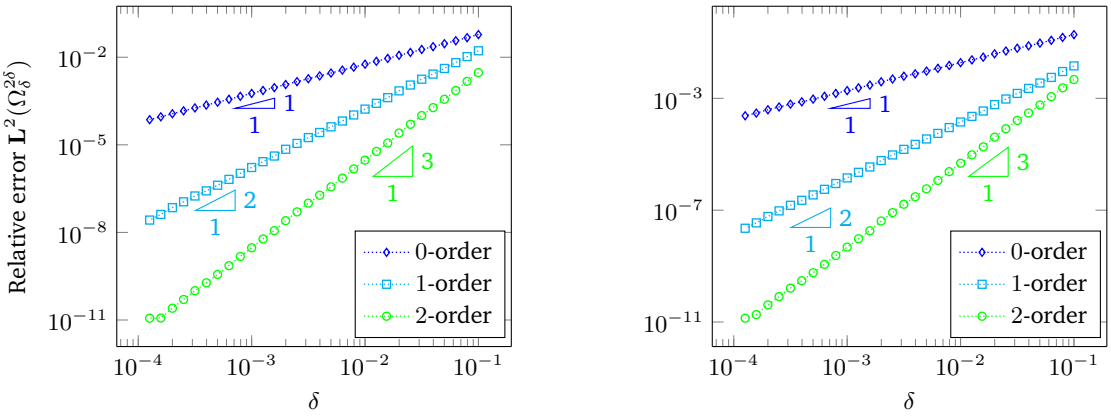

(a) Electric field (b) Magnetic field

Figure 10: Relative $\mathbf{L}^2$-errors for near-field approximations associated to Test 1 with $\lambda = 5$

4 The matched asymptotic expansions

In this section, we apply the method of matched asymptotic expansions to tackle the exterior time-harmonic Maxwell problem (2.2). Assuming that the obstacle size δ is significantly small in comparison with the incident wavelength $\lambda = \frac{2\pi}{\kappa}$, this method consists in defining an approximate solution using multi-scale expansions over far and near fields, related in a matching area. We introduce the geometrical setting, the problems satisfied by any term of the asymptotics at any order and the matching conditions applied on spectral coefficients. It is only in the last paragraph that we focus on the first terms of the asymptotics.

4.1 Geometrical setting

Before postulating *Ansatz* of the far and near field expansions, we define the asymptotic domains where the expansions will be defined. The far-field domain $\Omega_\delta^{\mathrm{F}}$ is the exterior domain defined by

$$\Omega_\delta^{\mathrm{F}} = \left\{\mathbf{x} \in \mathbb{R}^3,\ |\mathbf{x}| > \eta_\delta^{\mathrm{F}}\right\} \qquad \text{with } \lim_{\delta\to 0} \eta_\delta^{\mathrm{F}} = 0. \tag{4.1}$$

The far-field expansion is then defined in $\Omega^\star$ that is the limit of the far-field domain when δ tends to 0, see Figure 13,

$$\Omega^\star = \lim_{\delta\to 0} \Omega_\delta^{\mathrm{F}} = \mathbb{R}^3 \setminus \{0\}\,. \tag{4.2}$$

The definition of the near-field domain $\Omega_\delta^{\mathrm{N}}$ goes through the coordinate change $\mathbf{X} = \frac{\mathbf{x}}{\delta}$. Then, $\Omega_\delta^{\mathrm{N}}$ is the interior domain defined in fast variable by

$$\Omega_\delta^{\mathrm{N}} = \left\{\mathbf{X} \in \mathbb{R}^3,\ \delta < \delta|\mathbf{X}| < \eta_\delta^{\mathrm{N}}\right\} \qquad \text{with } \lim_{\delta\to 0} \frac{\eta_\delta^{\mathrm{N}}}{\delta} = +\infty. \tag{4.3}$$

The near-field expansion is then defined in $\widehat{\Omega}$ that is the near-field domain when δ tends to 0, see Figure 13 ,

$$\widehat{\Omega} = \lim_{\delta\to 0} \Omega_\delta^{\mathrm{N}} = \mathbb{R}^3 \setminus \overline{\mathcal{B}(0,1)}. \tag{4.4}$$

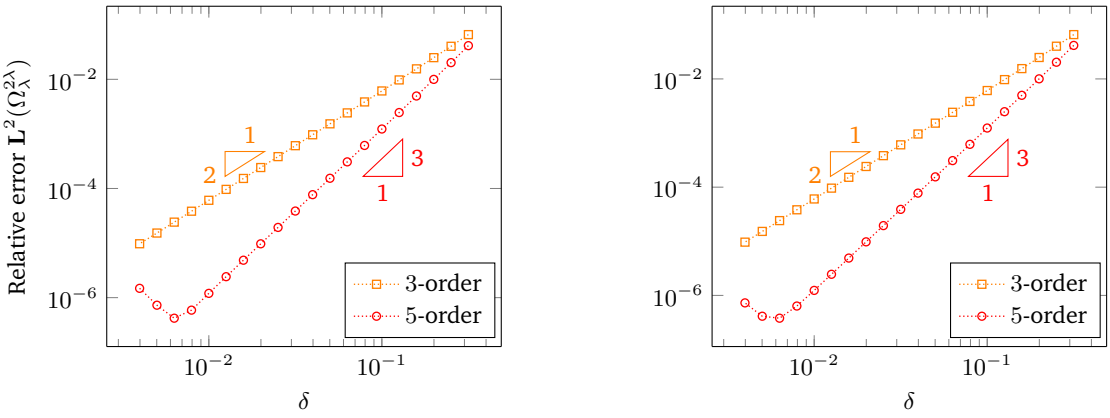

(a) Electric field (b) Magnetic field

Figure 11: Relative $\mathbf{L}^2$-errors for far-field approximations associated to Test 1 with $\lambda = 5$

4.2 Far-field expansion

Far from the obstacle, the exact solution is approximated by the far-field expansion

$$\mathbf{E}_\delta(\mathbf{x}) \underset{\delta\to 0}{\sim} \sum_{p=0}^{\infty} \delta^p \widetilde{\mathbf{E}}_p(\mathbf{x}) \,, \qquad \mathbf{H}_\delta(\mathbf{x}) \underset{\delta\to 0}{\sim} \sum_{p=0}^{\infty} \delta^p \widetilde{\mathbf{H}}_p(\mathbf{x}), \tag{4.5}$$

where $\mathbf{x} = r\widehat{x}$ is the spatial variable in spherical coordinates. This expansion begins at the third order since all previous terms are reduced to null-fields, see Remark 19 in Section 4.4. The set of $(\widetilde{\mathbf{E}}_p, \widetilde{\mathbf{H}}_p)$ with $p \geq 3$ is *singular* solution, reading as (C.6), of the time-harmonic Maxwell equations in $\Omega^\star$ given by (4.2),

$$\begin{cases} \mathbf{curl}\, \widetilde{\mathbf{E}}_p - i\kappa \widetilde{\mathbf{H}}_p = 0 & \text{in } \Omega^\star, \\ \mathbf{curl}\, \widetilde{\mathbf{H}}_p + i\kappa \widetilde{\mathbf{E}}_p = 0 & \text{in } \Omega^\star, \\ \lim\limits_{r\to\infty} r\big(\widetilde{\mathbf{H}}_p \times \widehat{x} - \widetilde{\mathbf{E}}_p\big) = 0 & \text{uniformly in } \widehat{x}. \end{cases} \tag{4.6}$$

These problems are ill-posed in $\mathbf{H}_{\rm loc}(\mathbf{curl}\,, \Omega^\star)$ which is the space of vector fields $\mathbf{u}$ such that

$$\forall \psi \in \mathscr{C}_c^\infty(\mathbb{R}^3), \quad \psi = 0 \text{ in a neighbourhood of } 0, \quad \psi\mathbf{u} \in \mathbf{L}^2(\mathbb{R}^3),\ \mathbf{curl}\,(\psi\mathbf{u}) \in \mathbf{L}^2(\mathbb{R}^3),$$

because it lacks a piece of information about their behavior at the origin. Actually, the terms $(\widetilde{\mathbf{E}}_p, \widetilde{\mathbf{H}}_p)$ are finite sums of multipoles that are explicitly known up to their spectral coefficients [32]. Obtaining these coefficients allows to define the far-field asymptotic expansion at any order.

Remark 15. The far-field expansion is defined in $\Omega^\star$ but is a suitable approximation of the solution into the exterior domains $\Omega_\delta^{\rm F}$, see (4.1). The proof goes through error estimates. For the numerical results in Section 3.4, we have chosen $\eta_\delta^{\rm F} = (\delta\lambda)^{\frac{1}{2}}$.

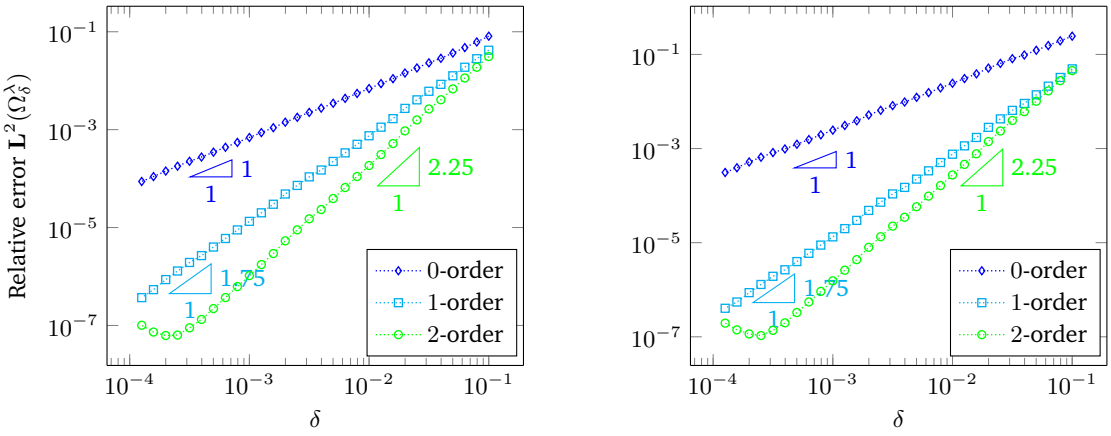

(a) Electric field (b) Magnetic field

Figure 12: Relative $\mathbf{L}^2$-errors for global approximations associated to Test 1 with $\lambda = 5$

4.3 Near-field expansion

In the vicinity of the obstacle, the solution can be approximated by the near-field expansion

$$\mathbf{E}_\delta(\delta\mathbf{X}) \underset{\delta\to 0}{\sim} \sum_{p=0}^{\infty} \delta^p \widehat{\mathbf{E}}_p(\mathbf{X})\,, \qquad \mathbf{H}_\delta(\delta\mathbf{X}) \underset{\delta\to 0}{\sim} \sum_{p=0}^{\infty} \delta^p \widehat{\mathbf{H}}_p(\mathbf{X}), \tag{4.7}$$

where $\mathbf{X} = \frac{\mathbf{x}}{\delta} = \mathrm{R}\widehat{x}$ denotes the fast variable. The set of $(\widehat{\mathbf{E}}_p, \widehat{\mathbf{H}}_p)$ for $p \geq 0$ satisfies the nested Maxwell equations given by

$$\begin{cases} \mathbf{curl}\, \widehat{\mathbf{E}}_p = i\kappa \widehat{\mathbf{H}}_{p-1} & \text{in } \widehat{\Omega}, \\ \mathbf{curl}\, \widehat{\mathbf{H}}_p = -i\kappa \widehat{\mathbf{E}}_{p-1} & \text{in } \widehat{\Omega}, \end{cases} \tag{4.8}$$

where $\widehat{\Omega}$ is defined in (4.4). In (4.8), we use the convention $\widehat{\mathbf{E}}_{-1} = \widehat{\mathbf{H}}_{-1} = 0$.

Remark 16. These equations are said *nested* because the problem of order p depends on the previous term, of order $p-1$. They can be read as Maxwell static problems with a non-homogeneous source term. Moreover, we can deduce from the problem of order $p+1$, complementary equations for the divergence of the fields of order p, that are

$$\begin{cases} \operatorname{div} \widehat{\mathbf{E}}_p = 0 & \text{in } \widehat{\Omega}, \\ \operatorname{div} \widehat{\mathbf{H}}_p = 0 & \text{in } \widehat{\Omega}. \end{cases} \tag{4.9}$$

The boundary conditions are obtained by identifying the Taylor series expansion of the incident field in a neighborhood of the origin in the fast variable $\mathbf{X} = \frac{\mathbf{x}}{\delta}$,

$$\mathbf{E}^{\mathrm{inc}}(\mathbf{x}) = \sum_{p=0}^{\infty} \delta^p \widehat{\mathbf{E}}_p^{\mathrm{inc}}(\mathbf{X})\,, \qquad \mathbf{H}^{\mathrm{inc}}(\mathbf{x}) = \sum_{p=0}^{\infty} \delta^p \widehat{\mathbf{H}}_p^{\mathrm{inc}}(\mathbf{X}),$$

where

$$\widehat{\mathbf{E}}_p^{\mathrm{inc}}(\mathbf{X}) = \sum_{|\alpha|=p} \frac{1}{\alpha!} \mathrm{d}^\alpha \mathbf{E}^{\mathrm{inc}}(0) \cdot \mathbf{X}^\alpha\,, \qquad \widehat{\mathbf{H}}_p^{\mathrm{inc}}(\mathbf{X}) = \sum_{|\alpha|=p} \frac{1}{\alpha!} \mathrm{d}^\alpha \mathbf{H}^{\mathrm{inc}}(0) \cdot \mathbf{X}^\alpha,$$

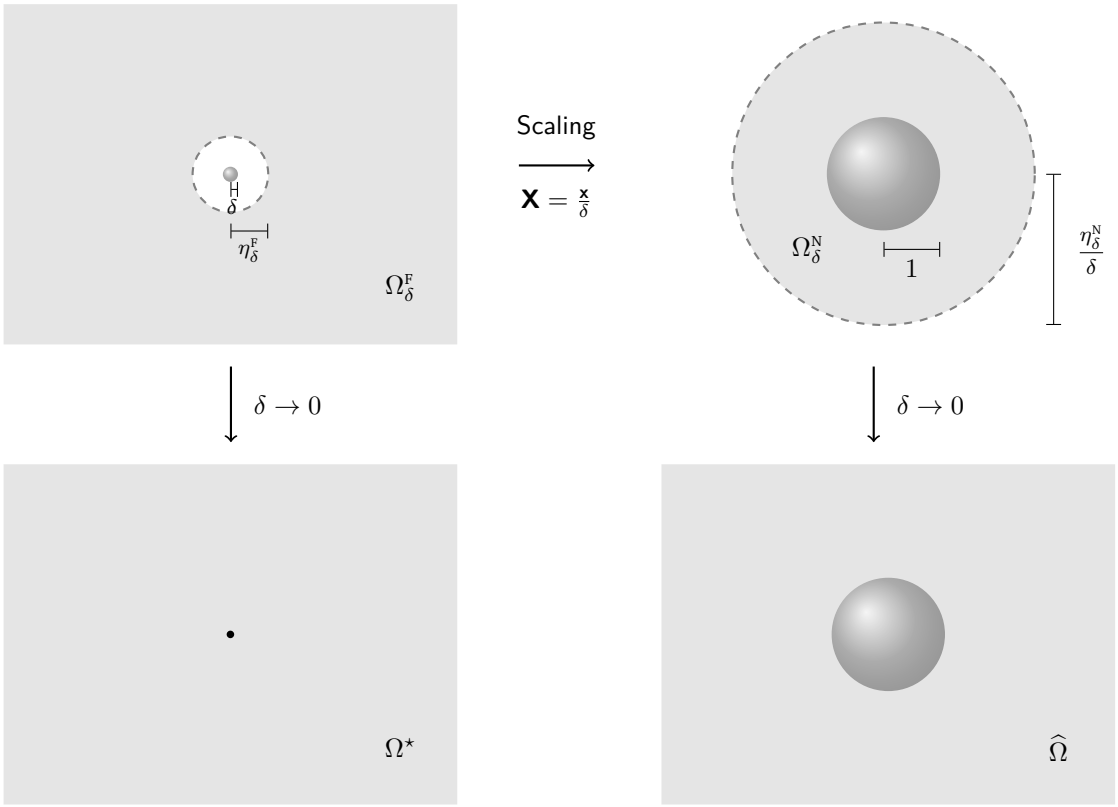

Figure 13: Far-field and near-field domains $\Omega_\delta^{\mathrm{F}}$ and $\Omega_\delta^{\mathrm{N}}$ and their limit $\Omega^\star$ and $\widehat{\Omega}$

with the boundary conditions satisfied by the near-field expansion. In particular, on the boundary $\partial\widehat{\Omega} = \mathcal{S}^2 = \widehat{\Gamma}$, we have

$$\begin{cases} \mathbf{e}_r \times \widehat{\mathbf{E}}_p = -\mathbf{e}_r \times \widehat{\mathbf{E}}_p^{\mathrm{inc}} & \text{on } \widehat{\Gamma}, \\ \mathbf{e}_r \cdot \widehat{\mathbf{H}}_p = -\mathbf{e}_r \cdot \widehat{\mathbf{H}}_p^{\mathrm{inc}} & \text{on } \widehat{\Gamma}. \end{cases} \tag{4.10}$$

Remark 17. The terms of order p depend on the zero value of the p-order derivative of the incident field.

The problems made up of Equations (4.8)-(4.10) with $p = 0$ satisfied by $\widehat{\mathbf{E}}_0$ and $\widehat{\mathbf{H}}_0$, are well-posed in the weighted Sobolev space

$$\mathbf{W} = \left\{ \frac{\mathbf{u}}{(1+\mathrm{R}^2)^{\frac{1}{2}}} \in \mathbf{L}^2(\widehat{\Omega}),\ \mathbf{curl}\,\mathbf{u} \in \mathbf{L}^2(\widehat{\Omega}),\ \mathrm{div}\,\mathbf{u} = 0 \text{ in } \widehat{\Omega} \right\}. \tag{4.11}$$

However, for $p \geq 1$ the nested problems made up of the equations (4.8)-(4.10) are ill-posed in $\mathbf{W}$ because it lacks a piece of information about the behavior of the *non-leading* terms towards the infinity. Actually, the terms $(\widehat{\mathbf{E}}_p, \widehat{\mathbf{H}}_p)$ for $p \geq 1$ can be described as the superposition of a regular solution $(\widehat{\mathbf{E}}_{p,0}, \widehat{\mathbf{H}}_{p,0})$ in $\mathbf{W}$ of the static Maxwell equations and a finite sum of growing vector fields which is a particular solution of the nested equations (4.8) satisfying

$$\max_{|\mathbf{X}|=\mathrm{R}} \left| \widehat{\mathbf{E}}_p(\mathbf{X}) - \widehat{\mathbf{E}}_{p,0}(\mathbf{X}) \right| = \underset{\mathrm{R}\to\infty}{O}(\mathrm{R}^{p-3})\,; \qquad \max_{|\mathbf{X}|=\mathrm{R}} \left| \widehat{\mathbf{H}}_p(\mathbf{X}) - \widehat{\mathbf{H}}_{p,0}(\mathbf{X}) \right| = \underset{\mathrm{R}\to\infty}{O}(\mathrm{R}^{p-3}). \tag{4.12}$$

These singularities also called *shadow* terms are produced by previous near-field terms. Then, the near-field problems can be solved by induction, where the computation of the shadows goes through previous terms and the computation of the leading term is done by solving a well-posed problem in $\mathbf{W}$.

Remark 18. The near-field expansion is defined in $\widehat{\Omega}$ but is a suitable approximation of the solution into the bounded domains $\Omega_\delta^{\mathrm{N}}$, see (4.3). The proof goes through error estimates. For the numerical results in Section 3.4, we have chosen $\eta_\delta^{\mathrm{N}} = 2(\delta\lambda)^{\frac{1}{2}}$.

4.4 Matching conditions

The far-field and near-field expansions are related thanks to a matching procedure which requires the behavior of $(\widetilde{\mathbf{E}}_p, \widetilde{\mathbf{H}}_p)$ close to the origin and the behavior of $(\widehat{\mathbf{E}}_p, \widehat{\mathbf{H}}_p)$ towards the infinity. In a formal way, for $p \geq 0$ we develop $(\widetilde{\mathbf{E}}_p, \widetilde{\mathbf{H}}_p)$ in a neighborhood of the origin as

$$\widetilde{\mathbf{E}}_p(r\widehat{x}) \underset{r\to 0}{\sim} \sum_{q=-\infty}^{+\infty} (\kappa r)^q \widetilde{\mathbf{E}}_p^q(\widehat{x}) \,, \qquad \widetilde{\mathbf{H}}_p(r\widehat{x}) \underset{r\to 0}{\sim} \sum_{q=-\infty}^{+\infty} (\kappa r)^q \widetilde{\mathbf{H}}_p^q(\widehat{x}), \tag{4.13}$$

and $(\widehat{\mathbf{E}}_p, \widehat{\mathbf{H}}_p)$ with fast variable $\mathrm{R} = \frac{r}{\delta}$ in a neighborhood of infinity as

$$\widehat{\mathbf{E}}_p(\mathrm{R}\widehat{x}) \underset{\mathrm{R}\to+\infty}{\sim} \sum_{q=-\infty}^{+\infty} (\kappa \mathrm{R})^q \widehat{\mathbf{E}}_p^q(\widehat{x}) \,, \qquad \widehat{\mathbf{H}}_p(\mathrm{R}\widehat{x}) \underset{\mathrm{R}\to+\infty}{\sim} \sum_{q=-\infty}^{+\infty} (\kappa \mathrm{R})^q \widehat{\mathbf{H}}_p^q(\widehat{x}). \tag{4.14}$$

The expansions (4.5) and (4.7) are matched in the overlapping area by using the expansions (4.13)- (4.14) and identifying the terms with respect to the δ-powers. Then, the matching conditions read as

$$\begin{cases} (\widetilde{\mathbf{E}}_p^q, \widetilde{\mathbf{H}}_p^q) = (\widehat{\mathbf{E}}_{p+q}^q, \widehat{\mathbf{H}}_{p+q}^q) & -p \leq q < 0, \\ (\widetilde{\mathbf{E}}_p^q, \widetilde{\mathbf{H}}_p^q) = 0 & p \leq 0 \text{ or } q < -p, \end{cases} \tag{4.15}$$

and

$$\begin{cases} (\widehat{\mathbf{E}}_p^q, \widehat{\mathbf{H}}_p^q) = (\widetilde{\mathbf{E}}_{p-q}^q, \widetilde{\mathbf{H}}_{p-q}^q) & 0 \leq q \leq p, \\ (\widehat{\mathbf{E}}_p^q, \widehat{\mathbf{H}}_p^q) = 0 & p < 0 \text{ or } q > p, \end{cases} \tag{4.16}$$

The conditions (4.15) allow to determine entirely the successive far-field terms while the conditions (4.16) are redundant regarding (C.15). This step is formally expressed but fundamental to the justification of the approximate models. Modal decomposition of the solutions allow to define the angular terms $(\widetilde{\mathbf{E}}_p^q, \widetilde{\mathbf{H}}_p^q)$ and $(\widehat{\mathbf{E}}_p^q, \widehat{\mathbf{H}}_p^q)$ and make explicit these conditions through the spectral coefficients.

Proposition 1. *The formal matching conditions* (4.15) *are equivalent to*

$$\begin{cases} u_{n,m}^{(p),\times} = \dfrac{\kappa^{n+2}}{i\, n\, \mathfrak{h}_{n,-n-1}} \widehat{h}_{n,m}^{(p-n-2)}, \\ u_{n,m}^{(p),t} = \dfrac{\kappa^{n+2}}{i\, n\, \mathfrak{h}_{n,-n-1}} \widehat{e}_{n,m}^{(p-n-2)}, \end{cases} \tag{4.17}$$

for any $p \geq 0$, $n \geq 1$ and $-n \leq m \leq n$. The coefficients $u_{n,m}^{(p),\times}$ and $u_{n,m}^{(p),t}$ are given by (C.5) *with $\boldsymbol{u} = \widetilde{\boldsymbol{E}}_p$. The coefficients $\widehat{e}_{n,m}^{(p-n-2)}$ and $\widehat{h}_{n,m}^{(p-n-2)}$ are given by* (C.9)-(C.10) *at the rank $p-n-2$. The coefficients $\mathfrak{h}_{n,\ell}$ come from the Laurent series expansion of the Hankel function of the first kind $h_n^{(1)}$, see Proposition 3 in Appendix* (C.1).

Remark 19. The coefficients $u_{n,m}^{(p),\times}$ and $u_{n,m}^{(p),\mathrm{t}}$ are equal to 0 when $p<3$. That implies that the asymptotic far-field expansion is starting at the third order.

Proof. Inserting Laurent series expansions (C.7) of the modal coefficients $\widetilde{\diamond}_{n,m}^{(p),\times}$, $\widetilde{\diamond}_{n,m}^{(p),\mathrm{t}}$ and $\widetilde{\diamond}_{n,m}^{(p),\mathrm{r}}$ for $\diamond=e$ or h into the modal decomposition (C.6), we obtain (4.13) with

$$\widetilde{\mathbf{E}}_p^q=\sum_{n=1}^{\infty}\sum_{m=-n}^{n} u_{n,m}^{\times}\mathfrak{h}_{n,q}\mathbf{curl}_{\mathbb{S}^2}Y_{n,m}+u_{n,m}^{\mathrm{t}}\frac{\mathfrak{h}_{n,q+1}}{i}\Big[(q+2)\nabla_{\mathbb{S}^2}Y_{n,m}+n(n+1)Y_{n,m}\mathbf{e}_r\Big],$$
$$\widetilde{\mathbf{H}}_p^q=\sum_{n=1}^{\infty}\sum_{m=-n}^{n} -u_{n,m}^{\mathrm{t}}\mathfrak{h}_{n,q}\mathbf{curl}_{\mathbb{S}^2}Y_{n,m}+u_{n,m}^{\times}\frac{\mathfrak{h}_{n,q+1}}{i}\Big[(q+2)\nabla_{\mathbb{S}^2}Y_{n,m}+n(n+1)Y_{n,m}\mathbf{e}_r\Big].$$

On the other hand, inserting the coefficients $\widehat{\diamond}_{n,m}^{(p),\times}$, $\widehat{\diamond}_{n,m}^{(p),\mathrm{t}}$ and $\widehat{\diamond}_{n,m}^{(p),\mathrm{r}}$ for $\diamond=e$ or h into the modal decompositions of $(\widehat{\mathbf{E}}_p,\widehat{\mathbf{H}}_p)$, see Proposition 4 in Section C.3.2, and making the index change $q=\ell-n-2$, we obtain (4.14) with

$$\widehat{\mathbf{E}}_p^q=\sum_{n=1}^{\infty}\sum_{m=-n}^{n}\Big(-i\kappa^{n+2}\frac{1}{n\,\mathfrak{h}_{n,-n-1}}\widehat{h}_{n,m}^{(p-q-n-2)}\Big)\mathfrak{h}_{n,q}\mathbf{curl}_{\mathbb{S}^2}Y_{n,m}$$
$$+\Big(-i\kappa^{n+2}\frac{1}{n\,\mathfrak{h}_{n,-n-1}}\widehat{e}_{n,m}^{(p-q-n-2)}\Big)\frac{\mathfrak{h}_{n,q+1}}{i}\Big[(q+2)\nabla_{\mathbb{S}^2}Y_{n,m}+n(n+1)Y_{n,m}\mathbf{e}_r\Big],$$
$$\widehat{\mathbf{H}}_p^q=\sum_{n=1}^{\infty}\sum_{m=-n}^{n}\Big(i\kappa^{n+2}\frac{1}{n\,\mathfrak{h}_{n,-n-1}}\widehat{h}_{n,m}^{(p-q-n-2)}\Big)\mathfrak{h}_{n,q}\mathbf{curl}_{\mathbb{S}^2}Y_{n,m}$$
$$+\Big(-i\kappa^{n+2}\frac{1}{n\,\mathfrak{h}_{n,-n-1}}\widehat{h}_{n,m}^{(p-q-n-2)}\Big)\frac{\mathfrak{h}_{n,q+1}}{i}\Big[(q+2)\nabla_{\mathbb{S}^2}Y_{n,m}+n(n+1)Y_{n,m}\mathbf{e}_r\Big].$$

Finally, according to the matching conditions (4.15), we deduce (4.17). □

Remark 20. The conditions (4.17) give us some pieces of information about the asymptotic expansions. Since we have assumed that the near-field expansion starts at the zeroth order, the coefficients $\widehat{e}_{n,m}^{(p)}$ and $\widehat{h}_{n,m}^{(p)}$ associated to an order $p<0$ are equal to zero. In particular, conditions (4.17) imply that the coefficients $u_{n,m}^{(p),\times}$ and $u_{n,m}^{(p),\mathrm{t}}$ are equal to zero when $n>p-2$. Then, the modal decomposition (C.6) for the far-field terms of order $p\geq 3$ is a finite sum of multipoles which needs the knowledge of the near-field terms of order p' such that $0\leq p'\leq p-3$ to be calculated.

4.5 First terms of the asymptotics

In this section, we introduce the problems satisfied by the first terms of the asymptotics and we make it explicit. We recall that the near-field problems are solved by induction because the calculation of the near-field term of order p requires the knowledge of the previous near-field terms. In Figure 14, we illustrate the construction of the first near-field terms, where the arrows describe the different contributions in order to compute the current term.

We can observe that the construction of the near-field terms does not depend on the far-field terms. The far-field terms are found through their modal decomposition given by (C.6) where the series are actually finite sums going up to $n=p-2$. In Figure 15, we illustrate the algorithm to construct the far-field terms.

Hereafter, we make explicit the near-field terms $(\widehat{\mathbf{E}}_p,\widehat{\mathbf{H}}_p)$ for $p=0,1,2$ and the far-field terms $(\widetilde{\mathbf{E}}_p,\widetilde{\mathbf{H}}_p)$ for $p=3,4,5$.

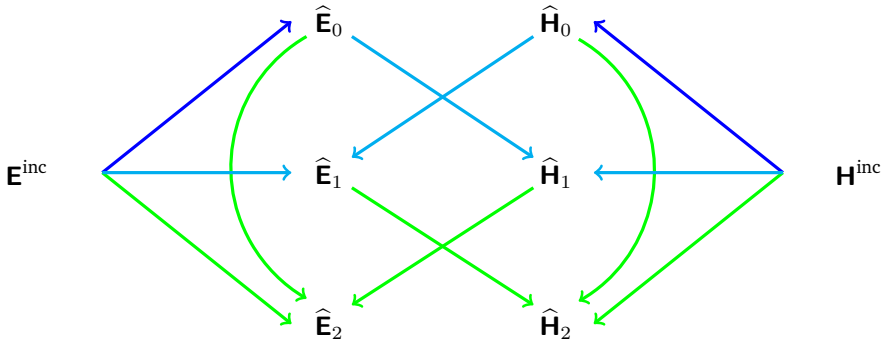

Figure 14: Construction of the near-field asymptotics (— Step 1, — Step 2, — Step 3)

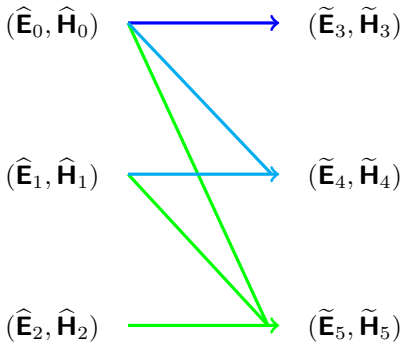

Figure 15: Construction of the far-field expansion (— Step 1, — Step 2, — Step 3)

4.5.1 Near-field terms

Zeroth order terms. The zeroth-order near-field terms $\widehat{\mathbf{E}}_0$ and $\widehat{\mathbf{H}}_0$ are solutions of the static Maxwell problems,

$$\begin{cases} \mathbf{curl}\, \widehat{\mathbf{E}}_0 = 0 & \text{in } \widehat{\Omega}, \\ \operatorname{div} \widehat{\mathbf{E}}_0 = 0 & \text{in } \widehat{\Omega}, \\ \mathbf{e}_r \times \widehat{\mathbf{E}}_0 = -\mathbf{e}_r \times \mathbf{E}^{\text{inc}}(0) & \text{on } \widehat{\Gamma}, \end{cases} \tag{4.18}$$

and

$$\begin{cases} \mathbf{curl}\, \widehat{\mathbf{H}}_0 = 0 & \text{in } \widehat{\Omega}, \\ \operatorname{div} \widehat{\mathbf{H}}_0 = 0 & \text{in } \widehat{\Omega}, \\ \mathbf{e}_r \cdot \widehat{\mathbf{H}}_0 = -\mathbf{e}_r \cdot \mathbf{H}^{\text{inc}}(0) & \text{on } \widehat{\Gamma}. \end{cases} \tag{4.19}$$

These problems are obtained by taking $p = 0$ into Equations (4.8), (4.9) and (4.10). The unique solution of (4.18), respectively of (4.19), in $\mathbf{W}$ see (4.11), is defined for $\mathbf{X} \in \widehat{\Omega}$, by

$$\widehat{\mathbf{E}}_0(\mathbf{X}) = \frac{1}{\mathrm{R}^3}\Big[3(\mathbf{E}^{\text{inc}}(0)\cdot\mathbf{e}_r)\mathbf{e}_r - \mathbf{E}^{\text{inc}}(0)\Big], \quad \widehat{\mathbf{H}}_0(\mathbf{X}) = -\frac{1}{2\mathrm{R}^3}\Big[3(\mathbf{H}^{\text{inc}}(0)\cdot\mathbf{e}_r)\mathbf{e}_r - \mathbf{H}^{\text{inc}}(0)\Big]. \tag{4.20}$$

First order terms. The first-order near-field terms $\widehat{\mathbf{E}}_1$ and $\widehat{\mathbf{H}}_1$ are solutions of the nested Maxwell problems

$$\begin{cases} \mathbf{curl}\,\widehat{\mathbf{E}}_1 = i\kappa\widehat{\mathbf{H}}_0 & \text{in } \widehat{\Omega}, \\ \operatorname{div}\widehat{\mathbf{E}}_1 = 0 & \text{in } \widehat{\Omega}, \\ \mathbf{e}_r \times \widehat{\mathbf{E}}_1 = -\mathbf{e}_r \times \Big(\mathbb{J}_{\mathbf{E}^{\rm inc}}(0)\mathbf{e}_r\Big) & \text{on } \widehat{\Gamma}, \end{cases} \tag{4.21}$$

and

$$\begin{cases} \mathbf{curl}\,\widehat{\mathbf{H}}_1 = -i\kappa\widehat{\mathbf{E}}_0 & \text{in } \widehat{\Omega}, \\ \operatorname{div}\widehat{\mathbf{H}}_1 = 0 & \text{in } \widehat{\Omega}, \\ \mathbf{e}_r \cdot \widehat{\mathbf{H}}_1 = -\mathbf{e}_r \cdot \Big(\mathbb{J}_{\mathbf{H}^{\rm inc}}(0)\mathbf{e}_r\Big) & \text{on } \widehat{\Gamma}. \end{cases} \tag{4.22}$$

These problems are obtained by taking $p = 1$ into Equations (4.8), (4.9) and (4.10). Let us decompose the vector fields $\widehat{\mathbf{E}}_1$ and $\widehat{\mathbf{H}}_1$ under the form

$$\widehat{\mathbf{E}}_1 = \widehat{\mathbf{E}}_{1,0} + \widehat{\mathbf{E}}_{1,1} \qquad \text{and} \qquad \widehat{\mathbf{H}}_1 = \widehat{\mathbf{H}}_{1,0} + \widehat{\mathbf{H}}_{1,1},$$

where $\widehat{\mathbf{E}}_{1,1}$ and $\widehat{\mathbf{H}}_{1,1}$ are particular solutions of the respective nested volumical equations

$$\begin{cases} \mathbf{curl}\,\widehat{\mathbf{E}}_{1,1} = i\kappa\widehat{\mathbf{H}}_0 & \text{in } \widehat{\Omega}, \\ \operatorname{div}\widehat{\mathbf{E}}_{1,1} = 0 & \text{in } \widehat{\Omega}, \end{cases} \qquad \begin{cases} \mathbf{curl}\,\widehat{\mathbf{H}}_{1,1} = -i\kappa\widehat{\mathbf{E}}_0 & \text{in } \widehat{\Omega}, \\ \operatorname{div}\widehat{\mathbf{H}}_{1,1} = 0 & \text{in } \widehat{\Omega}, \end{cases} \tag{4.23}$$

and $\widehat{\mathbf{E}}_{1,0} \in \mathbf{W}$ and $\widehat{\mathbf{H}}_{1,0} \in \mathbf{W}$ satisfy the static Maxwell equations in $\mathbf{W}$ with homogeneous volumical source term

$$\begin{cases} \mathbf{curl}\,\mathbf{u} = 0 & \text{in } \widehat{\Omega}, \\ \operatorname{div}\mathbf{u} = 0 & \text{in } \widehat{\Omega}. \end{cases} \tag{4.24}$$

The boundary conditions satisfied by the leading terms $\widehat{\mathbf{E}}_{1,0}$ and $\widehat{\mathbf{H}}_{1,0}$ are determined by the expression of $\widehat{\mathbf{E}}_{1,1}$ and $\widehat{\mathbf{H}}_{1,1}$. As a result,

$$\begin{cases} \mathbf{e}_r \times \widehat{\mathbf{E}}_{1,0} = -\mathbf{e}_r \times (\mathbb{J}_{\mathbf{E}^{\rm inc}}(0)\mathbf{e}_r) - \mathbf{e}_r \times \widehat{\mathbf{E}}_{1,1} & \text{on } \widehat{\Gamma}, \\ \mathbf{e}_r \cdot \widehat{\mathbf{H}}_{1,0} = -\mathbf{e}_r \cdot (\mathbb{J}_{\mathbf{H}^{\rm inc}}(0)\mathbf{e}_r) - \mathbf{e}_r \cdot \widehat{\mathbf{H}}_{1,1} & \text{on } \widehat{\Gamma}. \end{cases} \tag{4.25}$$

A particular couple of solutions of nested problems (4.23) is given by the modal decompositions (C.19) which require the knowledge of the tangential traces on $\widehat{\Gamma}$ of the zeroth-order near-field terms. On one hand, according to (C.17), we have

$$\gamma_t\widehat{\mathbf{E}}_0 = \sum_{m=-1}^{1} \widehat{e}^{(0)}_{1,m}\nabla_{\mathbb{S}^2}Y_{1,m} \qquad \text{and} \qquad \gamma_t\widehat{\mathbf{H}}_0 = \sum_{m=-1}^{1} \widehat{h}^{(0)}_{1,m}\nabla_{\mathbb{S}^2}Y_{1,m} \qquad \text{on } \widehat{\Gamma}. \tag{4.26}$$

On the other hand, according to (4.20), the tangential traces of $\widehat{\mathbf{E}}_0$ and $\widehat{\mathbf{H}}_0$ on $\widehat{\Gamma}$ are given by

$$\gamma_t\widehat{\mathbf{E}}_0 = -\gamma_t\mathbf{E}^{\rm inc}(0) \qquad \text{and} \qquad \gamma_t\widehat{\mathbf{H}}_0 = \frac{1}{2}\gamma_t\mathbf{H}^{\rm inc}(0) \qquad \text{on } \widehat{\Gamma}. \tag{4.27}$$

Hence, using that $\mathbf{curl}_{\mathbb{S}^2} = \nabla_{\mathbb{S}^2} \times \mathbf{e}_r$, we get from (C.19),

$$\widehat{\mathbf{E}}_{1,1}(\mathbf{X}) = -\frac{i\kappa}{2\mathrm{R}^2}\gamma_t\mathbf{H}^{\rm inc}(0) \times \mathbf{e}_r, \qquad \widehat{\mathbf{H}}_{1,1}(\mathbf{X}) = -\frac{i\kappa}{\mathrm{R}^2}\gamma_t\mathbf{E}^{\rm inc}(0) \times \mathbf{e}_r, \qquad \mathbf{X} \in \widehat{\Omega}.$$

Consequently, the boundary conditions (4.25) are uniquely determined thanks to the relation

$$\begin{cases} -\,\mathbf{e}_r \times \widehat{\mathbf{E}}_{1,1} = \dfrac{i\kappa}{2}\gamma_t \mathbf{H}^{\text{inc}}(0) & \text{on } \widehat{\Gamma}, \\ -\,\mathbf{e}_r \cdot \widehat{\mathbf{H}}_{1,1} = 0 & \text{on } \widehat{\Gamma}. \end{cases}$$

Remark 21. Noting that

$$\frac{i\kappa}{2}\mathbf{H}^{\text{inc}}(0) \times \mathbf{e}_r = \frac{1}{2}\left((\mathbb{J}_{\mathbf{E}^{\text{inc}}}(0)\mathbf{e}_r - (\mathbb{J}_{\mathbf{E}^{\text{inc}}}(0)\mathbf{e}_r)^\top\right) \qquad \text{on } \widehat{\Gamma},$$

the boundary conditions (4.25) can be put under the form

$$\begin{cases} \mathbf{e}_r \times \widehat{\mathbf{E}}_{1,0} = -\mathbf{e}_r \times \left(\mathbb{J}^{\text{sym}}_{\mathbf{E}^{\text{inc}}}(0)\mathbf{e}_r\right) & \text{on } \widehat{\Gamma}, \\ \mathbf{e}_r \cdot \widehat{\mathbf{H}}_{1,0} = -\mathbf{e}_r \cdot \left(\mathbb{J}_{\mathbf{H}^{\text{inc}}}(0)\mathbf{e}_r\right) & \text{on } \widehat{\Gamma}, \end{cases} \tag{4.28}$$

where $\mathbb{J}^{\text{sym}} = \frac{1}{2}(\mathbb{J} + \mathbb{J}^\top)$ denotes the symmetric part of the Jacobian operator.

The unique solutions in $\mathbf{W}$ of problems made up of static Maxwell equations (4.24) equipped with the respective boundary conditions (4.28) are

$$\begin{aligned} \widehat{\mathbf{E}}_{1,0}(\mathbf{X}) &= \frac{1}{\mathrm{R}^4}\left[-\gamma_t\left(\mathbb{J}^{\text{sym}}_{\mathbf{E}^{\text{inc}}}(0)\mathbf{e}_r\right) + \frac{3}{2}\gamma_n\left(\mathbb{J}_{\mathbf{E}^{\text{inc}}}(0)\mathbf{e}_r\right)\mathbf{e}_r\right], && \mathbf{X} \in \widehat{\Omega}, \\ \widehat{\mathbf{H}}_{1,0}(\mathbf{X}) &= \frac{1}{\mathrm{R}^4}\left[\frac{2}{3}\gamma_t\left(\mathbb{J}^{\text{sym}}_{\mathbf{H}^{\text{inc}}}(0)\mathbf{e}_r\right) - \gamma_n\left(\mathbb{J}_{\mathbf{H}^{\text{inc}}}(0)\mathbf{e}_r\right)\mathbf{e}_r\right], && \mathbf{X} \in \widehat{\Omega}. \end{aligned}$$

Second order terms. The second-order near-field terms $\widehat{\mathbf{E}}_2$ and $\widehat{\mathbf{H}}_2$ are solutions of the nested Maxwell problems

$$\begin{cases} \mathbf{curl}\,\widehat{\mathbf{E}}_2 = i\kappa\widehat{\mathbf{H}}_1 & \text{in } \widehat{\Omega}, \\ \operatorname{div}\widehat{\mathbf{E}}_2 = 0 & \text{in } \widehat{\Omega}, \\ \mathbf{e}_r \times \widehat{\mathbf{E}}_2 = -\dfrac{1}{2}\mathbf{e}_r \times \left(\mathbf{e}_r^\top \mathbb{H}_{\mathbf{E}^{\text{inc}}}(0)\mathbf{e}_r\right) & \text{on } \widehat{\Gamma}, \end{cases} \tag{4.29}$$

and

$$\begin{cases} \mathbf{curl}\,\widehat{\mathbf{H}}_2 = -i\kappa\widehat{\mathbf{E}}_1 & \text{in } \widehat{\Omega}, \\ \operatorname{div}\widehat{\mathbf{H}}_2 = 0 & \text{in } \widehat{\Omega}, \\ \mathbf{e}_r \cdot \widehat{\mathbf{H}}_2 = -\dfrac{1}{2}\mathbf{e}_r \cdot \left(\mathbf{e}_r^\top \mathbb{H}_{\mathbf{H}^{\text{inc}}}(0)\mathbf{e}_r\right) & \text{on } \widehat{\Gamma}. \end{cases} \tag{4.30}$$

These problems are obtained by taking $p = 2$ into Equations (4.8), (4.9) and (4.10). Let us decompose the vector fields $\widehat{\mathbf{E}}_2$ and $\widehat{\mathbf{H}}_2$ under the form

$$\widehat{\mathbf{E}}_2 = \widehat{\mathbf{E}}_{2,0} + \widehat{\mathbf{E}}_{2,1} + \widehat{\mathbf{E}}_{2,2} \qquad \text{and} \qquad \widehat{\mathbf{H}}_2 = \widehat{\mathbf{H}}_{2,0} + \widehat{\mathbf{H}}_{2,1} + \widehat{\mathbf{H}}_{2,2},$$

where $\widehat{\mathbf{E}}_{2,\ell}$ and $\widehat{\mathbf{H}}_{2,\ell}$ for $\ell = 1, 2$, are particular solutions of the respective nested volumical equations, see (C.16),

$$\begin{cases} \mathbf{curl}\,\widehat{\mathbf{E}}_{2,\ell} = i\kappa\widehat{\mathbf{H}}_{1,\ell-1} & \text{in } \widehat{\Omega}, \\ \operatorname{div}\widehat{\mathbf{E}}_{2,\ell} = 0 & \text{in } \widehat{\Omega}, \end{cases} \qquad \begin{cases} \mathbf{curl}\,\widehat{\mathbf{H}}_{2,\ell} = -i\kappa\widehat{\mathbf{E}}_{1,\ell-1} & \text{in } \widehat{\Omega}, \\ \operatorname{div}\widehat{\mathbf{H}}_{2,\ell} = 0 & \text{in } \widehat{\Omega}, \end{cases} \tag{4.31}$$

and $\widehat{\mathbf{E}}_{2,0} \in \mathbf{W}$ and $\widehat{\mathbf{H}}_{2,0} \in \mathbf{W}$ satisfy the static Maxwell equations (4.24) in $\mathbf{W}$. The boundary conditions satisfied by the leading terms $\widehat{\mathbf{E}}_{2,0}$ and $\widehat{\mathbf{H}}_{2,0}$ result from the derivation of the shadow terms $\widehat{\mathbf{E}}_{2,\ell}$ and $\widehat{\mathbf{H}}_{2,\ell}$ with $\ell = 1, 2$. Indeed,

$$\begin{cases} \mathbf{e}_r \times \widehat{\mathbf{E}}_{2,0} = -\dfrac{1}{2}\mathbf{e}_r \times \big(\mathbf{e}_r^\top \mathbb{H}_{\mathbf{E}^{\rm inc}}(0)\mathbf{e}_r\big) - \mathbf{e}_r \times \Big(\widehat{\mathbf{E}}_{2,1} + \widehat{\mathbf{E}}_{2,2}\Big) & \text{on } \widehat{\Gamma}, \\ \mathbf{e}_r \cdot \widehat{\mathbf{H}}_{2,0} = -\dfrac{1}{2}\mathbf{e}_r \cdot \big(\mathbf{e}_r^\top \mathbb{H}_{\mathbf{H}^{\rm inc}}(0)\mathbf{e}_r\big) - \mathbf{e}_r \cdot \Big(\widehat{\mathbf{H}}_{2,1} + \widehat{\mathbf{H}}_{2,2}\Big) & \text{on } \widehat{\Gamma}. \end{cases} \tag{4.32}$$

A particular couple of solutions of nested problems (4.31) for $\ell = 1, 2$ is given by the modal decompositions (C.14) with $p = 2$ and $\ell = 1, 2$. This calculation requires the knowledge of the tangential traces on $\widehat{\Gamma}$ of $\widehat{\mathbf{E}}_{1,0}$ and $\widehat{\mathbf{H}}_{1,0}$ for $\ell = 1$ and the normal traces on $\widehat{\Gamma}$ of $\widehat{\mathbf{E}}_0$ and $\widehat{\mathbf{H}}_0$ for $\ell = 2$.

- $\ell = 2$. On one hand, according to (C.17), we have

$$\gamma_n \widehat{\mathbf{E}}_0 = \sum_{m=-1}^{1} \widehat{e}_{1,m}^{(0)} Y_{1,m} \qquad \text{and} \qquad \gamma_n \widehat{\mathbf{H}}_0 = \sum_{m=-1}^{1} \widehat{h}_{1,m}^{(0)} Y_{1,m} \qquad \text{on } \widehat{\Gamma}. \tag{4.33}$$

On the other hand, according to (2.8),the normal traces of $\widehat{\mathbf{E}}_0$ and $\widehat{\mathbf{H}}_0$ on $\widehat{\Gamma}$ are given by

$$\gamma_n \widehat{\mathbf{E}}_0 = 2\gamma_n \mathbf{E}^{\rm inc}(0) \qquad \text{and} \qquad \gamma_n \widehat{\mathbf{H}}_0 = -\gamma_n \mathbf{H}^{\rm inc}(0) \qquad \text{on } \widehat{\Gamma}. \tag{4.34}$$

By using the relations (4.26) and (4.33)-(4.34), we get from (C.14) for $p = \ell = 2$,

$$\begin{aligned} \widehat{\mathbf{E}}_{2,2}(\mathbf{X}) &= \frac{\kappa^2}{2\mathrm{R}}\bigg[\gamma_t \mathbf{E}^{\rm inc}(0) + 2\Big(\gamma_n \mathbf{E}^{\rm inc}(0)\Big)\mathbf{e}_r\bigg], && \mathbf{X} \in \widehat{\Omega}, \\ \widehat{\mathbf{H}}_{2,2}(\mathbf{x}) &= -\frac{\kappa^2}{2\mathrm{R}}\bigg[\frac{1}{2}\gamma_t \mathbf{H}^{\rm inc}(0) + \Big(\gamma_n \mathbf{H}^{\rm inc}(0)\Big)\mathbf{e}_r\bigg], && \mathbf{X} \in \widehat{\Omega}. \end{aligned}$$

- $\ell = 1$. On one hand, according to (C.18), we have

$$\gamma_t \widehat{\mathbf{E}}_{1,0} = \sum_{m=-2}^{2} \widehat{e}_{2,m}^{(1)} \nabla_{\mathbb{S}^2} Y_{2,m} \qquad \text{and} \qquad \gamma_t \widehat{\mathbf{H}}_{1,0} = \sum_{m=-2}^{2} \widehat{h}_{2,m}^{(1)} \nabla_{\mathbb{S}^2} Y_{2,m} \qquad \text{on } \widehat{\Gamma}. \tag{4.35}$$

On the other hand, according to , the tangential traces of $\widehat{\mathbf{E}}_{1,0}$ and $\widehat{\mathbf{H}}_{1,0}$ on $\widehat{\Gamma}$ are given by

$$\gamma_t \widehat{\mathbf{E}}_{1,0} = -\gamma_t\Big(\mathbb{J}^{\rm sym}_{\mathbf{E}^{\rm inc}}(0)\mathbf{e}_r\Big) \qquad \text{and} \qquad \gamma_t \widehat{\mathbf{H}}_{1,0} = \frac{2}{3}\gamma_t\Big(\mathbb{J}^{\rm sym}_{\mathbf{H}^{\rm inc}}(0)\mathbf{e}_r\Big) \qquad \text{on } \widehat{\Gamma}. \tag{4.36}$$

By using (4.35)-(4.36), we get from (C.14) for $p = 2$ and $\ell = 1$,

$$\widehat{\mathbf{E}}_{2,1}(\mathbf{X}) = -\frac{i\kappa}{3\mathrm{R}^3}\Big(\mathbb{J}^{\rm sym}_{\mathbf{H}^{\rm inc}}(0)\mathbf{e}_r\Big) \times \mathbf{e}_r, \qquad \widehat{\mathbf{H}}_{2,1}(\mathbf{X}) = -\frac{i\kappa}{2\mathrm{R}^3}\Big(\mathbb{J}^{\rm sym}_{\mathbf{E}^{\rm inc}}(0)\mathbf{e}_r\Big) \times \mathbf{e}_r, \qquad \mathbf{X} \in \widehat{\Omega}.$$

As a result, the boundary conditions (4.32) are uniquely determined by

$$\begin{cases} \mathbf{e}_r \times \widehat{\mathbf{E}}_{2,0} = -\dfrac{1}{2}\mathbf{e}_r \times \Big(\mathbf{e}_r^\top \mathbb{H}_{\mathbf{E}^{\rm inc}}(0)\mathbf{e}_r\Big) + \dfrac{i\kappa}{3}\gamma_t\Big(\mathbb{J}^{\rm sym}_{\mathbf{H}^{\rm inc}}(0)\mathbf{e}_r\Big) - \dfrac{\kappa^2}{2}\mathbf{e}_r \times \mathbf{E}^{\rm inc}(0) & \text{on } \widehat{\Gamma}, \\ \mathbf{e}_r \cdot \widehat{\mathbf{H}}_{2,0} = -\dfrac{1}{2}\mathbf{e}_r \cdot \Big(\mathbf{e}_r^\top \mathbb{H}_{\mathbf{H}^{\rm inc}}(0)\mathbf{e}_r\Big) + \dfrac{\kappa^2}{2}\mathbf{e}_r \cdot \mathbf{H}^{\rm inc}(0) & \text{on } \widehat{\Gamma}. \end{cases} \tag{4.37}$$

The unique solutions in $\mathbf{W}$ of problems made up of the static Maxwell equations (4.24) equipped with the respective boundary conditions (4.37) are

$$\widehat{\mathbf{E}}_{2,0}(\mathbf{X}) = \frac{1}{\mathrm{R}^5}\Bigg[-\frac{1}{2}\gamma_t\Big(\mathbf{e}_r^\top \mathbb{H}_{\mathbf{E}^{\mathrm{inc}}}(0)\mathbf{e}_r\Big) + \frac{i\kappa}{3}\Big(\mathbb{J}^{\mathrm{sym}}_{\mathbf{H}^{\mathrm{inc}}}(0)\mathbf{e}_r\Big)\times\mathbf{e}_r - \frac{\kappa^2}{5}\gamma_t\mathbf{E}^{\mathrm{inc}}(0) \\ - \frac{4}{3}\Bigg\{ -\frac{1}{2}\gamma_n\Big(\mathbf{e}_r^\top \mathbb{H}_{\mathbf{E}^{\mathrm{inc}}}(0)\mathbf{e}_r\Big) - \frac{\kappa^2}{10}\gamma_n\mathbf{E}^{\mathrm{inc}}(0)\Bigg\}\mathbf{e}_r\Bigg] + \frac{3\kappa^2}{10\mathrm{R}^3}\Bigg[3\Big(\gamma_n\mathbf{E}^{\mathrm{inc}}(0)\Big)\mathbf{e}_r - \mathbf{E}^{\mathrm{inc}}(0)\Bigg],$$

and

$$\widehat{\mathbf{H}}_{2,0}(\mathbf{X}) = \frac{1}{\mathrm{R}^5}\Bigg[-\frac{3}{4}\Bigg\{ -\frac{1}{2}\gamma_t\Big(\mathbf{e}_r^\top \mathbb{H}_{\mathbf{H}^{\mathrm{inc}}}(0)\mathbf{e}_r\Big) - \frac{i\kappa}{3}\Big(\mathbb{J}^{\mathrm{sym}}_{\mathbf{E}^{\mathrm{inc}}}(0)\mathbf{e}_r\Big)\times\mathbf{e}_r - \frac{\kappa^2}{5}\gamma_t\mathbf{H}^{\mathrm{inc}}(0)\Bigg\} \\ - \Bigg\{\frac{1}{2}\gamma_n\Big(\mathbf{e}_r^\top \mathbb{H}_{\mathbf{H}^{\mathrm{inc}}}(0)\mathbf{e}_r\Big) + \frac{\kappa^2}{10}\gamma_n\mathbf{H}^{\mathrm{inc}}(0)\Bigg\}\mathbf{e}_r\Bigg] + \frac{3\kappa^2}{10\mathrm{R}^3}\Bigg[3\Big(\gamma_n\mathbf{H}^{\mathrm{inc}}(0)\Big)\mathbf{e}_r - \mathbf{H}^{\mathrm{inc}}(0)\Bigg],$$

for $\mathbf{X}\in\widehat{\Omega}$.

4.5.2 Far-field terms

The third, fourth and fifth-order far-field terms are calculated thanks to their modal decomposition (C.6) where the series go up to $n = p-2$ and by applying the matching conditions (4.17) with $p = 3, 4, 5$. The third-order far-field terms $\widetilde{\mathbf{E}}_3$ and $\widetilde{\mathbf{H}}_3$ possess the following decomposition

$$\widetilde{\mathbf{E}}_3(\mathbf{x}) = \frac{\kappa^3}{i\mathfrak{h}_{1,-2}}h_1^{(1)}(\kappa r)\sum_{m=-1}^{1}\widehat{h}^{(0)}_{1,m}\mathbf{curl}_{\mathbb{S}^2}Y_{1,m} \\ -\frac{\kappa^2}{\mathfrak{h}_{1,-2}}\frac{h_1^{(1)}(\kappa r)+\kappa r h_1^{(1)'}(\kappa r)}{r}\sum_{m=-1}^{1}\widehat{e}^{(0)}_{1,m}\nabla_{\mathbb{S}^2}Y_{1,m} - \frac{2\kappa^2}{\mathfrak{h}_{1,-2}}\frac{h_1^{(1)}(\kappa r)}{r}\sum_{m=-1}^{1}\widehat{e}^{(0)}_{1,m}Y_{1,m}\mathbf{e}_r \tag{4.38}$$

and

$$\widetilde{\mathbf{H}}_3(\mathbf{x}) = -\frac{\kappa^3}{i\mathfrak{h}_{1,-2}}h_1^{(1)}(\kappa r)\sum_{m=-1}^{1}\widehat{e}^{(0)}_{1,m}\mathbf{curl}_{\mathbb{S}^2}Y_{1,m} \\ -\frac{\kappa^2}{\mathfrak{h}_{1,-2}}\frac{h_1^{(1)}(\kappa r)+\kappa r h_1^{(1)'}(\kappa r)}{r}\sum_{m=-1}^{1}\widehat{h}^{(0)}_{1,m}\nabla_{\mathbb{S}^2}Y_{1,m} - \frac{2\kappa^2}{\mathfrak{h}_{1,-2}}\frac{h_1^{(1)}(\kappa r)}{r}\sum_{m=-1}^{1}\widehat{h}^{(0)}_{1,m}Y_{1,m}\mathbf{e}_r. \tag{4.39}$$

This is a sum of electromagnetic dipoles. The expressions (2.4) and (2.5) are obtained by substituting the relations (4.26)- (4.27) and (4.33)-(4.34) into (4.38)-(4.39). The fourth-order

far-field terms $\widetilde{\mathbf{E}}_4$ and $\widetilde{\mathbf{H}}_4$ possess the following decomposition

$$\begin{aligned}\widetilde{\mathbf{E}}_4(\mathbf{x}) = &\frac{\kappa^4}{2i\,\mathfrak{h}_{2,-3}} h_2^{(1)}(\kappa r) \sum_{m=-2}^{2} \widehat{h}_{2,m}^{(0)} \mathbf{curl}_{\mathbb{S}^2} Y_{2,m} \\ &- \frac{\kappa^3}{2\mathfrak{h}_{2,-3}} \frac{h_2^{(1)}(\kappa r) + \kappa r h_2^{(1)'}(\kappa r)}{r} \sum_{m=-2}^{2} \widehat{e}_{2,m}^{(0)} \nabla_{\mathbb{S}^2} Y_{2,m} - \frac{3\kappa^3}{\mathfrak{h}_{2,-3}} \frac{h_2^{(1)}(\kappa r)}{r} \sum_{m=-2}^{2} \widehat{e}_{2,m}^{(0)} Y_{2,m} \mathbf{e}_r \\ &+ \frac{\kappa^3}{i\mathfrak{h}_{1,-2}} h_1^{(1)}(\kappa r) \sum_{m=-1}^{1} \widehat{h}_{1,m}^{(1)} \mathbf{curl}_{\mathbb{S}^2} Y_{1,m} - \frac{\kappa^2}{\mathfrak{h}_{1,-2}} \frac{h_1^{(1)}(\kappa r) + \kappa r h_1^{(1)'}(\kappa r)}{r} \sum_{m=-1}^{1} \widehat{e}_{1,m}^{(1)} \nabla_{\mathbb{S}^2} Y_{1,m} \\ &- \frac{2\kappa^2}{\mathfrak{h}_{1,-2}} \frac{h_1^{(1)}(\kappa r)}{r} \sum_{m=-1}^{1} \widehat{e}_{1,m}^{(1)} Y_{1,m} \mathbf{e}_r\end{aligned}$$

and

$$\begin{aligned}\widetilde{\mathbf{H}}_4(\mathbf{x}) = &-\frac{\kappa^4}{2i\mathfrak{h}_{2,-3}} h_2^{(1)}(\kappa r) \sum_{m=-2}^{2} \widehat{e}_{2,m}^{(0)} \mathbf{curl}_{\mathbb{S}^2} Y_{2,m} \\ &- \frac{\kappa^3}{2\mathfrak{h}_{2,-3}} \frac{h_2^{(1)}(\kappa r) + \kappa r h_2^{(1)'}(\kappa r)}{r} \sum_{m=-2}^{2} \widehat{h}_{2,m}^{(0)} \nabla_{\mathbb{S}^2} Y_{2,m} - \frac{3\kappa^3}{\mathfrak{h}_{2,-3}} \frac{h_2^{(1)}(\kappa r)}{r} \sum_{m=-2}^{2} \widehat{h}_{2,m}^{(0)} Y_{2,m} \mathbf{e}_r \\ &- \frac{\kappa^3}{i\,n\,\mathfrak{h}_{1,-2}} h_1^{(1)}(\kappa r) \sum_{m=-1}^{1} \widehat{e}_{1,m}^{(1)} \mathbf{curl}_{\mathbb{S}^2} Y_{1,m} - \frac{\kappa^2}{\mathfrak{h}_{1,-2}} \frac{h_1^{(1)}(\kappa r) + \kappa r h_1^{(1)'}(\kappa r)}{r} \sum_{m=-1}^{1} \widehat{h}_{1,m}^{(1)} \nabla_{\mathbb{S}^2} Y_{1,m} \\ &- \frac{2\kappa^2}{\mathfrak{h}_{1,-2}} \frac{h_1^{(1)}(\kappa r)}{r} \sum_{m=-1}^{1} \widehat{h}_{1,m}^{(1)} Y_{1,m} \mathbf{e}_r.\end{aligned}$$

but $\widehat{h}_{2,m}^{(0)} = \widehat{e}_{2,m}^{(0)} = \widehat{h}_{1,m}^{(1)} = \widehat{e}_{1,m}^{(1)} = 0$ for any $-n \leq m \leq n$ ($n = 1$ or $n = 2$) according to (C.17)-(C.18). Hence, we deduce that $\widetilde{\mathbf{E}}_4$ and $\widetilde{\mathbf{H}}_4$ are identically zero. The fifth-order far-field terms $\widetilde{\mathbf{E}}_5$ and $\widetilde{\mathbf{H}}_5$ possess the following decomposition

$$\begin{aligned}\widetilde{\mathbf{E}}_5(\mathbf{x}) = &\frac{\kappa^4}{2i\mathfrak{h}_{2,-3}} h_2^{(1)}(\kappa r) \sum_{m=-2}^{2} \widehat{h}_{2,m}^{(1)} \mathbf{curl}_{\mathbb{S}^2} Y_{2,m} \\ &+ \frac{\kappa^4}{2i\mathfrak{h}_{2,-3}} \frac{h_2^{(1)}(\kappa r) + \kappa r h_2^{(1)'}(\kappa r)}{i\kappa r} \sum_{m=-2}^{2} \widehat{e}_{2,m}^{(1)} \nabla_{\mathbb{S}^2} Y_{2,m} + \frac{3\kappa^4}{i\mathfrak{h}_{2,-3}} \frac{h_2^{(1)}(\kappa r)}{i\kappa r} \sum_{m=-2}^{2} \widehat{e}_{2,m}^{(1)} Y_{2,m} \mathbf{e}_r \\ &+ \frac{\kappa^3}{i\mathfrak{h}_{1,-2}} h_1^{(1)}(\kappa r) \sum_{m=-1}^{1} \widehat{h}_{1,m}^{(2)} \mathbf{curl}_{\mathbb{S}^2} Y_{1,m} + \frac{\kappa^3}{i\mathfrak{h}_{1,-2}} \frac{h_1^{(1)}(\kappa r) + \kappa r h_1^{(1)'}(\kappa r)}{i\kappa r} \sum_{m=-1}^{1} \widehat{e}_{1,m}^{(2)} \nabla_{\mathbb{S}^2} Y_{1,m} \\ &+ \frac{2\kappa^3}{i\mathfrak{h}_{1,-2}} \frac{h_1^{(1)}(\kappa r)}{i\kappa r} \sum_{m=-1}^{1} \widehat{e}_{1,m}^{(2)} Y_{1,m} \mathbf{e}_r \qquad (4.40)\end{aligned}$$

and

$$\widetilde{\mathbf{H}}_5(\mathbf{x}) = -\frac{\kappa^4}{2i\mathfrak{h}_{2,-3}} h_2^{(1)}(\kappa r) \sum_{m=-2}^{2} \widehat{e}_{2,m}^{(1)} \mathbf{curl}_{\mathbb{S}^2} Y_{2,m}$$
$$+ \frac{\kappa^4}{2i\mathfrak{h}_{2,-3}} \frac{h_2^{(1)}(\kappa r) + \kappa r h_2^{(1)'}(\kappa r)}{i\kappa r} \sum_{m=-2}^{2} \widehat{h}_{2,m}^{(1)} \nabla_{\mathbb{S}^2} Y_{2,m} + \frac{3\kappa^4}{i\mathfrak{h}_{2,-3}} \frac{h_2^{(1)}(\kappa r)}{i\kappa r} \sum_{m=-2}^{2} \widehat{h}_{2,m}^{(1)} Y_{2,m} \mathbf{e}_r$$
$$- \frac{\kappa^3}{i\mathfrak{h}_{1,-2}} h_1^{(1)}(\kappa r) \sum_{m=-1}^{1} \widehat{e}_{1,m}^{(2)} \mathbf{curl}_{\mathbb{S}^2} Y_{1,m} + \frac{\kappa^3}{i\mathfrak{h}_{1,-2}} \frac{h_1^{(1)}(\kappa r) + \kappa r h_1^{(1)'}(\kappa r)}{i\kappa r} \sum_{m=-1}^{1} \widehat{h}_{1,m}^{(2)} \nabla_{\mathbb{S}^2} Y_{1,m}$$
$$+ \frac{2\kappa^2}{i\mathfrak{h}_{1,-2}} \frac{h_1^{(1)}(\kappa r)}{i\kappa r} \sum_{m=-1}^{1} \widehat{h}_{1,m}^{(2)} Y_{1,m} \mathbf{e}_r. \quad (4.41)$$

That is a sum of electromagnetic dipoles and quadrupoles. The normal and tangential part of the electric and magnetic dipoles are given by

$$\sum_{m=-1}^{1} \widehat{e}_{1,m}^{(2)} \nabla_{\mathbb{S}^2} Y_{1,m} = -\frac{3\kappa^2}{10} \gamma_t\big(\mathbf{E}^{\text{inc}}(0)\big) ; \qquad \sum_{m=-1}^{1} \widehat{e}_{1,m}^{(2)} Y_{1,m} = -\frac{3\kappa^2}{10} \gamma_n\big(\mathbf{E}^{\text{inc}}(0)\big),$$
$$\sum_{m=-1}^{1} \widehat{h}_{1,m}^{(2)} \nabla_{\mathbb{S}^2} Y_{1,m} = -\frac{3\kappa^2}{10} \gamma_t\big(\mathbf{H}^{\text{inc}}(0)\big) ; \qquad \sum_{m=-1}^{1} \widehat{h}_{1,m}^{(2)} Y_{1,m} = -\frac{3\kappa^2}{10} \gamma_n\big(\mathbf{H}^{\text{inc}}(0)\big).$$

The normal and tangential part of the electric and magnetic quadrupoles are given by

$$\sum_{m=-2}^{2} \widehat{e}_{2,m}^{(1)} \nabla_{\mathbb{S}^2} Y_{2,m} = -\gamma_t\Big(\mathbb{J}^{\text{sym}}_{\mathbf{E}^{\text{inc}}}(0)\mathbf{e}_r\Big) ; \qquad \sum_{m=-2}^{2} \widehat{e}_{2,m}^{(1)} Y_{2,m} = -\frac{1}{2} \gamma_n\Big(\mathbb{J}_{\mathbf{E}^{\text{inc}}}(0)\mathbf{e}_r\Big),$$
$$\sum_{m=-2}^{2} \widehat{h}_{2,m}^{(1)} \nabla_{\mathbb{S}^2} Y_{2,m} = \frac{2}{3} \gamma_t\Big(\mathbb{J}^{\text{sym}}_{\mathbf{H}^{\text{inc}}}(0)\mathbf{e}_r\Big) ; \qquad \sum_{m=-2}^{2} \widehat{h}_{2,m}^{(1)} Y_{2,m} = \frac{1}{3} \gamma_n\Big(\mathbb{J}_{\mathbf{H}^{\text{inc}}}(0)\mathbf{e}_r\Big).$$

It suffices to substitute these expressions into (4.40)-(4.41) to obtain the result.

5 Conclusion and perspectives

In this report, we have applied the method of matched asymptotic expansions on the electromagnetic wave scattering problem by a small sphere. We have performed the near-field expansion up to the second order and the far-field expansion up to the fifth order. This work is essentially concerned with numerical objectives. The theoretical justification of the matched asymptotic expansions, in particular the proof of error estimates, will be tackled in a further work. In this conclusion, we introduce two different applications of the asymptotic expansions, in particular

- the derivation of collected dipolar models improving the third-order far-field approximation,
- the application of the Born theory for the extension to the multiple scattering, neglecting interactions between the obstacles.

We will end this section with on-going works and perspectives.

5.1 Collected models

The main interest of asymptotic analysis lies in describing the leading behavior of the solution when one of their parameters tends to zero or to infinity, here the size of the obstacle tending towards zero. For numerical analysis, information is exploitable if we can indeed calculate the leading term, hoping that the computation will be less expensive than the computation of the numerical solution. Besides, we observed that the more we increase orders of the approximations, the more we consume derivatives of the incident fields. But, for realistic applications, it is not always possible to have access to these derivatives. With this in mind, we are interested to collected models which consist in gathering the different terms, not with respect to the δ-powers, but, with respect to their nature in terms of multipoles. In particular, if we do not want to use derivatives of the incident fields, we consider only the dipolar terms stemed from the expansions. From a far-field point of view, the dipolar collected model reads as

$$\begin{aligned}\mathbf{E}_\delta^{\text{Col}} &= \Big[-\frac{(\kappa\delta)^3}{2} + \frac{3(\kappa\delta)^5}{10}\Big] h_1^{(1)}(\kappa r)\gamma_\times(\mathbf{H}^{\text{inc}}(0)) \\ &- \Big[(\kappa\delta)^3 + \frac{3(\kappa\delta)^5}{10}\Big]\frac{h_1^{(1)}(\kappa r) + \kappa r h_1^{(1)'}(\kappa r)}{i\kappa r}\gamma_t(\mathbf{E}^{\text{inc}}(0)) - 2\Big[(\kappa\delta)^3 + \frac{3(\kappa\delta)^5}{10}\Big]\frac{h_1^{(1)}(\kappa r)}{i\kappa r}\gamma_n(\mathbf{E}^{\text{inc}}(0))\mathbf{e}_r\end{aligned}$$

and

$$\begin{aligned}\mathbf{H}_\delta^{\text{Col}} &= -\Big[(\kappa\delta)^3 + \frac{3(\kappa\delta)^5}{10}\Big] h_1^{(1)}(\kappa r)\gamma_\times(\mathbf{E}^{\text{inc}}(0)) \\ &+ \Big[\frac{(\kappa\delta)^3}{2} - \frac{3(\kappa\delta)^5}{10}\Big]\frac{h_1^{(1)}(\kappa r) + \kappa r h_1^{(1)'}(\kappa r)}{i\kappa r}\gamma_t(\mathbf{H}^{\text{inc}}(0)) + 2\Big[\frac{(\kappa\delta)^3}{2} - \frac{3(\kappa\delta)^5}{10}\Big]\frac{h_1^{(1)}(\kappa r)}{i\kappa r}\gamma_n(\mathbf{H}^{\text{inc}}(0))\mathbf{e}_r,\end{aligned}$$

where $\gamma_\times$, γ_t and γ_n are defined by (2.3). This approximation improves the third-order far-field approximation $(\delta^3\widetilde{\mathbf{E}}_3, \delta^3\widetilde{\mathbf{H}}_3)$ and its computation time is unchanged because it is only amplitude of the dipole which have been changed. According to (B.8)-(B.9) and (B.13)-(B.14), the previous expressions can be written in the compact form

$$\begin{aligned}\mathbf{E}_\delta^{\text{Col}} &= \delta^3\Big\{\mathbf{E}_{\text{dip}}^{\text{elec}}\Big[4\pi(1 + \frac{3(\kappa\delta)^2}{10})\mathbf{E}^{\text{inc}}(0)\Big] + \mathbf{E}_{\text{dip}}^{\text{mag}}\Big[-2\pi(1 - \frac{3(\kappa\delta)^2}{5})\mathbf{H}^{\text{inc}}(0)\Big]\Big\}, \\ \mathbf{H}_\delta^{\text{Col}} &= \delta^3\Big\{\mathbf{H}_{\text{dip}}^{\text{elec}}\Big[4\pi(1 + \frac{3(\kappa\delta)^2}{10})\mathbf{E}^{\text{inc}}(0)\Big] + \mathbf{H}_{\text{dip}}^{\text{mag}}\Big[-2\pi(1 - \frac{3(\kappa\delta)^2}{5})\mathbf{H}^{\text{inc}}(0)\Big]\Big\}.\end{aligned}$$

In Figure 16, we illustrate the performance of the collected approximation $(\mathbf{E}_\delta^{\text{Col}}, \mathbf{H}_\delta^{\text{Col}})$ and we compare it with to the third-order far-field approximation $(\delta^3\widetilde{\mathbf{E}}_3, \delta^3\widetilde{\mathbf{H}}_3)$.

In pre-asymptotic regime, we can remark that the order of convergence for the collected approximation is close to six but the error does not decrease a lot in comparison with the third-order far-field approximation. Actually, in the fifth-order far-field term, the predominant term when δ is large enough is the dipolar term while the dominant term is the quadrupolar term when δ decreases. For the same computation cost, the error decreases with a factor approximately equal to 6.0.

5.2 Born approximation

The extension to the multiple scattering can be done directly thanks to the Born model. It consists in superposing the scattered fields generated by the K isolated obstacles centered in c_k,

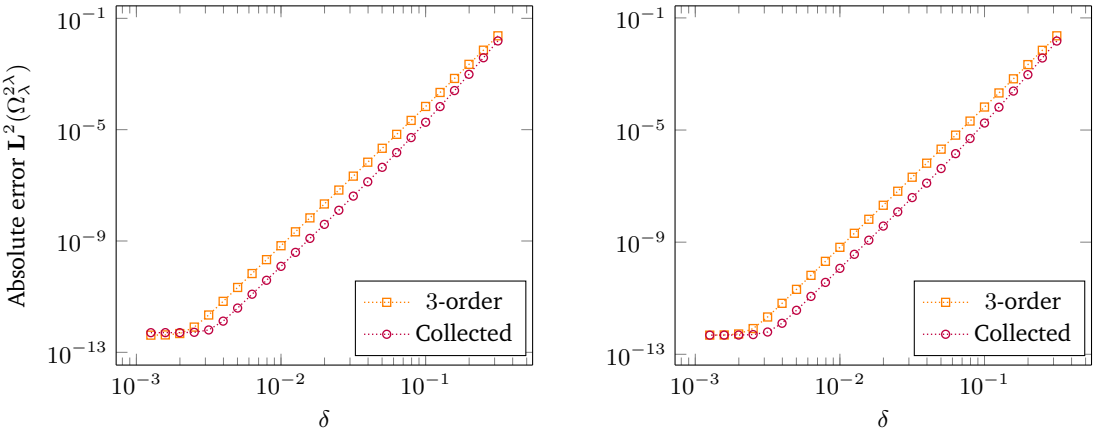

(a) Electric field (b) Magnetic field

Figure 16: Absolute $\mathbf{L}^2$-errors for far-field approximations of the electric and magnetic fields

$k = 1, \dots, K$. Interactions between obstacles are neglected. By considering this approximation, the third-order far-field terms are given by

$$\widetilde{\mathbf{E}}_3^{\text{Born}}(\mathbf{x}) = \kappa^3 \sum_{k=1}^{K} \Big\{ -\frac{1}{2} h_1^{(1)}(\kappa|\mathbf{x}-c_k|)\gamma_\times^{(k)} \mathbf{H}^{\text{inc}}(c_k)$$
$$- \frac{h_1^{(1)}(\kappa|\mathbf{x}-c_k|) + \kappa|\mathbf{x}-c_k| h_1^{(1)}(\kappa|\mathbf{x}-c_k|)}{i\kappa|\mathbf{x}-c_k|} \gamma_t^{(k)} \mathbf{E}^{\text{inc}}(c_k) - 2\frac{h_1^{(1)}(\kappa|\mathbf{x}-c_k|)}{i\kappa|\mathbf{x}-c_k|} \gamma_n^{(k)}(\mathbf{E}^{\text{inc}}(c_k))\mathbf{e}_r^{(k)} \Big\}$$

and

$$\widetilde{\mathbf{H}}_3^{\text{Born}}(\mathbf{x}) = \kappa^3 \sum_{k=1}^{K} \Big\{ -h_1^{(1)}(\kappa|\mathbf{x}-c_k|)\gamma_\times^{(k)} \mathbf{E}^{\text{inc}}(c_k)$$
$$+ \frac{1}{2} \frac{h_1^{(1)}(\kappa|\mathbf{x}-c_k|) + \kappa|\mathbf{x}-c_k| h_1^{(1)}(\kappa|\mathbf{x}-c_k|)}{i\kappa|\mathbf{x}-c_k|} \gamma_t^{(k)} \mathbf{H}^{\text{inc}}(c_k) + \frac{h_1^{(1)}(\kappa|\mathbf{x}-c_k|)}{i\kappa|\mathbf{x}-c_k|} \gamma_n^{(k)}(\mathbf{H}^{\text{inc}}(c_k))\mathbf{e}_r^{(k)} \Big\},$$

where $\mathbf{e}_r^{(k)}$ denotes the unit vector $\frac{\mathbf{x}-c_k}{|\mathbf{x}-c_k|}$ and the trace operators $\gamma_n^{(k)}$, $\gamma_\times^{(k)}$ and $\gamma_t^{(k)}$ are defined by (2.3) relatively to $\mathbf{e}_r^{(k)}$. It is also possible to mix the Born approximation with a collected approximation. In Figure 17, we illustrate the third-order Born approximation for $K = 13$ obstacles, where the physical parameters are given by (3.1) with $\lambda = 5$. We draw cross sections of the x and y-coordinates of the approximate electric field given by $\delta^3 \widetilde{\mathbf{E}}_3^{\text{Born}}$, in a logarithmic scale.

By virtue of (2.12), the previous expressions can be put into the compact form,

$$\widetilde{\mathbf{E}}_3^{\text{Born}}(\mathbf{x}) = \sum_{k=1}^{K} \mathbf{E}_{\text{dip}}^{\text{elec}}\big[4\pi\mathbf{E}^{\text{inc}}(c_k)\big](\mathbf{x}-c_k) + \mathbf{E}_{\text{dip}}^{\text{mag}}\big[-2\pi\mathbf{H}^{\text{inc}}(c_k)\big](\mathbf{x}-c_k),$$
$$\widetilde{\mathbf{H}}_3^{\text{Born}}(\mathbf{x}) = \sum_{k=1}^{K} \mathbf{H}_{\text{dip}}^{\text{elec}}\big[4\pi\mathbf{E}^{\text{inc}}(c_k)\big](\mathbf{x}-c_k) + \mathbf{H}_{\text{dip}}^{\text{mag}}\big[-2\pi\mathbf{H}^{\text{inc}}(c_k)\big](\mathbf{x}-c_k).$$

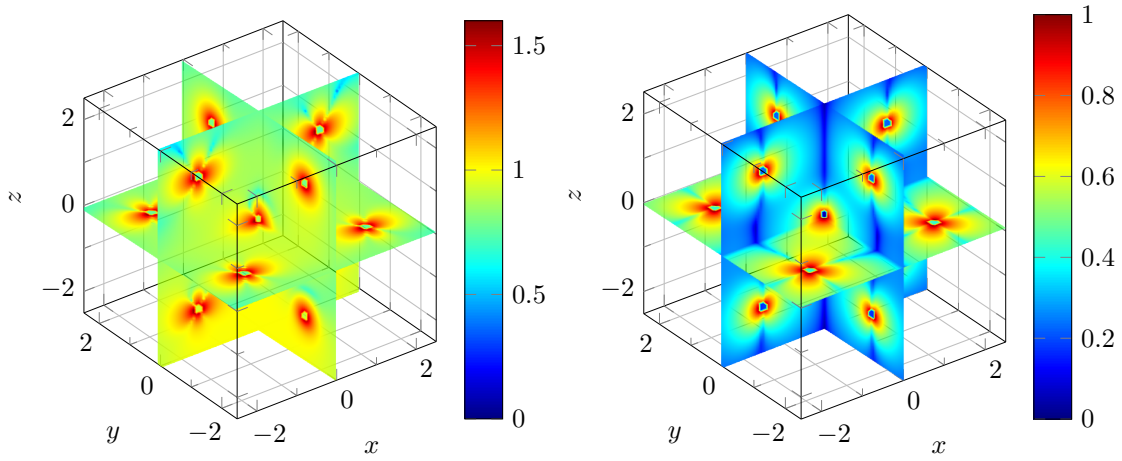

Figure 17: Cross sections of the x and y-coordinates of the scattered electric field in a logarithmic scale

Moreover, each of the K near-field expansions are defined in the fast variable $\mathbf{X}^{(k)}$ centered around the k-th obstacle,

$$\mathbf{X}^{(k)} = \frac{\mathbf{x} - c_k}{\delta}.$$

For any $k = 1, \ldots, K$, the near-field terms $(\widehat{\mathbf{E}}_p^{(k)}, \widehat{\mathbf{H}}_p^{(k)})$ are the same than for one obstacle except the awareness of translations. However, the Born model is restricted to very small obstacles, that are sufficiently far enough away from each other.

5.3 Other perspectives

A better approximation for the multiple scattering is the Foldy-Lax model which takes into account the interactions between the obstacles. Actually, the total scattered field is obtained by considering the superposition of scattered fields generated by the incident field and by considering also that all the isolated scattered fields as new sources for the other obstacles. The scattering problem related to this model is set by looking for an approximation of the scattered field as a superposition of K unknowns electromagnetic dipoles

$$\mathbf{E}_\delta^{\text{Foldy}} = \sum_{k=1}^{K} \Big\{ \mathbf{E}_{\text{dip}}^{\text{elec}}\big[\mathbf{d}_k^{\text{E}}\big](\mathbf{x} - c_k) + \mathbf{E}_{\text{dip}}^{\text{mag}}\big[\mathbf{d}_k^{\text{H}}\big](\mathbf{x} - c_k) \Big\},$$
$$\mathbf{H}_\delta^{\text{Foldy}} = \sum_{k=1}^{K} \Big\{ \mathbf{H}_{\text{dip}}^{\text{elec}}\big[\mathbf{d}_k^{\text{E}}\big](\mathbf{x} - c_k) + \mathbf{H}_{\text{dip}}^{\text{mag}}\big[\mathbf{d}_k^{\text{H}}\big](\mathbf{x} - c_k) \Big\},$$

whose directions can be written thanks to the collected model,

$$\mathbf{d}_k^{\text{E}} = 4\pi\big(1 + \frac{3(\kappa\delta)^2}{10}\big)\mathbf{w}_k^{\text{E}}(c_k), \qquad \mathbf{d}_k^{\text{H}} = -2\pi\big(1 - \frac{3(\kappa\delta)^2}{5}\big)\mathbf{w}_k^{\text{H}}(c_k).$$

The vector fields $\mathbf{w}_k^{\mathrm{E}}(c_k)$ and $\mathbf{w}_k^{\mathrm{H}}(c_k)$ can be determined by solving the following linear systems

$$\mathbf{w}_k^{\mathrm{E}}(c_k) = \delta^3 \Big\{ \mathbf{E}^{\mathrm{inc}}(c_k) + \sum_{\substack{\ell=1 \\ \ell\neq k}}^{K} \mathbf{E}_{\mathrm{dip}}^{\mathrm{elec}}[4\pi \mathbf{w}_\ell^{\mathrm{E}}(c_\ell)](c_k - c_\ell) + \mathbf{E}_{\mathrm{dip}}^{\mathrm{mag}}[-2\pi \mathbf{w}_\ell^{\mathrm{H}}(c_\ell)](c_k - c_\ell) \Big\}, \quad k = 1, \dots, K,$$

$$\mathbf{w}_k^{\mathrm{H}}(c_k) = \delta^3 \Big\{ \mathbf{H}^{\mathrm{inc}}(c_k) + \sum_{\substack{\ell=1 \\ \ell\neq k}}^{K} \mathbf{H}_{\mathrm{dip}}^{\mathrm{elec}}[4\pi \mathbf{w}_\ell^{\mathrm{E}}(c_\ell)](c_k - c_\ell) + \mathbf{H}_{\mathrm{dip}}^{\mathrm{mag}}[-2\pi \mathbf{w}_\ell^{\mathrm{H}}(c_\ell)](c_k - c_\ell) \Big\}, \quad k = 1, \dots, K.$$

We are still investigating the Foldy-Lax model for electromagnetic waves. We are interested by the numerical comparison between the two models, Born and Foldy-Lax, with a spectral method looking like the Ganesh's method in [23] but adapted to small obstacles as in [4]. Besides, the proofs of existence and uniqueness for solutions of elementary problems as well as the convergence proofs justifying the asymptotic expansions have to be developed in order to validate theoretically our results. The theoretical aspects will be performed in a further paper, for obstacles of arbitrary shape. Since the method of matched asymptotic expansions allows to define analytical approximations in geometries for which a parametrization give us explicit eigenfunctions of the vectorial Laplace-Beltrami operator, we could adapt the process and develop the first terms of the asymptotic expansions for ellipsoidal or spheroidal obstacles. An other perspective is the extension to time-dependent Maxwell scattering problems. Thanks to the identification of the time-harmonic symbol $-i\omega$ with the partial time-derivative ∂_t, we plan to adapt this work on the Maxwell's equations in time-dependant domain, that have been already done for the wave equation in [30] in contrast with the Helmholtz equation in [6].

Aknowledgements

We would like to thank very warmly Monique Dauge for her relevant remarks on this work which allowed to propose a richer second version.

A Comparison with the existing literature

In this appendix, we make the relation between the matched asympotic expansions and the multiscale expansions provided by the work of Korikov and Plamenevskii [26] for the study of electromagnetic scattering by a small obstacle. We summarize the results of [26] related to the time-harmonic Maxwell problem and we make explicit the first terms of the multiscale expansions when the scatterer is a small sphere.

A.1 Summary of the results

In [26], Korikov and Plamenevskii make the asymptotic analysis of the scattering problem of electromagnetic waves by a small obstacle with smooth boundary included in a bounded domain. They consider either a perfect conductor condition or an impedance condition on the boundary of the domain of propagation. They deal with the time-harmonic Maxwell problem including elliptic regularization and the time-dependent Maxwell problem. Here, we are concerned by the results that they obtained for the time-harmonic Maxwell problem. Let Ω and ω be bounded domains of $\mathbb{R}^3$ with smooth boundaries, containing the coordinate origin. We denote the small cavity $\omega_\delta = \frac{1}{\delta}\omega$, where $\delta > 0$ is a small parameter, the domain of propagation $\Omega_\delta = \Omega \setminus \overline{\omega_\delta}$ and

Γ_δ its boundary. We introduce the time-harmonic Maxwell system with elliptic regularization, also called the extended Maxwell problem, which consists in seeking $\mathbf{E}_\delta^{\rm tot}$, $\mathbf{H}_\delta^{\rm tot} \in \mathbf{H}^1(\Omega_\delta)$ and a_δ^1, $a_\delta^2 \in H^1(\Omega_\delta)$ satisfying

$$\begin{cases} i\,\mathbf{curl}\,\mathbf{H}_\delta^{\rm tot} - i\,\nabla a_\delta^1 + \tau\mathbf{E}_\delta^{\rm tot} = f^1 & \text{in } \Omega_\delta, \\ -i\,\mathbf{curl}\,\mathbf{E}_\delta^{\rm tot} - i\,\nabla a_\delta^2 + \tau\mathbf{H}_\delta^{\rm tot} = f^2 & \text{in } \Omega_\delta, \\ -i\,\mathrm{div}\,\mathbf{E}_\delta^{\rm tot} + \tau a_\delta^1 = g^1 & \text{in } \Omega_\delta, \\ -i\mathrm{div}\,\mathbf{H}_\delta^{\rm tot} + \tau a_\delta^2 = g^2 & \text{in } \Omega_\delta, \\ \mathbf{n}\times\mathbf{E}_\delta^{\rm tot} = 0 & \text{on } \Gamma_\delta, \\ \mathbf{n}\cdot\mathbf{H}_\delta^{\rm tot} = 0 & \text{on } \Gamma_\delta, \\ a_\delta^1 = 0 & \text{on } \Gamma_\delta, \end{cases} \tag{A.1}$$

with f^1, $f^2 \in \mathbf{L}^2(\Omega_\delta)$ and g^1, $g^2 \in L^2(\Omega_\delta)$. In (A.1), the parameter τ is related to the wave-number by $\tau = -\kappa$ and they assume that $\tau = \alpha - i\gamma$ with $\alpha \in \mathbb{R}$ and $\gamma > 0$. The system (A.1) can be put in the compact form

$$\begin{cases} \big(A(D_{\mathbf{x}}) + \tau\big)\mathbf{u}_\delta = \mathbf{f} & \text{in } \Omega_\delta, \\ \Gamma\mathbf{u}_\delta = 0 & \text{on } \Gamma_\delta, \end{cases} \tag{A.2}$$

where $D_{\mathbf{x}} = -i\partial_{\mathbf{x}}$, $\mathbf{u}_\delta = (\mathbf{E}_\delta^{\rm tot}, \mathbf{H}_\delta^{\rm tot}, a_\delta^1, a_\delta^2)^\top$ belongs to the vector Sobolev space $\mathbb{H}^1(\Omega_\delta)$ given by

$$\mathbb{H}^1(\Omega_\delta) = \mathbf{H}^1(\Omega_\delta)\times\mathbf{H}^1(\Omega_\delta)\times H^1(\Omega_\delta)\times H^1(\Omega_\delta)$$

and

$$A(D_{\mathbf{x}})\mathbf{u}_\delta = \begin{pmatrix} i\,\mathbf{curl}\,\mathbf{H}_\delta^{\rm tot} - i\,\nabla a_\delta^1 \\ -i\,\mathbf{curl}\,\mathbf{E}_\delta^{\rm tot} - i\,\nabla a_\delta^2 \\ -i\,\mathrm{div}\,\mathbf{E}_\delta^{\rm tot} \\ -i\,\mathrm{div}\,\mathbf{H}_\delta^{\rm tot} \end{pmatrix}, \qquad \Gamma\mathbf{u}_\delta = \begin{pmatrix} -\mathbf{E}_\delta^{\rm tot}\cdot\boldsymbol{\tau}_2 \\ \mathbf{E}_\delta^{\rm tot}\cdot\boldsymbol{\tau}_1 \\ \mathbf{H}_\delta^{\rm tot}\cdot\mathbf{n} \\ a^1 \end{pmatrix}.$$

Hereinabove, $\boldsymbol{\tau}_1$ and $\boldsymbol{\tau}_2$ are unit tangent vectors such that $\mathbf{n}\times\mathbf{E}_\delta^{\rm tot} = -(\mathbf{E}_\delta^{\rm tot}\cdot\boldsymbol{\tau}_2)\boldsymbol{\tau}_1 + (\mathbf{E}_\delta^{\rm tot}\cdot\boldsymbol{\tau}_1)\boldsymbol{\tau}_2$. The regularized operator satisfies the relation

$$A(D_{\mathbf{x}})^2 = -\Delta_{\mathbf{x}}.$$

Remark 22. According to [26, Proposition 6.7], if the wave-number τ and the right-hand side $\mathbf{f} = (f^1, f^2, g^1, g^2)$ of (A.2) are subject to the compatibility conditions

$$\begin{cases} \mathrm{div}\, f^k - i\tau g^k = 0 & \text{in } \Omega_\delta, \quad \text{for } k = 1, 2, \\ f^2\cdot\mathbf{n} = 0 & \text{on } \Gamma_\delta, \end{cases}$$

then the components a_δ^1 and a_δ^2 of the corresponding solution $\mathbf{u}_\delta = (\mathbf{E}_\delta^{\rm tot}, \mathbf{H}_\delta^{\rm tot}, a_\delta^1, a_\delta^2)$ vanish in Ω_δ while $(\mathbf{E}_\delta^{\rm tot}, \mathbf{H}_\delta^{\rm tot})$ satisfies the non-extended Maxwell system.

The method of compound solutions, or the *multiscale expansion* method, allows to derive an asymptotic expansion for the solution $\mathbf{u}_\delta$ of (A.2) and to justify it by proving error estimates. For the sake of shortness, we present their results by considering only the terms that appear for the non-extended Maxwell problem. The solution $\mathbf{u}_\delta$ has the following asymptotic expansion for almost any $\mathbf{x} \in \Omega_\delta$

$$\mathbf{u}_\delta(\mathbf{x}) \approx \sum_{n=0}^{\infty} \delta^n \Big(\mathbf{v}_n(\mathbf{x}) + \chi(|\mathbf{x}|)\mathbf{w}_n(\mathbf{X})\Big), \tag{A.3}$$

where $\mathbf{X} = \frac{\mathbf{x}}{\delta}$ denotes the fast variable and $\chi \in \mathscr{C}_c^\infty(\Omega)$ is a cut-off function which is equal to 1 in a neighborhood of the origin and to 0 at infinity. Let us denote

$$\mathbf{u}_\delta \approx \mathbf{u}_\delta^N + \widetilde{\mathbf{u}}_\delta^{N+1},$$

where

$$\mathbf{u}_\delta^N(\mathbf{x}) = \sum_{n=0}^{N+1} \delta^n \mathbf{v}_n(\mathbf{x}) + \chi(|\mathbf{x}|) \sum_{n=0}^{N} \delta^n \mathbf{w}_n(\mathbf{X}),$$

and $\widetilde{\mathbf{u}}_\delta^{N+1}$ denotes the remainder of (A.3). The shift into the outer and inner expansions is chosen such that the remainder $\widetilde{\mathbf{u}}_\delta^{N+1}$ be subject to the following error estimate

$$\|\widetilde{\mathbf{u}}_\delta^{N+1}\|_{0,\Omega_\delta} \leq c\, \delta^{N+\frac{3}{2}-\epsilon}, \tag{A.4}$$

for any $\epsilon > 0$ where the constant c does not depend on δ, see [26, Theorem 7.2]. Hereafter, we present the problems satisfied by the different terms of the asymptotic expansion. Firstly, we introduce the Taylor series expansion of $\mathbf{v}_n$ in a neighborhood of the origin, respectively of $\mathbf{w}_n$ at infinity,

$$\mathbf{v}_n(\mathbf{x}) = \sum_{q=0}^{p-1} \mathbf{v}_n^{(q)}(\theta,\varphi)|\mathbf{x}|^q + \widetilde{\mathbf{v}}_n^{(p)}(\mathbf{x})\,; \qquad \mathbf{w}_n(\mathbf{X}) = \sum_{q=1}^{p} \mathbf{w}_n^{(q)}(\theta,\varphi)\frac{1}{|\mathbf{X}|^q} + \widetilde{\mathbf{w}}_n^{(p+1)}(\mathbf{X}), \tag{A.5}$$

for any positive integer p.

***Far-field* problems.** The first term $\mathbf{v}_0$ in the asymptotic expansion belongs to $\mathbb{H}^1(\Omega)$ and corresponds to the solution of the limit problem,

$$\begin{cases} (A(D_\mathbf{x}) + \tau)\mathbf{v}_0 = \mathbf{f} & \text{in } \Omega, \\ \Gamma\mathbf{v}_0 = 0 & \text{on } \partial\Omega. \end{cases}$$

For any $n \in \mathbb{N}^*$, $\mathbf{v}_n \in \mathbb{H}^1(\Omega)$ solves

$$\begin{cases} (A(D_\mathbf{x}) + \tau)\mathbf{v}_n = -\chi(|\mathbf{x}|)\tau\mathbf{w}_{n-1}^{(1)}(\theta,\varphi)\dfrac{1}{|\mathbf{x}|} - [A(D_\mathbf{x}), \chi(|\mathbf{x}|)]\displaystyle\sum_{k=1}^{n} \mathbf{w}_{n-k}^{(k)}(\theta,\varphi)\frac{1}{|\mathbf{x}|^k} & \text{in } \Omega, \\ \Gamma\mathbf{v}_n = 0 & \text{on } \partial\Omega. \end{cases}$$

***Near-field* problems.** The first term $\mathbf{w}_0$ in the asymptotic expansion satisfies the static Maxwell problem

$$\begin{cases} A(D_\mathbf{X})\mathbf{w}_0 = 0 & \text{in } \mathbb{R}^3 \setminus \overline{\omega}, \\ \Gamma\mathbf{w}_0 = -\Gamma\mathbf{v}_0(0) & \text{on } \partial\omega. \end{cases} \tag{A.6}$$

This problem is well-posed in the vector weighted Sobolev space $\mathbb{W}_1^1(\mathbb{R}^3 \setminus \overline{\omega})$ defined by

$$\mathbb{W}_1^1(\mathbb{R}^3 \setminus \overline{\omega}) = \left\{ \mathbf{u} \mid \nabla\mathbf{u} \in \mathbb{L}^2(\mathbb{R}^3 \setminus \overline{\omega}) \text{ and } \frac{1}{|\mathbf{X}|}\mathbf{u} \in \mathbb{L}^2(\mathbb{R}^3 \setminus \overline{\omega}) \right\},$$

where $\mathbb{L}^2(\mathbb{R}^3 \setminus \overline{\omega})$ denotes the vector Lebesgue space given by

$$\mathbb{L}^2(\mathbb{R}^3 \setminus \overline{\omega}) = \mathbf{L}^2(\mathbb{R}^3 \setminus \overline{\omega}) \times \mathbf{L}^2(\mathbb{R}^3 \setminus \overline{\omega}) \times L^2(\mathbb{R}^3 \setminus \overline{\omega}) \times L^2(\mathbb{R}^3 \setminus \overline{\omega}).$$

For any $n \in \mathbb{N}^*$, $\mathbf{w}_n \in \mathbb{W}_1^1(\mathbb{R}^3 \setminus \overline{\omega})$ solves

$$\begin{cases} A(D_{\mathbf{X}})\mathbf{w}_n = -\tau \widetilde{\mathbf{w}}_{n-1}^{(2)} & \text{in } \mathbb{R}^3 \setminus \overline{\omega}, \\ \Gamma \mathbf{w}_n = -\Gamma \displaystyle\sum_{k=0}^{n} \mathbf{v}_{n-k}^{(k)}(\theta,\varphi)|\mathbf{X}|^k & \text{on } \partial\omega. \end{cases}$$

A.2 Comparison with the matched asymptotic expansions

In this paragraph, we compare the different terms of the asymptotics involved by the method of compound solutions and the method of matched asymptotic expansions. Indeed, the two asymptotic expansions involved by these two different methods are closely related. In the particular case of the scattering by a small sphere, we make explicit the first terms of the asymptotics derived by Korikov and Plamenevskii. The zeroth-order term $\mathbf{v}_0$ defined in the slow variable and corresponding to the solution of the limit problem can be identified with the incident wave,

$$\mathbf{v}_0 = (\mathbf{E}^{\text{inc}}, \mathbf{H}^{\text{inc}}, 0, 0).$$

The zeroth-order term $\mathbf{w}_0$ defined in the fast variable satisfies the static equation (A.6) and the boundary condition reads as

$$\Gamma \mathbf{w}_0 = -\Gamma(\mathbf{E}^{\text{inc}}(0), \mathbf{H}^{\text{inc}}(0), 0, 0) \qquad \text{on } \partial\omega.$$

Hence, in virtue of problems (4.18) and (4.19), $\mathbf{w}_0$ can be identified with the zeroth-order near-field term. As a result,

$$\mathbf{w}_0 = (\widehat{\mathbf{E}}_0, \widehat{\mathbf{H}}_0, 0, 0).$$

The Taylor series expansion (A.5) of $\mathbf{v}_0$ in a neigborhood of the origin corresponds to the Taylor series expansion of the incident field,

$$\mathbf{v}_0(\mathbf{x}) = \mathbf{v}_0(0) + |\mathbf{x}|\, \mathbb{J}_{\mathbf{v}_0}(0)\widehat{x} + \frac{|\mathbf{x}|^2}{2}\, \widehat{x}^{\top} \mathbb{H}_{\mathbf{v}_0}(0)\widehat{x} + \underset{|\mathbf{x}|\to 0}{O}(|\mathbf{x}|^3). \tag{A.7}$$

Besides, the only term that is non-equal to 0 into the Taylor series expansion (A.5) of $\mathbf{w}_0$ at infinity is $\mathbf{w}_0^{(3)}$ and in the particular case where ω denotes the unit open ball, we have

$$\mathbf{w}_0^{(3)}(\theta,\varphi) = \Big(3(\gamma_n \mathbf{E}^{\text{inc}}(0))\widehat{x} - \mathbf{E}^{\text{inc}}(0), -\frac{1}{2}\big(3(\gamma_n \mathbf{H}^{\text{inc}}(0))\widehat{x} - \mathbf{H}^{\text{inc}}(0)\big), 0, 0\Big),$$

with $\widehat{x} = \frac{\mathbf{x}}{|\mathbf{x}|}$. The first-order term $\mathbf{v}_1$ defined in the slow variable is the unique solution in $\mathbb{H}^1(\Omega)$ of the homogeneous time-harmonic Maxwell problem

$$\begin{cases} (A(D_{\mathbf{x}}) + \tau)\mathbf{v}_1 = 0 & \text{in } \Omega, \\ \Gamma \mathbf{v}_1 = 0 & \text{on } \partial\Omega, \end{cases}$$

thus, $\mathbf{v}_1 \equiv (0,0,0,0)$. The first-order term $\mathbf{w}_1$ defined in the fast variable is the unique solution in $\mathbb{W}_1^1(\mathbb{R}^3 \setminus \overline{\omega})$ of the nested Maxwell problem

$$\begin{cases} A(D_{\mathbf{X}})\mathbf{w}_1 = -\tau \mathbf{w}_0 & \text{in } \mathbb{R}^3 \setminus \overline{\omega}, \\ \Gamma \mathbf{w}_1 = -\Gamma(\mathbf{v}_0^{(1)}(\theta,\varphi)|\mathbf{X}|) & \text{on } \partial\omega. \end{cases}$$

Noting that $\mathbf{v}_0^{(1)}$ corresponds to the term behaving in $|\mathbf{x}|$ into the Taylor series expansion (A.7) of $\mathbf{v}_0$, *i.e.*,

$$\mathbf{v}_0^{(1)}(\theta,\varphi) = \mathbb{J}_{\mathbf{v}_0}(0)\widehat{x},$$

in virtue of problems (4.21) and (4.22), $\mathbf{w}_1$ can be identified with the first-order near-field term

$$\mathbf{w}_1 = (\widehat{\mathbf{E}}_1, \widehat{\mathbf{H}}_1, 0, 0).$$

For the particular case of a sphere, the Taylor series expansion of $\mathbf{w}_1$ at infinity is given by

$$\mathbf{w}_1(\mathbf{X}) = \mathbf{w}_1^{(4)}(\theta,\varphi)\frac{1}{|\mathbf{X}|^4} + \mathbf{w}_1^{(2)}(\theta,\varphi)\frac{1}{|\mathbf{X}|^2},$$

with

$$\begin{aligned}
\mathbf{w}_1^{(4)}(\theta,\varphi) &= \Big(-\gamma_t(\mathbb{J}^{\text{sym}}_{\mathbf{E}^{\text{inc}}}(0)\widehat{x} + \frac{3}{2}\gamma_n(\mathbb{J}_{\mathbf{H}^{\text{inc}}}(0)\widehat{x})\widehat{x}, \frac{2}{3}\gamma_t(\mathbb{J}^{\text{sym}}_{\mathbf{E}^{\text{inc}}}(0)\widehat{x} - \gamma_n(\mathbb{J}_{\mathbf{H}^{\text{inc}}}(0)\widehat{x})\widehat{x}, 0, 0\Big),\\
\mathbf{w}_1^{(2)}(\theta,\varphi) &= \Big(-\frac{i\tau}{2}\gamma_\times(\mathbf{H}^{\text{inc}}(0)), i\tau\,\gamma_\times(\mathbf{E}^{\text{inc}}(0)), 0, 0\Big).
\end{aligned}$$

The second-order term $\mathbf{v}_2$ satisfies the same problem than $\mathbf{v}_1$, thus $\mathbf{v}_2 \equiv (0,0,0,0)$. The second-order term $\mathbf{w}_2$ is the unique solution in $\mathbb{W}_1^1(\mathbb{R}^3 \setminus \overline{\omega})$ of the nested Maxwell problem

$$\begin{cases} A(D_{\mathbf{X}})\mathbf{w}_2 = -\tau\mathbf{w}_1 & \text{in } \mathbb{R}^3 \setminus \overline{\omega},\\ \Gamma\mathbf{w}_2 = -\Gamma(\mathbf{v}_0^{(2)}(\theta,\varphi)|\mathbf{X}|) & \text{on } \partial\omega, \end{cases}$$

where $\mathbf{v}_0^{(2)}$ corresponds to the term behaving in $|\mathbf{x}|^2$ into the Taylor series expansion (A.7) of $\mathbf{v}_0$, *i.e.*,

$$\mathbf{v}_0^{(2)}(\theta,\varphi) = \frac{1}{2}\widehat{x}^\top\mathbb{H}_{\mathbf{v}_0}(0)\widehat{x}.$$

As a result, regarding problems (4.29) and (4.30), $\mathbf{w}_2$ can be identified with the second-order near-field term

$$\mathbf{w}_2 = (\widehat{\mathbf{E}}_2, \widehat{\mathbf{H}}_2, 0, 0).$$

Furthermore, for the particular case of a sphere, the Taylor series expansion of $\mathbf{w}_2$ at infinity is given by

$$\mathbf{w}_2(\mathbf{X}) = \mathbf{w}_2^{(5)}(\theta,\varphi)\frac{1}{|\mathbf{X}|^5} + \mathbf{w}_2^{(3)}(\theta,\varphi)\frac{1}{|\mathbf{X}|^3} + \mathbf{w}_2^{(1)}(\theta,\varphi)\frac{1}{|\mathbf{X}|},$$

with

$$\begin{aligned}
\mathbf{w}_2^{(5)}(\theta,\varphi) = \Big(&\frac{2}{3}\gamma_n\big(\widehat{x}^\top\mathbb{H}_{\mathbf{E}^{\text{inc}}}(0)\,\widehat{x}\big)\widehat{x} + \frac{2\tau^2}{15}\gamma_n\big(\mathbf{E}^{\text{inc}}(0)\big)\widehat{x} - \frac{1}{2}\gamma_t\big(\widehat{x}^\top\mathbb{H}_{\mathbf{E}^{\text{inc}}}(0)\,\widehat{x}\big)\\
&\qquad + \frac{i\tau}{3}\gamma_\times\big(\mathbb{J}^{\text{sym}}_{\mathbf{H}^{\text{inc}}}(0)\,\widehat{x}\big) - \frac{\tau^2}{5}\gamma_t\big(\mathbf{E}^{\text{inc}}(0)\big),\\
&-\frac{1}{2}\gamma_n\big(\widehat{x}^\top\,\mathbb{H}_{\mathbf{H}^{\text{inc}}}(0)\,\widehat{x}\big)\widehat{x} - \frac{\tau^2}{10}\gamma_n\big(\mathbf{H}^{\text{inc}}(0)\big)\widehat{x} + \frac{3}{8}\gamma_t\big(\widehat{x}^\top\mathbb{H}_{\mathbf{H}^{\text{inc}}}(0)\widehat{x}\big)\\
&\qquad + \frac{i\tau}{4}\gamma_\times\big(\mathbb{J}^{\text{sym}}_{\mathbf{E}^{\text{inc}}}(0)\widehat{x}\big) + \frac{3\tau^2}{20}\gamma_t\big(\mathbf{H}^{\text{inc}}(0)\big), 0, 0\Big)
\end{aligned}$$

and

$$\mathbf{w}_2^{(3)}(\theta,\varphi) = \Big(-\frac{i\tau}{3}\gamma_\times(\mathbb{J}^{\mathrm{sym}}_{\mathbf{H}^{\mathrm{inc}}}(0)\widehat{x}) - \frac{3\tau^2}{10}\big(\mathbf{E}^{\mathrm{inc}}(0) - 3\gamma_n(\mathbf{E}^{\mathrm{inc}}(0))\widehat{x}\big), \\ -\frac{i\tau}{2}\gamma_\times(\mathbb{J}^{\mathrm{sym}}_{\mathbf{E}^{\mathrm{inc}}}(0)\widehat{x}) + \frac{3\tau^2}{10}\big(\mathbf{H}^{\mathrm{inc}}(0) - 3\gamma_n(\mathbf{H}^{\mathrm{inc}}(0))\widehat{x}\big), 0, 0\Big),$$

$$\mathbf{w}_2^{(1)}(\theta,\varphi) = \Big(\frac{\tau^2}{2}\big(\mathbf{E}^{\mathrm{inc}}(0) + \gamma_n(\mathbf{E}^{\mathrm{inc}}(0))\widehat{x}\big), -\frac{\tau^2}{4}\big(\mathbf{H}^{\mathrm{inc}}(0) + \gamma_n(\mathbf{H}^{\mathrm{inc}}(0))\widehat{x}\big), 0, 0\Big).$$

The third-order term $\mathbf{v}_3$ is the unique solution in $\mathbb{H}^1(\Omega)$ of the time-harmonic Maxwell problem

$$\begin{cases} (A(D_{\mathbf{x}}) + \tau)\mathbf{v}_3 = -\chi(|\mathbf{x}|)\tau\mathbf{w}_2^{(1)}(\theta,\varphi)\dfrac{1}{|\mathbf{x}|} \\ \qquad\qquad - [A(D_{\mathbf{x}}),\chi]\left(\mathbf{w}_2^{(1)}(\theta,\varphi)\dfrac{1}{|\mathbf{x}|} + \mathbf{w}_1^{(2)}(\theta,\varphi)\dfrac{1}{|\mathbf{x}|^2} + \mathbf{w}_0^{(3)}(\theta,\varphi)\dfrac{1}{|\mathbf{x}|^3}\right) \qquad \text{in } \Omega, \\ \Gamma\mathbf{v}_3 = 0 \qquad\qquad \text{on } \partial\Omega. \end{cases}$$

Hereinabove, the right-hand side is not equal to 0 that implies the term $\mathbf{v}_3$ is not identically zero. If we denote

$$\mathbf{V}_3(\mathbf{x}) = \mathbf{v}_3(\mathbf{x}) + \chi(|\mathbf{x}|)\Big(\mathbf{w}_2^{(1)}(\theta,\varphi)\frac{1}{|\mathbf{x}|} + \mathbf{w}_1^{(2)}(\theta,\varphi)\frac{1}{|\mathbf{x}|^2} + \mathbf{w}_0^{(3)}(\theta,\varphi)\frac{1}{|\mathbf{x}|^3}\Big),$$

then, $\mathbf{V}_3$ satisfies the time-harmonic Maxwell problem outside the origin coordinate,

$$\begin{cases} (A(D_x) + \tau)\mathbf{V}_3 = 0 \qquad \text{in } \Omega \setminus \{0\}, \\ \Gamma\mathbf{V}_3 = 0 \qquad\qquad \text{on } \partial\Omega. \end{cases}$$

Thus, in virtue of problem (4.6), the term $\mathbf{V}_3$ can be identified with the third-order far-field term

$$\mathbf{V}_3 = (\widetilde{\mathbf{E}}_3, \widetilde{\mathbf{H}}_3, 0, 0).$$

Remark 23. A difference between the asymptotics involved by the two different methods appears at the third-order term (and not before).

A.3 Error estimates

According the previous paragraph, we can state that, at least for the first terms, the asymptotic expansions involved by the method of matched asymptotic expansions and the method of compound solutions locally coincide. In addition, according to the article [16] of Dauge *et al.* in which it is shown how the terms involved by the two different approaches can be split into a finite number of sub-terms in order to reconstruct the other expansion, we can assume that the two different expansions will locally coincide at any order. From the error estimate (A.4) which evaluates the $\mathbb{L}^2$-norm of the remainder into the whole domain Ω_δ, we could deduce local estimates for the matched asymptotic expansions. However, our frameworks are slightly different. The first noteworthy difference is that they consider dissipative medium which guarantees the coercivity of the Maxwell operator whereas we consider real wave-numbers. That implies the loss of coercivity and consequently the loss of stability. The second difference is the consideration of a bounded whole domain whereas we consider unbounded domains. Hence, we should adapt the estimates in local Sobolev spaces. In spite of that, it seems possible not only to adapt

error estimates to a more general framework but also to improve it because these estimates appear non-optimal in the sense where an order-upgrading is required. For $P = 3, 4$ or 5, let us introduce the vector fields $(\widetilde{\mathbf{E}}_{\delta,P}, \widetilde{\mathbf{H}}_{\delta,P})$ reading as the sum of the first far-field terms

$$\widetilde{\mathbf{E}}_{\delta,P} = \sum_{p=3}^{P} \delta^p \widetilde{\mathbf{E}}_p \, ; \qquad \widetilde{\mathbf{H}}_{\delta,P} = \sum_{p=3}^{P} \delta^p \widetilde{\mathbf{H}}_p \tag{A.9}$$

and for $P = 0, 1$ or 2, the vector fields $(\widehat{\mathbf{E}}_{\delta,P}, \widehat{\mathbf{H}}_{\delta,P})$ as the sum of the first near-field terms,

$$\widehat{\mathbf{E}}_{\delta,P} = \sum_{p=0}^{P} \delta^p \widehat{\mathbf{E}}_p \, ; \qquad \widehat{\mathbf{H}}_{\delta,P} = \sum_{p=0}^{P} \delta^p \widehat{\mathbf{H}}_p. \tag{A.10}$$

Adapting the error estimates of Korikov and Plamenevski [26], we can postulate two theorems which precise the expected order of convergence.

Theorem 1. *For any $P = 3, 4$ or 5, there exists a positive δ_0 such that for any $r_1 > r_0 > \delta_0$ there exists $c > 0$ such that for any positive $\delta < \delta_0$, we have*

$$\|\boldsymbol{E}_\delta - \widetilde{\boldsymbol{E}}_{\delta,P}\|_{0,\mathcal{C}(r_0,r_1)} \leq c\, \delta^{P+1} \, ; \qquad \|\boldsymbol{H}_\delta - \widetilde{\boldsymbol{H}}_{\delta,P}\|_{0,\mathcal{C}(r_0,r_1)} \leq c\, \delta^{P+1}.$$

Theorem 2. *For $P = 0, 1$ or 2, there exist δ_0, $\mathrm{R}^\star$ satisfying $\mathrm{R}^\star > \delta_0 > 0$ such that for any R_0 satisfying $1 < \mathrm{R}_0 < \mathrm{R}^\star$, there exists $c > 0$ such that for any positive $\delta < \delta_0$, we have*

$$\|\boldsymbol{E}_\delta(\delta\,\cdot) - \widehat{\boldsymbol{E}}_{\delta,P}\|_{0,\mathcal{C}(1,\mathrm{R}_0)} \leq c\, \delta^{P+\frac{5}{2}} \, ; \qquad \|\boldsymbol{H}_\delta(\delta\,\cdot) - \widehat{\boldsymbol{H}}_{\delta,P}\|_{0,\mathcal{C}(1,\mathrm{R}_0)} \leq c\, \delta^{P+\frac{5}{2}}.$$

Remark 24. In [3], Ammari *et al.* showed that estimates in Theorem 2 hold for $P = 0$.

The rigorous proof of error estimates for the matched asymptotic expansions will be done in a further paper.

B Multipole theory in electromagnetism

If fields are associated with forces, potentials are associated with energy and work. In the presence of a charge distribution ρ and a current distribution $\boldsymbol{\mathcal{J}}$ in the free-space with a time-harmonic dependency, electromagnetic fields $(\boldsymbol{\mathcal{E}}, \boldsymbol{\mathcal{H}})$ are generated and can be described by their potential decomposition

$$\boldsymbol{\mathcal{E}} = -\nabla \mathcal{V} + i\omega \boldsymbol{\mathcal{A}}, \qquad \boldsymbol{\mathcal{H}} = \frac{1}{\mu} \mathbf{curl}\, \boldsymbol{\mathcal{A}}, \tag{B.1}$$

where the electric potential $\mathcal{V}$ and magnetic potential $\boldsymbol{\mathcal{A}}$ are given by

$$\mathcal{V}(\mathbf{x}) = \frac{1}{4\pi\varepsilon} \int_{\mathbb{R}^3} \exp(i\kappa|\mathbf{x}-\mathbf{y}|) \frac{\rho(\mathbf{y})}{|\mathbf{x}-\mathbf{y}|}\, \mathrm{d}\mathbf{y}, \qquad \boldsymbol{\mathcal{A}}(\mathbf{x}) = \frac{\mu}{4\pi} \int_{\mathbb{R}^3} \exp(i\kappa|\mathbf{x}-\mathbf{y}|) \frac{\boldsymbol{\mathcal{J}}(\mathbf{y})}{|\mathbf{x}-\mathbf{y}|}\, \mathrm{d}\mathbf{y}.$$

According to Equation (B.1), applying the normalization of Table 1, the normalized electromagnetic fields $(\mathbf{E}, \mathbf{H})$ read as

$$\mathbf{E} = -\nabla \mathsf{V} + i\kappa \mathbf{A}, \qquad \mathbf{H} = \mathbf{curl}\, \mathbf{A}, \tag{B.2}$$

where the electric potential V and the magnetic potential $\mathbf{A}$ are given by

$$\mathsf{V}(\mathbf{x}) = \frac{1}{4\pi} \int_{\mathbb{R}^3} \exp(i\kappa|\mathbf{x}-\mathbf{y}|) \frac{\varrho(\mathbf{y})}{|\mathbf{x}-\mathbf{y}|}\, \mathrm{d}\mathbf{y}, \qquad \mathbf{A}(\mathbf{x}) = \frac{1}{4\pi c} \int_{\mathbb{R}^3} \exp(i\kappa|\mathbf{x}-\mathbf{y}|) \frac{\mathbf{j}(\mathbf{y})}{|\mathbf{x}-\mathbf{y}|}\, \mathrm{d}\mathbf{y}. \tag{B.3}$$

Remark 25. These formulas are also valid in electrostatics or magnetostatics, *i.e.* with $\omega = 0$ and where we deal with the following equations

$$\textbf{curl}\,\mathbf{E} = 0 \text{ and } \operatorname{div}\mathbf{E} = \varrho \qquad \text{or} \qquad \textbf{curl}\,\mathbf{H} = \frac{\mathbf{j}}{c} \text{ and } \operatorname{div}\mathbf{H} = 0.$$

B.1 Electric multipoles

A N-point charge distribution is an idealistic configuration for electric charge distributions. It can be represented as a combination of Dirac distributions $\delta_{\mathbf{x}_k}$ at points $\mathbf{x}_k$ for $k \in [1, N]$ with charge amplitudes q_k that are constants in static or time-harmonic regime,

$$\varrho(\mathbf{x}) = \sum_{k=1}^{N} q_k \delta_{\mathbf{x}_k}(\mathbf{x}).$$

The electric multipoles stem from an asymptotic process describing an ideal electric charge distribution. An electric multipole of order 2^N, or electric dipole for $N = 1$, electric quadrupole for $N = 2$, electric octupole and so forth, is obtained in bringing together a 2^N-point charge such that:

- there are 2^{N-1} positive charges $(+q)$ and 2^{N-1} opposite ones $(-q)$ such that the geometric centers of the positive charges and the negative ones are blended.
- the charge amplitudes are given by $q = \frac{q_0}{\epsilon^N}$, where q_0 is measured in Coulomb and any distance between two opposite charges is proportional to ϵ.

By *in bringing together*, we mean that any distance between two charges are tending towards 0, while the amplitudes are tending towards infinity. In Figure 18, we schematize an electrostatic dipole and quadrupole, where we have denoted by ϵ the parameter supposed to tend to 0.

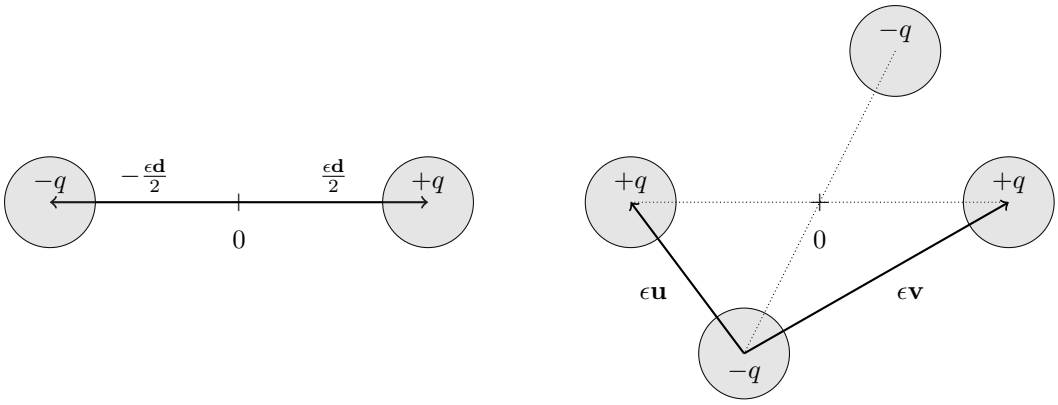

Figure 18: Electrostatic dipole on the left ; Electrostatic quadrupole on the right

Electric fields are produced through a such configuration thanks to the relation $\mathbf{E} = -\nabla \mathsf{V}_\varrho$ where V_ϱ is the scalar electric potential induced by ϱ in a multipolar configuration. In particular, Equations (B.2)-(B.3) with $\kappa = 0$ allow to deduce a general form of the electric field $\mathbf{E}^{\text{elec}}_{\text{dip}}$ created in the presence of an electric dipole centered at the origin along a direction $\mathbf{d}$,

$$\mathbf{E}^{\text{elec}}_{\text{dip}}[\mathbf{d}, \kappa = 0](r, \theta, \varphi) = \frac{q_0}{4\pi r^3}\Big\{3(\mathbf{d}\cdot\mathbf{e}_r(\theta,\varphi))\mathbf{e}_r(\theta,\varphi) - \mathbf{d}\Big\}, \tag{B.4}$$

where $\mathbf{e}_r = (\sin\theta\cos\varphi, \sin\theta\sin\varphi, \cos\theta)^\top$. Moreover, the electric field $\mathbf{E}^{\text{elec}}_{\text{quad}}$ created in the presence of an electric quadrupole centered at the origin along directions $(\mathbf{u}, \mathbf{v})$, in a static regime, can be represented as

$$\mathbf{E}^{\text{elec}}_{\text{quad}}[\mathbf{u},\mathbf{v},\kappa=0](r,\theta,\varphi) = \frac{3q_0}{16\pi r^4}\Big\{\big[(\mathbf{u}\cdot\mathbf{v}) - 3(\mathbf{u}\cdot\mathbf{e}_r)(\mathbf{v}\cdot\mathbf{e}_r)\big]\mathbf{e}_r + \big[(\mathbf{u}\cdot\mathbf{e}_r)(\mathbf{v}\cdot\mathbf{e}_\theta) + (\mathbf{v}\cdot\mathbf{e}_r)(\mathbf{u}\cdot\mathbf{e}_\theta)\big]\mathbf{e}_\theta + \big[(\mathbf{u}\cdot\mathbf{e}_r)(\mathbf{v}\cdot\mathbf{e}_\varphi) + (\mathbf{v}\cdot\mathbf{e}_r)(\mathbf{u}\cdot\mathbf{e}_\varphi)\big]\mathbf{e}_\varphi\Big\}, \tag{B.5}$$

where $(\mathbf{e}_r, \mathbf{e}_\theta, \mathbf{e}_\varphi)$ denotes the spherical coordinate system.

Remark 26. The formula (B.4) can be found in [28, Section 1.16] as well as a discussion about multipole of superior order but we have not found the formula (B.5) in the literature. The computation of $\mathbf{E}^{\text{elec}}_{\text{quad}}$ goes through its potential decomposition (B.2) with

$$\mathsf{V}_{\text{quad}}[\mathbf{u},\mathbf{v},\kappa=0] = \lim_{\epsilon\to 0}\frac{q(\epsilon)}{4\pi}\left[\frac{1}{|\mathbf{x}-c_1(\epsilon)|} + \frac{1}{|\mathbf{x}-c_2(\epsilon)|} - \frac{1}{|\mathbf{x}-c_3(\epsilon)|} - \frac{1}{|\mathbf{x}-c_4(\epsilon)|}\right],$$

where $c_k(\epsilon)$ denotes the center of the k-th charge. In the configuration of Figure 18, the centers read as $c_1(\epsilon) = \frac{\epsilon\mathbf{d}_1}{2}$, $c_2(\epsilon) = -\frac{\epsilon\mathbf{d}_1}{2}$, $c_3(\epsilon) = \frac{\epsilon\mathbf{d}_2}{2}$, $c_4(\epsilon) = -\frac{\epsilon\mathbf{d}_2}{2}$ with $\mathbf{d}_2 - \mathbf{d}_1 = \mathbf{u}$ and $\mathbf{d}_2 + \mathbf{d}_1 = \mathbf{v}$. Moreover, the charge q is given by $q(\epsilon) = \frac{q_0}{\epsilon^2}$.

In classical magnetostatics, the presence of an electric current distribution $\mathbf{j}$ on a system of electric dipole, drag the creation of a magnetic field. A filiform electric current distribution is described by a curve γ and a constant intensity I_γ,

$$I_\gamma = \int_S \mathbf{j}\cdot\mathbf{n}\,\mathsf{d}s,$$

where S denotes any wire section, $\mathsf{d}s$ its surface element and $\mathbf{n}$ its unit normal vector oriented with respect to γ, see Figure 19. For γ parametrized along a direction $\mathbf{d}$ as in Figure 19, this current affects the vectorial magnetic potential as

$$\mathbf{A}_{\text{dip}}[\mathbf{d},\kappa=0] = \lim_{\epsilon\to 0}\frac{I_\gamma}{4\pi c}\left(\int_{-\frac{\epsilon}{2}}^{\frac{\epsilon}{2}}\frac{1}{|\mathbf{x}-s\mathbf{d}|}\,\mathsf{d}s\right)\mathbf{d}. \tag{B.6}$$

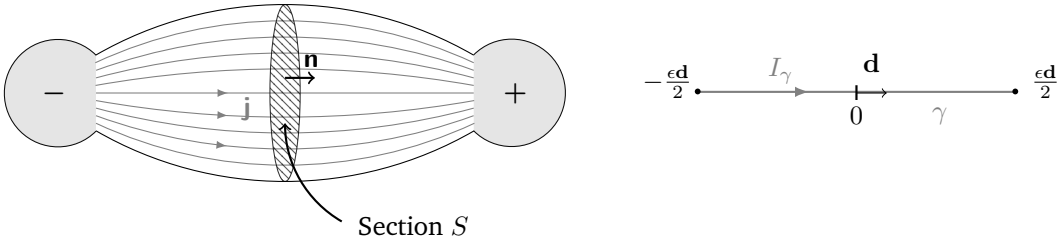

Figure 19: Filiform current between two opposite charges

In particular, Equations (B.2)-(B.6) allow to deduce a general form for the magnetic field $\mathbf{H}^{\text{elec}}_{\text{dip}}$ created in the presence of a filiform electric current of intensity I_γ between two opposite electric point charges along the direction $\mathbf{d}$,

$$\mathbf{H}^{\text{elec}}_{\text{dip}}[\mathbf{d},\kappa=0](r,\theta,\varphi) = \frac{I_\gamma}{4\pi c r^2}(\mathbf{d}\times\mathbf{e}_r). \tag{B.7}$$

In the time-harmonic regime, the charge conservation principle involves the creation of currents in the presence of charges and reciprocally the creation of charges in the presence of currents. In particular, the charge q is linked with the current intensity I_γ as $I_\gamma = -i\omega q$. The presence of an electric dipole along a direction $\mathbf{d}$ generates electromagnetic fields $(\mathbf{E}_{\rm dip}^{\rm elec}, \mathbf{H}_{\rm dip}^{\rm elec})$. The two following expressions generalize the previous ones that are expressed for $\kappa \neq 0$. According to Equations (B.2)-(B.3) and Remark 2, electromagnetic fields read as

$$\mathbf{E}_{\rm dip}^{\rm elec}[\mathbf{d},\kappa](r,\theta,\varphi) = \frac{\exp(i\kappa r)}{4\pi r}\left\{\Big(\frac{3}{r^2} - \frac{3i\kappa}{r} - \kappa^2\Big)(\mathbf{d}\cdot\mathbf{e}_r)\mathbf{e}_r + \Big(-\frac{1}{r^2} + \frac{i\kappa}{r} + \kappa^2\Big)\mathbf{d}\right\} \tag{B.8}$$

and

$$\mathbf{H}_{\rm dip}^{\rm elec}[\mathbf{d},\kappa](r,\theta,\varphi) = \frac{\exp(i\kappa r)}{4\pi r}\Big(\frac{1}{r} - i\kappa\Big)(-i\kappa\mathbf{d})\times\mathbf{e}_r. \tag{B.9}$$

B.2 Magnetic multipoles

The notion of magnetic multipole, although very controversial in classical physics and running counter to the existing theory, enriches the theoretical background of Maxwell's equations. Theoretically, it consists in adding magnetic sources to the Maxwell's system - a magnetic charge density ν and a magnetic current density $\mathbf{m}$ - related with a similar *magnetic* charge conservation principle $-i\omega\nu + \mathrm{div}\,\mathbf{m} = 0$. These densities become sources for the following equations

$$\mathrm{div}\,\mathbf{H} = \nu \qquad \text{and} \qquad \mathbf{curl}\,\mathbf{E} - i\kappa\mathbf{H} = -\frac{\mathbf{m}}{c}.$$

In this case, when we consider that the two other equations are homogeneous, we would have

$$\mathbf{H} = -\nabla \mathsf{V}_\nu + i\kappa\mathbf{A}_\mathbf{m} \qquad \text{and} \qquad \mathbf{E} = -\mathbf{curl}\,\mathbf{A}_\mathbf{m}.$$

By analogy with the previous section, the magnetic fields $\mathbf{H}_{\rm dip}^{\rm mag}$ and $\mathbf{H}_{\rm quad}^{\rm mag}$ created in the presence of a magnetic dipole/quadrupole depending on respective directions $\mathbf{d}_\nu$ and $(\mathbf{u}_\nu, \mathbf{v}_\nu)$ have the following representations in static regime

$$\mathbf{H}_{\rm dip}^{\rm mag}[\mathbf{d}_\nu,\kappa=0](r,\theta,\varphi) = \frac{n_0}{4\pi r^3}\Big\{3(\mathbf{d}_\nu\cdot\mathbf{e}_r)\mathbf{e}_r - \mathbf{d}_\nu\Big\} \tag{B.10}$$

and

$$\begin{aligned}\mathbf{H}_{\rm quad}^{\rm mag}[\mathbf{u}_\nu,\mathbf{v}_\nu,\kappa=0](r,\theta,\varphi) = \frac{3n_0}{16\pi r^4}\Big\{&\big[(\mathbf{u}_\nu\cdot\mathbf{v}_\nu) - 3(\mathbf{u}_\nu\cdot\mathbf{e}_r)(\mathbf{v}_\nu\cdot\mathbf{e}_r)\big]\mathbf{e}_r\\ &+ \big[(\mathbf{u}_\nu\cdot\mathbf{e}_r)(\mathbf{v}_\nu\cdot\mathbf{e}_\theta) + (\mathbf{v}_\nu\cdot\mathbf{e}_r)(\mathbf{u}_\nu\cdot\mathbf{e}_\theta)\big]\mathbf{e}_\theta + \big[(\mathbf{u}_\nu\cdot\mathbf{e}_r)(\mathbf{v}_\nu\cdot\mathbf{e}_\varphi) + (\mathbf{v}_\nu\cdot\mathbf{e}_r)(\mathbf{u}_\nu\cdot\mathbf{e}_\varphi)\big]\mathbf{e}_\varphi\Big\}.\end{aligned} \tag{B.11}$$

Moreover, the electric field $\mathbf{E}_{\rm dip}^{\rm mag}$ created in the presence of a filiform magnetic current density $\mathbf{m}$ between two opposite magnetic point charges of direction $\mathbf{d}_\mathbf{m}$ in static regime reads as

$$\mathbf{E}_{\rm dip}^{\rm mag}[\mathbf{d}_\mathbf{m},\kappa=0](r,\theta,\varphi) = -\frac{I_\gamma}{4\pi c r^2}(\mathbf{d}\times\mathbf{e}_r). \tag{B.12}$$

Finally, the electromagnetic fields $(\mathbf{E}_{\rm dip}^{\rm mag}, \mathbf{H}_{\rm dip}^{\rm mag})$ created in the presence of a time-harmonic magnetic dipole along a direction $\mathbf{d}$, are given by

$$\mathbf{H}_{\rm dip}^{\rm mag}[\mathbf{d},\kappa](r,\theta,\varphi) = \frac{\exp(i\kappa r)}{4\pi r}\left\{\Big(\frac{3}{r^2} - \frac{3i\kappa}{r} - \kappa^2\Big)(\mathbf{d}\cdot\mathbf{e}_r)\mathbf{e}_r + \Big(-\frac{1}{r^2} + \frac{i\kappa}{r} + \kappa^2\Big)\mathbf{d}\right\} \tag{B.13}$$

and

$$\mathbf{E}_{\rm dip}^{\rm mag}[\mathbf{d},\kappa](r,\theta,\varphi) = \frac{\exp(i\kappa r)}{4\pi r}\Big(\frac{1}{r} - i\kappa\Big)(i\kappa\mathbf{d})\times\mathbf{e}_r. \tag{B.14}$$

C Solutions of time-harmonic and nested Maxwell equations

C.1 Well-known properties on the scattering by spheres

Modal decomposition of solutions of Maxwell equations results from the spectral decomposition of tangential vector fields in $\mathbf{L}^2(\mathcal{S}^2)$, where $\mathcal{S}^2$ is the unit sphere. A tangential vector field $\boldsymbol{\lambda}$ in $\mathbf{L}^2(\mathcal{S}_\rho)$ reads as a series which converges into $\mathbf{L}^2(\mathcal{S}_\rho)$

$$\boldsymbol{\lambda} = \sum_{n=1}^{\infty} \sum_{m=-n}^{n} \lambda^{\times}_{n,m} \nabla_{\mathcal{S}^2} Y_{n,m} + \lambda^{\mathsf{t}}_{n,m} \mathbf{curl}_{\mathcal{S}^2} Y_{n,m}, \tag{C.1}$$

where $\mathcal{S}_\rho$ denotes the sphere of radius ρ, see for instance [17, 32, 33]. The coefficients $\lambda^{\times}_{n,m}$ and $\lambda^{\mathsf{t}}_{n,m}$ are defined as the projections of $\boldsymbol{\lambda}$ onto the orthogonal basis of the tangential vector fields in $\mathbf{L}^2(\mathcal{S}^2)$, composed of vectorial spherical harmonics $\nabla_{\mathcal{S}^2} Y_{n,m}$ and $\mathbf{curl}_{\mathcal{S}^2} Y_{n,m}$

$$\lambda^{\times}_{n,m} = \frac{1}{n(n+1)} \int_{\mathcal{S}_\rho} \boldsymbol{\lambda} \cdot \nabla_{\mathcal{S}^2} \overline{Y_{n,m}}(\widehat{x}) \, \mathsf{d}s \, ; \qquad \lambda^{\mathsf{t}}_{n,m} = \frac{1}{n(n+1)} \int_{\mathcal{S}_\rho} \boldsymbol{\lambda} \cdot \mathbf{curl}_{\mathcal{S}^2} \overline{Y_{n,m}}(\widehat{x}) \, \mathsf{d}s. \tag{C.2}$$

The spherical harmonics $Y_{n,m}$ constitute an orthonormal basis of $L^2(\mathcal{S}^2)$, see [33],

$$Y_{n,m}(\theta, \varphi) = \sqrt{\frac{2n+1}{4\pi} \frac{(n-|m|)!}{(n+|m|)!}} P_{n,|m|}(\cos\theta) \exp(im\varphi).$$

For any integer $m \in [0, n]$, $P_{n,m}$ is the m-th Legendre function of order n defined for $t \in [-1, 1]$ by

$$P_{n,m}(t) = (1-t^2)^{\frac{m}{2}} \left(\frac{\mathsf{d}}{\mathsf{d}t} \right)^m P_n(t),$$

where $t \longmapsto P_n(t)$ is the Legendre polynomial of order n

$$P_n(t) = \frac{(-1)^n}{2^n n!} \left(\frac{\mathsf{d}}{\mathsf{d}t} \right)^n (1-t^2)^n.$$

The tangential operators $\nabla_{\mathcal{S}^2}$ and $\mathbf{curl}_{\mathcal{S}^2}$ are given in spherical coordinates by

$$\nabla_{\mathcal{S}^2} = \partial_\theta \, \mathbf{e}_\theta + \frac{1}{\sin\theta} \partial_\varphi \, \mathbf{e}_\varphi \, ; \qquad \mathbf{curl}_{\mathcal{S}^2} = \nabla_{\mathcal{S}^2} \times \mathbf{e}_r = \frac{1}{\sin\theta} \partial_\varphi \, \mathbf{e}_\theta - \partial_\theta \, \mathbf{e}_\varphi.$$

Proposition 2. *The vectorial spherical harmonics $\nabla_{\mathcal{S}^2} Y_{n,m}$ and $\mathbf{curl}_{\mathcal{S}^2} Y_{n,m}$ are the eigenvectors with multiplicity $2n+1$ associated to the eigenvalues $-n(n+1)$ of the vectorial Laplace-Beltrami operator $\boldsymbol{\Delta}_{\mathcal{S}^2}$ defined on the unit sphere, reading as*

$$\boldsymbol{\Delta}_{\mathcal{S}^2} = \nabla_{\mathcal{S}^2}(\mathrm{div}_{\mathcal{S}^2}) - \mathbf{curl}_{\mathcal{S}^2}(\mathrm{curl}_{\mathcal{S}^2}),$$

where surface operators $\mathrm{div}_{\mathcal{S}^2}$ and $\mathrm{curl}_{\mathcal{S}^2}$ are respectively dual operators of $\nabla_{\mathcal{S}^2}$ and $\mathbf{curl}_{\mathcal{S}^2}$ for the pivot space $L^2(\mathcal{S}_\rho)$. In particular, the following properties hold

1. $\|\nabla_{\mathcal{S}^2} Y_{n,m}\|^2_{0,\mathcal{S}^2} = \|\mathbf{curl}_{\mathcal{S}^2} Y_{n,m}\|^2_{0,\mathcal{S}^2} = n(n+1)$;
2. *the vectorial spherical harmonics are orthogonal in pairs and for $(n,m) \neq (n',m')$, we have*

$$\int_{\mathcal{S}^2} \nabla_{\mathcal{S}^2} Y_{n,m} \cdot \nabla_{\mathcal{S}^2} \overline{Y_{n',m'}} \, \mathsf{d}s = \int_{\mathcal{S}^2} \mathbf{curl}_{\mathcal{S}^2} Y_{n,m} \cdot \mathbf{curl}_{\mathcal{S}^2} \overline{Y_{n',m'}} \, \mathsf{d}s = 0.$$

The tangential trace decomposition (C.1) in $\mathbf{L}^2(\mathcal{S}^2)$ is the first step to determine modal decomposition of solutions of time-harmonic Maxwell equations. The second one is the use Debye potentials, see [32], which introduces a link between a scalar solution u of Helmholtz equation and vectorial solutions of time-harmonic Maxwell equations given by

$$\big(\mathbf{curl}\,(u\mathbf{x})\,,\,\frac{1}{i\kappa}\mathbf{curl}\,\mathbf{curl}\,(u\mathbf{x})\big).$$

When u is a singular solution of Helmholtz equation, u can be represented as the series which converges in $L^2_{\text{loc}}(\mathbb{R}^3\setminus\{0\})$,

$$u=\sum_{n=0}^{\infty}\sum_{m=-n}^{n} u_{n,m}\,h_n^{(1)}(\kappa r)Y_{n,m}(\widehat{x}), \tag{C.3}$$

where $L^2_{\text{loc}}(\mathbb{R}^3\setminus\{0\})$ is the space of scalar functions u such that

$$\forall\psi\in\mathscr{C}_c^{\infty}(\mathbb{R}^3),\qquad \psi=0 \text{ in a neighborhood of } 0,\quad \psi u\in L^2(\mathbb{R}^3).$$

The function $h_n^{(1)}$ denotes the n-order spherical Hankel function of first kind and we have the following properties:

Proposition 3. *For any $n\geq 0$, the spherical Hankel function of the first kind $h_n^{(1)}$ is defined as $h_n^{(1)}=j_n+iy_n$, where j_n denotes the spherical Bessel function of order n and y_n the spherical Neumann function of order n. Both are solutions of the spherical Bessel differential equation in $\mathbb{C}^*$,*

$$\frac{\mathsf{d}}{\mathsf{d}r}\Big(r^2\frac{\mathsf{d}u}{\mathsf{d}r}\Big)+\kappa^2r^2u=n(n+1)u.$$

The spherical Bessel functions are smooth nearby 0 whereas the Neumann functions are singular. Moreover, the spherical Hankel function can be described as a Laurent series expansion in a neighborhood of 0 as

$$h_n^{(1)}(z)=\sum_{\ell=-n-1}^{\infty}\mathfrak{h}_{n,\ell}\,z^{\ell}.$$

The coefficients $\mathfrak{h}_{n,\ell}$ read as

$$\mathfrak{h}_{n,\ell}=\begin{cases}\mathfrak{j}_{n,\ell} & \text{if } \ell-n \text{ is even and } \ell\geq n,\\ i\,\mathfrak{y}_{n,\ell} & \text{if } \ell-n \text{ is odd and } \ell\geq -n-1,\\ 0 & \text{otherwise},\end{cases}$$

where $\mathfrak{j}_{n,\ell}$ and $\mathfrak{y}_{n,\ell}$ are coefficients into series expansions of j_n and y_n given by

$$\mathfrak{j}_{n,\ell}=\begin{cases}\dfrac{\sqrt{\pi}}{2^{\ell+1}}\dfrac{(-1)^{\frac{\ell-n}{2}}}{(\frac{\ell-n}{2})!\,\Gamma(\frac{\ell+n+1}{2}+1)} & \text{if } \ell-n \text{ is even and } \ell\geq n,\\ 0 & \text{otherwise},\end{cases}$$

$$\mathfrak{y}_{n,\ell}=\begin{cases}(-1)^{n+1}\dfrac{\sqrt{\pi}}{2^{\ell+1}}\dfrac{(-1)^{\frac{\ell+n+1}{2}}}{(\frac{\ell+n+1}{2})!\,\Gamma(\frac{\ell-n}{2}+1)} & \text{if } \ell-n \text{ is odd and } \ell\geq -n-1,\\ 0 & \text{otherwise},\end{cases}$$

with Γ denotes the Euler gamma function, see [25] for more details.

The coefficients $u_{n,m}$ in (C.3) are defined as the projections of u onto the basis of $L^2(\mathcal{S}^2)$ composed of $Y_{n,m}$ on every sphere $\mathcal{S}_\rho$ of radius $\rho > 0$

$$u_{n,m} = \frac{1}{h_n^{(1)}(\kappa\rho)} \int_{\mathcal{S}_\rho} u(\mathbf{x})\overline{Y_{n,m}}(\widehat{x})\, \mathrm{d}s.$$

Then, the associated Maxwell solution $\mathbf{u}$ is also singular and reads as the following series which converges in $\mathbf{H}_{\text{loc}}(\mathbf{curl}\,, \mathbb{R}^3 \setminus \{0\})$,

$$\mathbf{u} = \sum_{n=1}^{\infty} \sum_{m=-n}^{n} \left\{ u_{n,m}^{\times} \mathbf{curl}\left(h_n^{(1)}(\kappa r) Y_{n,m}(\widehat{x})\mathbf{x}\right) + \frac{u_{n,m}^{\mathrm{t}}}{i\kappa} \mathbf{curl}\,\mathbf{curl}\left(h_n^{(1)}(\kappa r) Y_{n,m}(\widehat{x})\mathbf{x}\right) \right\}. \tag{C.4}$$

The complex magnitudes $u_{n,m}^{\times}$ and $u_{n,m}^{\mathrm{t}}$ are defined as the projections of $\mathbf{n} \times \mathbf{u}$ onto the basis of tangential vector fields in $\mathbf{L}^2(\mathcal{S}^2)$ on every sphere $\mathcal{S}_\rho$ of radius $\rho > 0$

$$u_{n,m}^{\times} = -\frac{\lambda_{n,m}^{\times}}{h_n^{(1)}(\kappa\rho)}, \qquad u_{n,m}^{\mathrm{t}} = -\frac{i\kappa\rho\lambda_{n,m}^{\mathrm{t}}}{h_n^{(1)}(\kappa\rho) + \kappa\rho h_n^{(1)'}(\kappa\rho)}, \tag{C.5}$$

with $\lambda_{n,m}^{\times}$ and $\lambda_{n,m}^{\mathrm{t}}$ are spectral coefficients (C.2) with $\boldsymbol{\lambda} = \mathbf{n} \times \mathbf{u}$.

C.2 Solutions of time-harmonic Maxwell equations as series

An outgoing solution $(\widetilde{\mathbf{E}}_p, \widetilde{\mathbf{H}}_p)$ with $p \geq 3$ of the time-harmonic Maxwell equations reads as the following series which converges into $\mathbf{H}_{\text{loc}}(\mathbf{curl}\,, \mathbb{R}^3 \setminus \{0\})$, see for instance [32],

$$\begin{aligned}
\widetilde{\mathbf{E}}_p(r,\widehat{x}) &= \sum_{n=1}^{\infty} \sum_{m=-n}^{n} \widetilde{e}_{n,m}^{(p),\times}(r)\mathbf{curl}_{\mathcal{S}^2} Y_{n,m}(\widehat{x}) + \widetilde{e}_{n,m}^{(p),\mathrm{t}}(r)\nabla_{\mathcal{S}^2} Y_{n,m}(\widehat{x}) + \widetilde{e}_{n,m}^{(p),\mathrm{r}}(r) Y_{n,m}(\widehat{x})\mathbf{e}_r, \\
\widetilde{\mathbf{H}}_p(r,\widehat{x}) &= \sum_{n=1}^{\infty} \sum_{m=-n}^{n} \widetilde{h}_{n,m}^{(p),\times}(r)\mathbf{curl}_{\mathcal{S}^2} Y_{n,m}(\widehat{x}) + \widetilde{h}_{n,m}^{(p),\mathrm{t}}(r)\nabla_{\mathcal{S}^2} Y_{n,m}(\widehat{x}) + \widetilde{h}_{n,m}^{(p),\mathrm{r}}(r) Y_{n,m}(\widehat{x})\mathbf{e}_r.
\end{aligned} \tag{C.6}$$

Convergence results are detailed in [27]. The radial coefficients are defined as projections of the vector fields onto the basis of $\mathbf{L}^2(\mathcal{S}^2)$ composed of $\mathbf{curl}_{\mathcal{S}^2} Y_{n,m}$, $\nabla_{\mathcal{S}^2} Y_{n,m}$ and onto $Y_{n,m}\mathbf{e}_r$

$$\begin{aligned}
\widetilde{e}_{n,m}^{(p),\times}(r) &= \frac{1}{n(n+1)} \int_{\mathcal{S}^2} \widetilde{\mathbf{E}}_p(r,\widehat{x}) \cdot \mathbf{curl}_{\mathcal{S}^2}\overline{Y_{n,m}}(\widehat{x})\, \mathrm{d}\widehat{x}, \\
\widetilde{e}_{n,m}^{(p),\mathrm{t}}(r) &= \frac{1}{n(n+1)} \int_{\mathcal{S}^2} \widetilde{\mathbf{E}}_p(r,\widehat{x}) \cdot \nabla_{\mathcal{S}^2}\overline{Y_{n,m}}(\widehat{x})\, \mathrm{d}\widehat{x}, \\
\widetilde{e}_{n,m}^{(p),\mathrm{r}}(r) &= \int_{\mathcal{S}^2} \left(\widetilde{\mathbf{E}}_p(r,\widehat{x}) \cdot \mathbf{e}_r\right) \overline{Y_{n,m}}(\widehat{x})\, \mathrm{d}\widehat{x}, \\
\widetilde{h}_{n,m}^{(p),\times}(r) &= \frac{1}{n(n+1)} \int_{\mathcal{S}^2} \widetilde{\mathbf{H}}_p(r,\widehat{x}) \cdot \mathbf{curl}_{\mathcal{S}^2}\overline{Y_{n,m}}(\widehat{x})\, \mathrm{d}\widehat{x}, \\
\widetilde{h}_{n,m}^{(p),\mathrm{t}}(r) &= \frac{1}{n(n+1)} \int_{\mathcal{S}^2} \widetilde{\mathbf{H}}_p(r,\widehat{x}) \cdot \nabla_{\mathcal{S}^2}\overline{Y_{n,m}}(\widehat{x})\, \mathrm{d}\widehat{x}, \\
\widetilde{h}_{n,m}^{(p),\mathrm{r}}(r) &= \int_{\mathcal{S}^2} \left(\widetilde{\mathbf{H}}_p(r,\widehat{x}) \cdot \mathbf{e}_r\right) \overline{Y_{n,m}}(\widehat{x})\, \mathrm{d}\widehat{x}.
\end{aligned}$$

According to Eq. (C.4), these projections can be expressed thanks to the Hankel functions $h_n^{(1)}$

$$\begin{aligned}
&\widetilde{e}_{n,m}^{(p),\times}(r) = u_{n,m}^{(p),\times}\, h_n^{(1)}(\kappa r), && \widetilde{h}_{n,m}^{(p),\times}(r) = -u_{n,m}^{(p),\mathrm{t}}\, h_n^{(1)}(\kappa r),\\
&\widetilde{e}_{n,m}^{(p),\mathrm{t}}(r) = \frac{u_{n,m}^{(p),\mathrm{t}}}{i\kappa r}\big(h_n^{(1)}(\kappa r) + \kappa r h_n^{(1)'}(\kappa r)\big), && \widetilde{h}_{n,m}^{(p),\mathrm{t}}(r) = \frac{u_{n,m}^{(p),\times}}{i\kappa r}\big(h_n^{(1)}(\kappa r) + \kappa r h_n^{(1)'}(\kappa r)\big),\\
&\widetilde{e}_{n,m}^{(p),\mathrm{r}}(r) = \frac{n(n+1)u_{n,m}^{(p),\mathrm{t}}}{i\kappa r}\, h_n^{(1)}(\kappa r, && \widetilde{h}_{n,m}^{(p),\mathrm{r}}(r) = \frac{n(n+1)u_{n,m}^{(p),\times}}{i\kappa r}\, h_n^{(1)}(\kappa r),
\end{aligned}$$

where the complex magnitudes $u_{n,m}^{(p),\times}$ and $u_{n,m}^{(p),\mathrm{t}}$ are modal coefficients (C.5) with $\mathbf{u} = \widetilde{\mathbf{E}}_p$. The magnitudes $u_{n,m}^{(p),\times}$ and $u_{n,m}^{(p),\mathrm{t}}$ are not only defined through the spectral decomposition of $\widetilde{\mathbf{E}}_p$ but are also related to the modal decomposition of near-field terms using the matching conditions (4.15). These conditions allow to establish that in (C.6), only a finite number of coefficients are not equal to zero. To give details of this dependence, the study of behavior of the far-field terms $(\widetilde{\mathbf{E}}_p, \widetilde{\mathbf{H}}_p)$ is required. That goes through a Laurent series expansion of the Hankel functions of the first kind $h_n^{(1)}$. According to Proposition 3, the radial coefficients $\widetilde{\diamond}_{n,m}^{(p),\times}$, $\widetilde{\diamond}_{n,m}^{(p),\mathrm{t}}$ and $\widetilde{\diamond}_{n,m}^{(p),\mathrm{r}}$ for $\diamond = e$ or h can be described as Laurent series expansions in a neighborhood of 0 as

$$\begin{aligned}
&\widetilde{e}_{n,m}^{(p),\times}(r) = u_{n,m}^{(p),\times} \sum_{\ell=-n-1}^{\infty} \mathfrak{h}_{n,\ell}(\kappa r)^\ell, && \widetilde{h}_{n,m}^{(p),\times}(r) = -u_{n,m}^{(p),\mathrm{t}} \sum_{\ell=0}^{\infty} \mathfrak{h}_{n,\ell}(\kappa r)^\ell,\\
&\widetilde{e}_{n,m}^{(p),\mathrm{t}}(r) = u_{n,m}^{(p),\mathrm{t}} \sum_{\ell=-n-2}^{\infty} \frac{\mathfrak{h}_{n,\ell+1}}{i}(\ell+2)(\kappa r)^\ell, && \widetilde{h}_{n,m}^{(p),\mathrm{t}}(r) = u_{n,m}^{(p),\times} \sum_{\ell=-n-2}^{\infty} \frac{\mathfrak{h}_{n,\ell+1}}{i}(\ell+2)(\kappa r)^\ell,\\
&\frac{\widetilde{e}_{n,m}^{(p),\mathrm{t}}(r)}{n(n+1)} = u_{n,m}^{(p),\mathrm{t}} \sum_{\ell=-n-2}^{\infty} \frac{\mathfrak{h}_{n,\ell+1}}{i}(\kappa r)^\ell, && \frac{\widetilde{h}_{n,m}^{(p),\mathrm{r}}(r)}{n(n+1)} = u_{n,m}^{(p),\times} \sum_{\ell=-n-2}^{\infty} \frac{\mathfrak{h}_{n,\ell+1}}{i}(\kappa r)^\ell.
\end{aligned} \tag{C.7}$$

C.3 Solutions of the static and nested Maxwell equations as series

C.3.1 Solutions of the static Maxwell equations as series

A regular solution $(\widehat{\mathbf{E}}_{p,0}, \widehat{\mathbf{H}}_{p,0})$ with $p \geq 0$ of the static Maxwell equations in the exterior domain $\widehat{\Omega}$ reads as the following series which converges into $\mathbf{H}(\mathbf{curl}\,, \widehat{\Omega})$,

$$\begin{aligned}
\widehat{\mathbf{E}}_{p,0}(\mathbf{X}) &= \sum_{n=1}^{\infty} \sum_{m=-n}^{n} \frac{\widehat{e}_{n,m}^{(p)}}{\mathrm{R}^{n+2}} \Big(\nabla_{\mathcal{S}^2} Y_{n,m}(\widehat{x}) - (n+1) Y_{n,m}(\widehat{x}) \mathbf{e}_r \Big),\\
\widehat{\mathbf{H}}_{p,0}(\mathbf{X}) &= \sum_{n=1}^{\infty} \sum_{m=-n}^{n} \frac{\widehat{h}_{n,m}^{(p)}}{\mathrm{R}^{n+2}} \Big(\nabla_{\mathcal{S}^2} Y_{n,m}(\widehat{x}) - (n+1) Y_{n,m}(\widehat{x}) \mathbf{e}_r \Big).
\end{aligned} \tag{C.8}$$

The spectral coefficients $\widehat{e}_{n,m}^{(p)}$ are defined as projections of $\widehat{\mathbf{E}}_{p,0}$ onto the vectorial spherical harmonics $\nabla_{\mathcal{S}^2} Y_{n,m}$ on the unit sphere $\mathcal{S}^2$,

$$\widehat{e}_{n,m}^{(p)} = \frac{1}{n(n+1)} \int_{\mathcal{S}^2} \big(\mathbf{e}_r \times \widehat{\mathbf{E}}_{p,0} \big) \cdot \mathbf{curl}_{\mathcal{S}^2} \overline{Y_{n,m}}\, \mathrm{d}s.$$

The others coefficients $\widehat{h}_{n,m}^{(p)}$ are projections of $\widehat{\mathbf{H}}_{p,0}$ onto the basis vector fields $Y_{n,m}\mathbf{e}_r$ on $\mathcal{S}^2$,

$$\widehat{h}_{n,m}^{(p)} = -\frac{1}{n+1} \int_{\mathcal{S}^2} \big(\mathbf{e}_r \cdot \widehat{\mathbf{H}}_{p,0} \big) \overline{Y_{n,m}}\, \mathrm{d}s.$$

In order to obtain the boundary conditions (4.10) and apply the calculation of these coefficients in pratice, we require the following recursive relations for any $p \geq 0$,

$$\widehat{e}_{n,m}^{(p)} = -\frac{1}{n(n+1)} \sum_{|\alpha|=p} \frac{1}{\alpha!} \int_{\mathbb{S}^2} \big(\mathbf{e}_r \times (\mathsf{d}^\alpha \mathbf{E}^{\text{inc}}(0) \cdot \mathbf{e}_r^\alpha)\big) \cdot \mathbf{curl}_{\mathbb{S}^2} \overline{Y_{n,m}} \, \mathsf{d}s \\ - \sum_{\ell=1}^{p} \kappa^\ell \, \frac{\ell - n}{n} \, \frac{\mathfrak{h}_{n,\ell-n-1}}{\mathfrak{h}_{n,-n-1}} \, \widehat{e}_{n,m}^{(p-\ell)} \tag{C.9}$$

and

$$\widehat{h}_{n,m}^{(p)} = \frac{1}{n+1} \sum_{|\alpha|=p} \frac{1}{\alpha!} \int_{\mathbb{S}^2} \big(\mathbf{e}_r \cdot (\mathsf{d}^\alpha \mathbf{H}^{\text{inc}}(0) \cdot \mathbf{e}_r^\alpha)\big) \overline{Y_{n,m}} \, \mathsf{d}s - \sum_{\ell=1}^{p} \kappa^\ell \, \frac{\mathfrak{h}_{n,\ell-n-1}}{\mathfrak{h}_{n,-n-1}} \, \widehat{h}_{n,m}^{(p-\ell)}. \tag{C.10}$$

The coefficients $\mathfrak{h}_{n,\ell}$ denote the coefficients before the ℓ-power of r into the expansion as Laurent series of the n-order Hankel function $h_n^{(1)}$ of the first kind, see Proposition 3 in Section C.1.

Remark 27. Expressions in Equations (C.8) define a regular solution of the static Maxwell equations in exterior domain $\widehat{\Omega}$. To show that, we go through intrinsic expressions of the rotational and the divergence of a smooth vector field $\mathbf{u} = u_{\mathrm{r}}\mathbf{e}_r + \mathbf{u}_{\mathrm{t}}$, given by

$$\mathbf{curl}\, \mathbf{u} = \frac{1}{\mathrm{R}} \mathrm{curl}_{\mathbb{S}^2} \mathbf{u}_{\mathrm{t}} + \frac{1}{\mathrm{R}} \mathbf{curl}_{\mathbb{S}^2} u_{\mathrm{r}} + \frac{1}{\mathrm{R}} \partial_{\mathrm{R}} \big[\mathrm{R}\mathbf{e}_r \times \mathbf{u}_{\mathrm{t}}\big], \quad \mathrm{div}\, \mathbf{u} = \frac{1}{\mathrm{R}^2} \partial_{\mathrm{R}} \big[\mathrm{R}^2 u_{\mathrm{r}}\big] + \frac{1}{\mathrm{R}} \mathrm{div}_{\mathbb{S}^2} \mathbf{u}_{\mathrm{t}}, \tag{C.11}$$

where the operators $\mathrm{curl}_{\mathbb{S}^2}$ and $\mathrm{div}_{\mathbb{S}^2}$ denote respectively the dual operators of $\mathbf{curl}_{\mathbb{S}^2}$ and $\nabla_{\mathbb{S}^2}$ for the pivot space $\mathbf{L}^2(\mathcal{S}^2)$. Since the following properties hold

$$\mathrm{curl}_{\mathbb{S}^2} \nabla_{\mathbb{S}^2} Y_{n,m} = 0 \, ; \, \mathbf{e}_r \times \nabla_{\mathbb{S}^2} Y_{n,m} = -\mathbf{curl}_{\mathbb{S}^2} Y_{n,m} \, ; \, \mathrm{div}_{\mathbb{S}^2} \nabla_{\mathbb{S}^2} Y_{n,m} = -n(n+1) Y_{n,m}, \tag{C.12}$$

we observe that $(\widehat{\mathbf{E}}_{p,0}, \widehat{\mathbf{H}}_{p,0})$ satisfies

$$\begin{cases} \mathbf{curl}\, \widehat{\mathbf{E}}_{p,0} = \dfrac{1}{\mathrm{R}} \displaystyle\sum_{n=1}^{\infty} \sum_{m=-n}^{n} \frac{\widehat{e}_{n,m}^{(p)}}{\mathrm{R}^{n+2}} \big[-(n+1)\mathbf{curl}_{\mathbb{S}^2} Y_{n,m} - (n+1)\mathbf{e}_r \times \nabla_{\mathbb{S}^2} Y_{n,m}\big] = 0, \\ \mathbf{curl}\, \widehat{\mathbf{H}}_{p,0} = \dfrac{1}{\mathrm{R}} \displaystyle\sum_{n=1}^{\infty} \sum_{m=-n}^{n} \frac{\widehat{h}_{n,m}^{(p)}}{\mathrm{R}^{n+2}} \big[-(n+1)\mathbf{curl}_{\mathbb{S}^2} Y_{n,m} - (n+1)\mathbf{e}_r \times \nabla_{\mathbb{S}^2} Y_{n,m}\big] = 0, \\ \mathrm{div}\, \widehat{\mathbf{E}}_{p,0} = \dfrac{1}{\mathrm{R}^2} \displaystyle\sum_{n=1}^{\infty} \sum_{m=-n}^{n} \frac{\widehat{e}_{n,m}^{(p)}}{\mathrm{R}^{n+1}} \big[n(n+1) Y_{n,m} + \mathrm{div}_{\mathbb{S}^2} \nabla_{\mathbb{S}^2} Y_{n,m}\big] = 0, \\ \mathrm{div}\, \widehat{\mathbf{H}}_{p,0} = \dfrac{1}{\mathrm{R}^2} \displaystyle\sum_{n=1}^{\infty} \sum_{m=-n}^{n} \frac{\widehat{h}_{n,m}^{(p)}}{\mathrm{R}^{n+1}} \big[n(n+1) Y_{n,m} + \mathrm{div}_{\mathbb{S}^2} \nabla_{\mathbb{S}^2} Y_{n,m}\big] = 0. \end{cases}$$

C.3.2 Solutions of the nested Maxwell equations as series

Proposition 4. *For any $p \geq 0$, a solution $(\widehat{\boldsymbol{E}}_p, \widehat{\boldsymbol{H}}_p)$ of the nested Maxwell equations reads as the following series which converges into $\mathbf{H}_{loc}(\boldsymbol{curl}, \mathbb{R}^3 \setminus \overline{\mathcal{B}(0,1)})$*

$$\widehat{\boldsymbol{E}}_p = \sum_{\ell=0}^{p} \widehat{\boldsymbol{E}}_{p,\ell}, \qquad \widehat{\boldsymbol{H}}_p = \sum_{\ell=0}^{p} \widehat{\boldsymbol{H}}_{p,\ell}, \tag{C.13}$$

where

$$\begin{aligned}
\widehat{\boldsymbol{E}}_{p,\ell} &= \sum_{n=1}^{\infty}\sum_{m=-n}^{n} \widehat{e}^{(p),\times}_{n,m,\ell}(\mathrm{R})\boldsymbol{curl}_{\mathbb{S}^2} Y_{n,m} + \widehat{e}^{(p),t}_{n,m,\ell}(\mathrm{R})\nabla_{\mathbb{S}^2} Y_{n,m} + \widehat{e}^{(p),r}_{n,m,\ell}(\mathrm{R}) Y_{n,m}\boldsymbol{e}_r,\\
\widehat{\boldsymbol{H}}_{p,\ell} &= \sum_{n=1}^{\infty}\sum_{m=-n}^{n} \widehat{h}^{(p),\times}_{n,m,\ell}(\mathrm{R})\boldsymbol{curl}_{\mathbb{S}^2} Y_{n,m} + \widehat{h}^{(p),t}_{n,m,\ell}(\mathrm{R})\nabla_{\mathbb{S}^2} Y_{n,m} + \widehat{h}^{(p),r}_{n,m,\ell}(\mathrm{R}) Y_{n,m}\boldsymbol{e}_r.
\end{aligned} \tag{C.14}$$

The radial coefficients are given by

$$\begin{aligned}
\widehat{e}^{(p),\times}_{n,m,\ell}(\mathrm{R}) &= -\frac{i\kappa^\ell}{\mathrm{R}^{n+2-\ell}}\,\frac{1}{n}\,\frac{\mathfrak{h}_{n,\ell-n-2}}{\mathfrak{h}_{n,-n-1}}\,\widehat{h}^{(p-\ell)}_{n,m},\\
\widehat{e}^{(p),t}_{n,m,\ell}(\mathrm{R}) &= -\frac{\kappa^\ell}{\mathrm{R}^{n+2-\ell}}\,\frac{\ell-n}{n}\,\frac{\mathfrak{h}_{n,\ell-n-1}}{\mathfrak{h}_{n,-n-1}}\,\widehat{e}^{(p-\ell)}_{n,m},\\
\widehat{e}^{(p),r}_{n,m,\ell}(\mathrm{R}) &= -\frac{\kappa^\ell}{\mathrm{R}^{n+2-\ell}}\,\frac{\mathfrak{h}_{n,\ell-n-1}}{\mathfrak{h}_{n,-n-1}}\,(n+1)\,\widehat{e}^{(p-\ell)}_{n,m},\\
\widehat{h}^{(p),\times}_{n,m,\ell}(\mathrm{R}) &= \frac{i\kappa^\ell}{\mathrm{R}^{n+2-\ell}}\,\frac{1}{n}\,\frac{\mathfrak{h}_{n,\ell-n-2}}{\mathfrak{h}_{n,-n-1}}\,\widehat{e}^{(p-\ell)}_{n,m},\\
\widehat{h}^{(p),t}_{n,m,\ell}(\mathrm{R}) &= -\frac{\kappa^\ell}{\mathrm{R}^{n+2-\ell}}\,\frac{\ell-n}{n}\,\frac{\mathfrak{h}_{n,\ell-n-1}}{\mathfrak{h}_{n,-n-1}}\,\widehat{h}^{(p-\ell)}_{n,m},\\
\widehat{h}^{(p),r}_{n,m,\ell}(\mathrm{R}) &= -\frac{\kappa^\ell}{\mathrm{R}^{n+2-\ell}}\,\frac{\mathfrak{h}_{n,\ell-n-1}}{\mathfrak{h}_{n,-n-1}}\,(n+1)\,\widehat{h}^{(p-\ell)}_{n,m}.
\end{aligned} \tag{C.15}$$

Remark 28. In (C.14), the series with $\ell = 0$ correspond to the series expansions of $(\widehat{\mathbf{E}}_{p,0}, \widehat{\mathbf{H}}_{p,0})$, according to the following identities

$$\begin{aligned}
&\widehat{e}^{(p),\times}_{n,m,0} = 0\,; \qquad \widehat{e}^{(p),\mathrm{t}}_{n,m,0} = \frac{\widehat{e}^{(p)}_{n,m}}{\mathrm{R}^{n+2}}\,; \qquad \widehat{e}^{(p),\mathrm{r}}_{n,m,0} = -\frac{n+1}{\mathrm{R}^{n+2}}\,\widehat{e}^{(p)}_{n,m};\\
&\widehat{h}^{(p),\times}_{n,m,0} = 0\,; \qquad \widehat{h}^{(p),\mathrm{t}}_{n,m,0} = \frac{\widehat{h}^{(p)}_{n,m}}{\mathrm{R}^{n+2}}\,; \qquad \widehat{h}^{(p),\mathrm{r}}_{n,m,0} = -\frac{n+1}{\mathrm{R}^{n+2}}\,\widehat{h}^{(p)}_{n,m}.
\end{aligned}$$

Remark 29. The sub-terms $(\widehat{\mathbf{E}}_{p,\ell}, \widehat{\mathbf{H}}_{p,\ell})$ are built such that they satisfy *sub-nested* Maxwell equations in the following sense

$$\mathbf{curl}\,\widehat{\mathbf{E}}_{p,\ell} = i\kappa\widehat{\mathbf{H}}_{p-1,\ell-1} \text{ in } \widehat{\Omega}, \qquad \mathbf{curl}\,\widehat{\mathbf{H}}_{p,\ell} = -i\kappa\widehat{\mathbf{E}}_{p-1,\ell-1} \text{ in } \widehat{\Omega}. \tag{C.16}$$

In (C.16), we use the convention $\widehat{\mathbf{E}}_{p,\ell} = \widehat{\mathbf{H}}_{p,\ell} = 0$ if $p < 0$ or $\ell < 0$. If each sub-term $(\widehat{\mathbf{E}}_{p,\ell}, \widehat{\mathbf{H}}_{p,\ell})$ satisfies the equations (C.16) then the near-field term $(\widehat{\mathbf{E}}_{p}, \widehat{\mathbf{H}}_{p})$ defined as (C.13) satisfies the nested Maxwell equations (4.8).

Proof of Proposition 4. The family $(\widehat{\mathbf{E}}_{p,\ell}, \widehat{\mathbf{H}}_{p,\ell})$ satisfies the nested Maxwell equations (C.16). Actually, we apply operators (C.11) on the previous series in order to compare them to the modal

coefficients of $(i\kappa\widehat{\mathbf{H}}_{p-1,\ell-1}, -i\kappa\widehat{\mathbf{E}}_{p-1,\ell-1})$,

$$\mathbf{curl}\,\widehat{\mathbf{E}}_{p,\ell} = \sum_{n=1}^{\infty}\sum_{m=-n}^{n} \big(\mathbf{curl}\,\widehat{\mathbf{E}}_{p,\ell}\big)^{\times}_{n,m}\mathbf{curl}_{\mathbb{S}^2}Y_{n,m} + \big(\mathbf{curl}\,\widehat{\mathbf{E}}_{p,\ell}\big)^{\mathrm{t}}_{n,m}\nabla_{\mathbb{S}^2}Y_{n,m} + \big(\mathbf{curl}\,\widehat{\mathbf{E}}_{p,\ell}\big)^{\mathrm{r}}_{n,m}Y_{n,m}\mathbf{e}_r,$$

$$\mathbf{curl}\,\widehat{\mathbf{H}}_{p,\ell} = \sum_{n=1}^{\infty}\sum_{m=-n}^{n} \big(\mathbf{curl}\,\widehat{\mathbf{H}}_{p,\ell}\big)^{\times}_{n,m}\mathbf{curl}_{\mathbb{S}^2}Y_{n,m} + \big(\mathbf{curl}\,\widehat{\mathbf{H}}_{p,\ell}\big)^{\mathrm{t}}_{n,m}\nabla_{\mathbb{S}^2}Y_{n,m} + \big(\mathbf{curl}\,\widehat{\mathbf{H}}_{p,\ell}\big)^{\mathrm{r}}_{n,m}Y_{n,m}\mathbf{e}_r,$$

where the modal coefficients of $(\mathbf{curl}\,\widehat{\mathbf{E}}_{p,\ell}, \mathbf{curl}\,\widehat{\mathbf{H}}_{p,\ell})$ are given by

$$\begin{aligned}
\big(\mathbf{curl}\,\widehat{\mathbf{E}}_{p,\ell}\big)^{\times}_{n,m} &= \frac{1}{\mathrm{R}}\widehat{e}^{(p),\mathrm{r}}_{n,m,\ell} - \frac{1}{\mathrm{R}}\partial_{\mathrm{R}}\big[\mathrm{R}\widehat{e}^{(p),\mathrm{t}}_{n,m,\ell}\big], & \big(\mathbf{curl}\,\widehat{\mathbf{H}}_{p,\ell}\big)^{\times}_{n,m} &= \frac{1}{\mathrm{R}}\widehat{h}^{(p),\mathrm{r}}_{n,m,\ell} - \frac{1}{\mathrm{R}}\partial_{\mathrm{R}}\big[\mathrm{R}\widehat{h}^{(p),\mathrm{t}}_{n,m,\ell}\big],\\
\big(\mathbf{curl}\,\widehat{\mathbf{E}}_{p,\ell}\big)^{\mathrm{t}}_{n,m} &= \frac{1}{\mathrm{R}}\partial_{\mathrm{R}}\big[\mathrm{R}\widehat{e}^{(p),\times}_{n,m,\ell}\big], & \big(\mathbf{curl}\,\widehat{\mathbf{H}}_{p,\ell}\big)^{\mathrm{t}}_{n,m} &= \frac{1}{\mathrm{R}}\partial_{\mathrm{R}}\big[\mathrm{R}\widehat{h}^{(p),\times}_{n,m,\ell}\big],\\
\big(\mathbf{curl}\,\widehat{\mathbf{E}}_{p,\ell}\big)^{\mathrm{r}}_{n,m} &= \frac{n(n+1)}{\mathrm{R}}\widehat{e}^{(p),\times}_{n,m,\ell}, & \big(\mathbf{curl}\,\widehat{\mathbf{H}}_{p,\ell}\big)^{\mathrm{r}}_{n,m} &= \frac{n(n+1)}{\mathrm{R}}\widehat{h}^{(p),\times}_{n,m,\ell}.
\end{aligned}$$

That is due to properties (C.12) and also to the following one

$$\mathrm{curl}_{\mathbb{S}^2}\mathbf{curl}_{\mathbb{S}^2}Y_{n,m} = n(n+1)Y_{n,m}.$$

Expanding radial coefficients of $(\mathbf{curl}\,\widehat{\mathbf{E}}_{p,\ell}, \mathbf{curl}\,\widehat{\mathbf{H}}_{p,\ell})$, we observe that

$$\begin{aligned}
\big(\mathbf{curl}\,\widehat{\mathbf{E}}_{p,\ell}\big)^{\mathrm{t}}_{n,m} &= i\kappa\,\frac{-\kappa^{\ell-1}}{\mathrm{R}^{n+2-(\ell-1)}}\,\frac{(\ell-1)-n}{n}\,\frac{\mathfrak{h}_{n,(\ell-1)-n-1}}{\mathfrak{h}_{n,-n-1}}\,\widehat{h}^{(p-\ell)}_{n,m} &&= i\kappa\,\widehat{e}^{(p-1),\mathrm{t}}_{n,m,\ell-1},\\
\big(\mathbf{curl}\,\widehat{\mathbf{E}}_{p,\ell}\big)^{\mathrm{r}}_{n,m} &= i\kappa\,\frac{\kappa^{\ell-1}}{\mathrm{R}^{n+2-(\ell-1)}}\,\frac{\mathfrak{h}_{(\ell-1)-n-1}}{\mathfrak{h}_{n,-n-1}}\,(n+1)\,\widehat{h}^{(p-\ell)}_{n,m} &&= i\kappa\,\widehat{e}^{(p-1),\mathrm{r}}_{n,m,\ell-1},\\
\big(\mathbf{curl}\,\widehat{\mathbf{H}}_{p,\ell}\big)^{\mathrm{t}}_{n,m} &= -i\kappa\,\frac{-\kappa^{\ell-1}}{\mathrm{R}^{n+2-(\ell-1)}}\,\frac{(\ell-1)-n}{n}\,\frac{\mathfrak{h}_{n,(\ell-1)-n-1}}{\mathfrak{h}_{n,-n-1}}\,\widehat{e}^{(p-\ell)}_{n,m} &&= -i\kappa\,\widehat{h}^{(p-1),\mathrm{t}}_{n,m,\ell-1},\\
\big(\mathbf{curl}\,\widehat{\mathbf{H}}_{p,\ell}\big)^{\mathrm{r}}_{n,m} &= -i\kappa\,\frac{-\kappa^{\ell-1}}{\mathrm{R}^{n+2-(\ell-1)}}\,\frac{\mathfrak{h}_{(\ell-1)-n-1}}{\mathfrak{h}_{n,-n-1}}\,(n+1)\,\widehat{e}^{(p-\ell)}_{n,m} &&= -i\kappa\,\widehat{h}^{(p-1),\mathrm{r}}_{n,m,\ell-1},
\end{aligned}$$

and

$$\begin{aligned}
\big(\mathbf{curl}\,\widehat{\mathbf{E}}_{p,\ell}\big)^{\times}_{n,m} &= i\kappa\,\frac{i\kappa^{\ell-1}}{\mathrm{R}^{n+2-(\ell-1)}}\,\frac{1}{n}\,\frac{\ell(1+2n-\ell)\mathfrak{h}_{n,\ell-n-1}}{\mathfrak{h}_{n,-n-1}}\,\widehat{e}^{(p-\ell)}_{n,m},\\
\big(\mathbf{curl}\,\widehat{\mathbf{H}}_{p,\ell}\big)^{\times}_{n,m} &= -i\kappa\,\frac{-i\kappa^{\ell-1}}{\mathrm{R}^{n+2-(\ell-1)}}\,\frac{1}{n}\,\frac{\ell(1+2n-\ell)\mathfrak{h}_{n,\ell-n-1}}{\mathfrak{h}_{n,-n-1}}\,\widehat{h}^{(p-\ell)}_{n,m}.
\end{aligned}$$

Furthermore, we have $\ell(1+2n-\ell)\mathfrak{h}_{n,\ell-n-1} = \mathfrak{h}_{n,\ell-n-3}$ and then, the set of shadows $(\widehat{\mathbf{E}}_{p,\ell}, \widehat{\mathbf{H}}_{p,\ell})$ satisfies the nested Maxwell equations (C.16). Finally, the sum of shadows satisfies the property (4.12) because $n+2-\ell \geq 3-p$ for any $n \geq 1$ and $\ell \leq p$. □

C.3.3 First terms of the near-field expansion as finite sums

The decomposition of solutions of the nested Maxwell equations can be extended to more complex geometries as well as those of the time-harmonic Maxwell equations, but in general with

infinite series, see [27, 32]. In the particular case of scattering by a sphere, considering the boundary conditions (4.10), these series are actually finite sums. The following corollary that is a consequence of (C.8) and (4.10), characterizes the zeroth-order near-field term $(\widehat{\mathbf{E}}_0, \widehat{\mathbf{H}}_0)$ as a finite sum of dipoles.

Corollary 1. *The zeroth-order near-field term $(\widehat{\boldsymbol{E}}_0, \widehat{\boldsymbol{H}}_0)$ have the following modal decomposition*

$$\widehat{\boldsymbol{E}}_0 = \frac{1}{\mathrm{R}^3}\sum_{m=-1}^{1} \widehat{e}_{1,m}^{(0)}\Big[\nabla_{\mathbb{S}^2} Y_{1,m} - 2Y_{1,m}\boldsymbol{e}_r\Big]\,; \qquad \widehat{\boldsymbol{H}}_0 = \frac{1}{\mathrm{R}^3}\sum_{m=-1}^{1} \widehat{h}_{1,m}^{(0)}\Big[\nabla_{\mathbb{S}^2} Y_{1,m} - 2Y_{1,m}\boldsymbol{e}_r\Big]. \quad \text{(C.17)}$$

The result is due to the following lemma in which we decompose a vector field in the basis of the spherical harmonics. Then, we observe that in (C.8), there is only a finite number of radial coefficients $\widehat{e}_{n,m}^{(0)}$ and $\widehat{h}_{n,m}^{(0)}$ not equal to zero. In particular, it is for $n = 1$.

Lemma 1. *Let $\boldsymbol{u}$ be a constant vector field of $\mathbb{R}^3$. Let us denote (u_1, u_2, u_3) its coordinates in the canonical basis of $\mathbb{R}^3$. The normal and tangential traces of $\boldsymbol{u}$ on $\mathbb{S}^2$ read in the basis of spherical harmonics as*

$$\gamma_n \boldsymbol{u} = \frac{u_1 + iu_2}{2}\sqrt{\frac{8\pi}{3}}Y_{1,-1} + \frac{u_1 - iu_2}{2}\sqrt{\frac{8\pi}{3}}Y_{1,1} + u_3\sqrt{\frac{4\pi}{3}}Y_{1,0},$$
$$\gamma_t \boldsymbol{u} = \frac{u_1 + iu_2}{2}\sqrt{\frac{8\pi}{3}}\nabla_{\mathbb{S}^2}Y_{1,-1} + \frac{u_1 - iu_2}{2}\sqrt{\frac{8\pi}{3}}\nabla_{\mathbb{S}^2}Y_{1,-1} + u_3\sqrt{\frac{4\pi}{3}}\nabla_{\mathbb{S}^2}Y_{1,0}.$$

The following corollary characterizes the first-order ner-field terms $(\widehat{\mathbf{E}}_1, \widehat{\mathbf{H}}_1)$ as a finite sum of dipoles and quadrupoles.

Corollary 2. *The leading part of the first-order near-field term $(\widehat{\boldsymbol{E}}_{1,0}, \widehat{\boldsymbol{H}}_{1,0})$ have the following modal decomposition*

$$\widehat{\boldsymbol{E}}_{1,0} = \frac{1}{\mathrm{R}^4}\sum_{m=-2}^{2} \widehat{e}_{2,m}^{(1)}\Big[\nabla_{\mathbb{S}^2} Y_{2,m} - 3Y_{2,m}\boldsymbol{e}_r\Big]\,;\ \widehat{\boldsymbol{H}}_{1,0} = \frac{1}{\mathrm{R}^4}\sum_{m=-2}^{2} \widehat{h}_{2,m}^{(1)}\Big[\nabla_{\mathbb{S}^2} Y_{2,m} - 3Y_{2,m}\boldsymbol{e}_r\Big]. \quad \text{(C.18)}$$

The associated shadows $(\widehat{\boldsymbol{E}}_{1,1}, \widehat{\boldsymbol{H}}_{1,1})$ have the following modal decomposition

$$\widehat{\boldsymbol{E}}_{1,1} = -\frac{i\kappa}{\mathrm{R}^2}\sum_{m=-1}^{1} \widehat{h}_{1,m}^{(0)}\boldsymbol{curl}_{\mathbb{S}^2} Y_{1,m}\,; \qquad \widehat{\boldsymbol{H}}_{1,1} = \frac{i\kappa}{\mathrm{R}^2}\sum_{m=-1}^{1} \widehat{e}_{1,m}^{(0)}\boldsymbol{curl}_{\mathbb{S}^2} Y_{1,m}. \quad \text{(C.19)}$$

The result is due to the following lemma in which we decompose a vector field reading as $\mathbf{M}\boldsymbol{e}_r$, where $\mathbf{M}$ is a constant matrix, in the basis of the spherical harmonics. Then, we observe that in (C.13)-(C.14), there is only a finite number of radial coefficients $\widehat{e}_{n,m}^{(1)}$ and $\widehat{h}_{n,m}^{(1)}$ not equal to zero. In particular, it is for $n = 2$.

Lemma 2. *Let $\boldsymbol{M}$ be a constant matrix of size 3×3. Let us denote $(m_{i,j})$ its coordinates relatively to the canonical basis of $\mathbb{R}^3$. The normal and tangential traces of the vector field $\boldsymbol{M}\boldsymbol{e}_r$ on $\mathbb{S}^2$ read in the basis of spherical harmonics as*

$$\gamma_n\Big(\boldsymbol{M}\boldsymbol{e}_r\Big) = \frac{m_{1,1} - m_{2,2}}{2}\sqrt{\frac{8\pi}{15}}\big(Y_{2,2} + Y_{2,-2}\big) + \frac{m_{1,2} + m_{2,1}}{2i}\sqrt{\frac{8\pi}{15}}\big(Y_{2,2} - Y_{2,-2}\big) +$$
$$\frac{m_{1,3} + m_{3,1}}{2}\sqrt{\frac{8\pi}{15}}\big(Y_{2,1} + Y_{2,-1}\big) + \frac{m_{2,3} + m_{3,2}}{2i}\sqrt{\frac{8\pi}{15}}\big(Y_{2,1} - Y_{2,-1}\big) + \frac{m_{3,3}}{2}\sqrt{\frac{16\pi}{5}}Y_{2,0},$$

$$\gamma_t\Big(\boldsymbol{Me}_r\Big) = \frac{2m_{3,3}-m_{1,1}-m_{2,2}}{2}\sqrt{\frac{4\pi}{45}}\nabla_{\mathbb{S}^2}Y_{2,0} + \frac{m_{1,1}-m_{2,2}}{4}\sqrt{\frac{8\pi}{15}}\big(\nabla_{\mathbb{S}^2}Y_{2,-2}+\nabla_{\mathbb{S}^2}Y_{2,2}\big)$$
$$+\frac{m_{1,3}+m_{3,1}}{4}\sqrt{\frac{8\pi}{15}}\big(\nabla_{\mathbb{S}^2}Y_{2,-1}+\nabla_{\mathbb{S}^2}Y_{2,1}\big) + \frac{m_{2,3}+m_{3,2}}{4i}\sqrt{\frac{8\pi}{15}}\big(\nabla_{\mathbb{S}^2}Y_{2,1}-\nabla_{\mathbb{S}^2}Y_{2,-1}\big)$$
$$+\frac{m_{1,2}+m_{2,1}}{4i}\sqrt{\frac{8\pi}{15}}\big(\nabla_{\mathbb{S}^2}Y_{2,2}-\nabla_{\mathbb{S}^2}Y_{2,-2}\big) + \frac{m_{3,1}-m_{1,3}}{4i}\sqrt{\frac{8\pi}{3}}\big(\boldsymbol{curl}_{\mathbb{S}^2}Y_{1,1}-\boldsymbol{curl}_{\mathbb{S}^2}Y_{1,-1}\big)$$
$$+\frac{m_{3,2}-m_{2,3}}{4}\sqrt{\frac{8\pi}{3}}\big(\boldsymbol{curl}_{\mathbb{S}^2}Y_{1,1}+\boldsymbol{curl}_{\mathbb{S}^2}Y_{1,-1}\big) + \frac{m_{2,1}-m_{1,2}}{2}\sqrt{\frac{4\pi}{3}}\boldsymbol{curl}_{\mathbb{S}^2}Y_{1,0}.$$

D Analytical solution of the scattering problem by one small sphere

In this section, we develop the Taylor expansion of the analytical solution of the electromagnetic scattering by a small sphere. The result validates the expression of the far-field expansion $(\delta^3\widetilde{\mathbf{E}}_3, \delta^3\widetilde{\mathbf{H}}_3)$. In a first time, we recall some results about regular solutions of Maxwell expansions in order to introduce the modal decomposition of the incident field.

D.1 Analytical decomposition of the incident field

The incident electromagnetic fields $(\mathbf{E}^{\text{inc}}, \mathbf{H}^{\text{inc}})$ are regular solutions of the time-harmonic Maxwell equations, in any bounded domain of $\mathbb{R}^3$. Then, we can decompose these ones into the basis of regular solutions of the Maxwell equations, related to the spherical Bessel functions j_n, see [32],

$$\mathbf{E}^{\text{inc}}(\mathbf{x}) = \sum_{n=1}^{\infty}\sum_{m=-n}^{n}\Big\{\mathtt{h}^{\text{inc}}_{n,m}j_n(\kappa r)\mathbf{curl}_{\mathbb{S}^2}Y_{n,m}(\widehat{x}) + \mathtt{e}^{\text{inc}}_{n,m}\Big[\frac{j_n(\kappa r)+\kappa r j_n'(\kappa r)}{i\kappa r}\nabla_{\mathbb{S}^2}Y_{n,m}(\widehat{x}) + \frac{j_n(\kappa r)}{i\kappa r}n(n+1)Y_{n,m}(\widehat{x})\mathbf{e}_r(\mathbf{x})\Big]\Big\} \tag{D.1}$$

and

$$\mathbf{H}^{\text{inc}}(\mathbf{x}) = \sum_{n=1}^{\infty}\sum_{m=-n}^{n}\Big\{-\mathtt{e}^{\text{inc}}_{n,m}j_n(\kappa r)\mathbf{curl}_{\mathbb{S}^2}Y_{n,m}(\widehat{x}) + \mathtt{h}^{\text{inc}}_{n,m}\Big[\frac{j_n(\kappa r)+\kappa r j_n'(\kappa r)}{i\kappa r}\nabla_{\mathbb{S}^2}Y_{n,m}(\widehat{x}) + \frac{j_n(\kappa r)}{i\kappa r}n(n+1)Y_{n,m}(\widehat{x})\mathbf{e}_r(\mathbf{x})\Big]\Big\}. \tag{D.2}$$

In (D.1)-(D.2), the modal coefficients have the following expression for any $\delta > 0$,

$$\begin{aligned}\mathtt{e}^{\text{inc}}_{n,m} &= -\frac{i\kappa\delta}{j_n(\kappa\delta)+\kappa\delta j_n'(\kappa\delta)}\frac{1}{n(n+1)}\int_{\{|\mathbf{x}|=\delta\}}(\mathbf{n}\times\mathbf{E}^{\text{inc}})(\mathbf{x})\cdot\mathbf{curl}_{\mathbb{S}^2}\overline{Y_{n,m}}(\widehat{x})\,\mathrm{d}s,\\ \mathtt{h}^{\text{inc}}_{n,m} &= -\frac{1}{j_n(\kappa\delta)}\frac{1}{n(n+1)}\int_{\{|\mathbf{x}|=\delta\}}(\mathbf{n}\times\mathbf{E}^{\text{inc}})(\mathbf{x})\cdot\nabla_{\mathbb{S}^2}\overline{Y_{n,m}}(\widehat{x})\,\mathrm{d}s,\end{aligned} \tag{D.3}$$

where $\mathbf{n}$ denotes the outward normal unit vector to $\mathcal{B}(0,\delta)$. This is the generic expression for regular electromagnetic waves. In general, there is not analytical expression for the coefficients

associated to this expansion. But, in specific cases, we can effectively compute it exactly. For instance, an electromagnetic plane wave directed through the z-axis and polarized by $\mathbf{e}_1$ possesses the Jacobi-Anger decomposition [18, Section A.3.4]

$$\exp(-i\kappa z)\mathbf{e}_1 = \sqrt{\pi}\sum_{n=1}^{\infty}(-i)^{n+1}\sqrt{\frac{2n+1}{n(n+1)}}\Big[j_n(\kappa\delta)\big(\mathbf{curl}_{\mathbb{S}^2}Y_{n,1}(\widehat{x}) - \mathbf{curl}_{\mathbb{S}^2}Y_{n,-1}(\widehat{x})\big) - \frac{j_n(\kappa\delta)+\kappa\delta j_n'(\kappa\delta)}{\kappa\delta}\big(\nabla_{\mathbb{S}^2}Y_{n,1}(\widehat{x}) + \nabla_{\mathbb{S}^2}Y_{n,-1}(\widehat{x})\big)\Big]. \quad \text{(D.4)}$$

Lemma 3. *The sums of dipoles in the modal decomposition of the incident field are given by*

$$\begin{aligned}
\sum_{m=-1}^{1}\mathsf{e}_{1,m}^{inc}\nabla_{\mathbb{S}^2}Y_{1,m} &= \frac{i}{2\mathrm{j}_{1,1}}\gamma_t\boldsymbol{E}^{inc}(0), & \sum_{m=-1}^{1}\mathsf{e}_{1,m}^{inc}Y_{1,m} &= \frac{i}{2\mathrm{j}_{1,1}}\gamma_n\boldsymbol{E}^{inc}(0),\\
\sum_{m=-1}^{1}\mathsf{h}_{1,m}^{inc}\nabla_{\mathbb{S}^2}Y_{1,m} &= \frac{i}{2\mathrm{j}_{1,1}}\gamma_t\boldsymbol{H}^{inc}(0), & \sum_{m=-1}^{1}\mathsf{h}_{1,m}^{inc}Y_{1,m} &= \frac{i}{2\mathrm{j}_{1,1}}\gamma_n\boldsymbol{H}^{inc}(0),
\end{aligned} \quad \text{(D.5)}$$

where $\mathrm{j}_{1,1} = \frac{1}{3}$ *denotes the first coefficient in the expansion of the spherical Bessel function* j_n*, see Proposition 3 in Appendix* (C.1).

Proof. The result is obtained by identifying the Taylor expansion of $(\mathbf{E}^{\text{inc}}, \mathbf{H}^{\text{inc}})$ in a neighborhood of 0

$$\mathbf{E}^{\text{inc}}(\mathbf{x}) = \mathbf{E}^{\text{inc}}(0) + \underset{r\to 0}{O}(r), \qquad \mathbf{H}^{\text{inc}}(\mathbf{x}) = \mathbf{H}^{\text{inc}}(0) + \underset{r\to 0}{O}(r),$$

with the expansion of the modal decomposition in a neighborhood of 0 given by

$$\begin{aligned}
\mathbf{E}^{\text{inc}}(\mathbf{x}) &= \frac{2\mathrm{j}_{1,1}}{i}\sum_{m=-1}^{1}\mathsf{e}_{1,m}^{\text{inc}}\Big[\nabla_{\mathbb{S}^2}Y_{1,m} + Y_{1,m}\mathbf{e}_r\Big] + \underset{r\to 0}{O}(r),\\
\mathbf{H}^{\text{inc}}(\mathbf{x}) &= \frac{2\mathrm{j}_{1,1}}{i}\sum_{m=-1}^{1}\mathsf{h}_{1,m}^{\text{inc}}\Big[\nabla_{\mathbb{S}^2}Y_{1,m} + Y_{1,m}\mathbf{e}_r\Big] + \underset{r\to 0}{O}(r).
\end{aligned}$$

□

D.2 Analytical decomposition of the scattered field

According to (C.6), the solution of the exterior Maxwell problem (2.2) have an analytical solution. Actually, the scattered fields $(\mathbf{E}_\delta, \mathbf{H}_\delta)$ can be decomposed in the basis of singular solutions of the Maxwell equations,

$$\begin{aligned}
\mathbf{E}_\delta(\mathbf{x}) = \sum_{n=1}^{\infty}\sum_{m=-n}^{n}\ &\mathsf{h}_{n,m}(\delta)h_n^{(1)}(\kappa r)\mathbf{curl}_{\mathbb{S}^2}Y_{n,m}(\widehat{x})\\
&+ \mathsf{e}_{n,m}(\delta)\Big[\frac{h_n^{(1)}(\kappa r)+\kappa r h_n^{(1)'}(\kappa r)}{i\kappa r}\nabla_{\mathbb{S}^2}Y_{n,m}(\widehat{x}) + \frac{h_n^{(1)}(\kappa r)}{i\kappa r}n(n+1)Y_{n,m}(\widehat{x})\mathbf{e}_r\Big]
\end{aligned} \quad \text{(D.6)}$$

and

$$\mathbf{H}_\delta(\mathbf{x}) = \sum_{n=1}^{\infty}\sum_{m=-n}^{n} -\mathtt{e}_{n,m}(\delta)h_n^{(1)}(\kappa r)\mathbf{curl}_{\mathbb{S}^2}Y_{n,m}(\widehat{x}) \\ + \mathtt{h}_{n,m}(\delta)\Big[\frac{h_n^{(1)}(\kappa r)+\kappa r h_n^{(1)'}(\kappa r)}{i\kappa r}\nabla_{\mathbb{S}^2}Y_{n,m}(\widehat{x}) + \frac{h_n^{(1)}(\kappa r)}{i\kappa r}n(n+1)Y_{n,m}(\widehat{x})\mathbf{e}_r\Big]. \quad \text{(D.7)}$$

In (D.6)-(D.7), the modal coefficients depend on the small parameter δ through the expression (C.5)

$$\begin{aligned}\mathtt{e}_{n,m}(\delta) &= \frac{i\kappa\delta}{h_n^{(1)}(\kappa\delta)+\kappa\delta h_n^{(1)'}(\kappa\delta)}\frac{1}{n(n+1)}\int_{\{|\mathbf{x}|=\delta\}}(\mathbf{n}\times\mathbf{E}^{\text{inc}})(\mathbf{x})\cdot\mathbf{curl}_{\mathbb{S}^2}\overline{Y_{n,m}}(\widehat{x})\,\mathrm{d}s,\\ \mathtt{h}_{n,m}(\delta) &= \frac{1}{h_n^{(1)}(\kappa\delta)}\frac{1}{n(n+1)}\int_{\{|\mathbf{x}|=\delta\}}(\mathbf{n}\times\mathbf{E}^{\text{inc}})(\mathbf{x})\cdot\nabla_{\mathbb{S}^2}\overline{Y_{n,m}}(\widehat{x})\,\mathrm{d}s.\end{aligned} \quad \text{(D.8)}$$

Remark 30. Identifying (D.3) and (D.8), we observe that

$$\mathtt{e}_{n,m}(\delta) = -\frac{j_n(\kappa\delta)+\kappa\delta j_n'(\kappa\delta)}{h_n^{(1)}(\kappa\delta)+\kappa\delta h_n^{(1)'}(\kappa\delta)}\mathtt{e}_{n,m}^{\text{inc}}\,; \qquad \mathtt{h}_{n,m}(\delta) = -\frac{j_n(\kappa\delta)}{h_n^{(1)}(\kappa\delta)}\mathtt{h}_{n,m}^{\text{inc}}. \quad \text{(D.9)}$$

This relation makes evident the dependence in δ.

The following proposition gives the Taylor expansion of the exact solution $(\mathbf{E}_\delta, \mathbf{H}_\delta)$ at the fifth order. That allows to find the third-order far-field terms given by (2.4)-(2.5) and also the expression of the collected model presented in Section 5.

Proposition 5. *The analytical solution $(\boldsymbol{E}_\delta, \boldsymbol{H}_\delta)$ have the Taylor series expansion when δ tends to 0,*

$$\boldsymbol{E}_\delta(\boldsymbol{x}) = (\kappa\delta)^3\Big\{\Big(\frac{1}{2}-\frac{3(\kappa\delta)^2}{10}\Big)h_1^{(1)}(\kappa r)\gamma_t\boldsymbol{H}^{inc}(0)\times\boldsymbol{e}_r \\ -\Big(1+\frac{3(\kappa\delta)^2}{10}\Big)\frac{h_1^{(1)}(\kappa r)+\kappa r h_1^{(1)'}(\kappa r)}{i\kappa r}\gamma_t\boldsymbol{E}^{inc}(0) - 2\Big(1+\frac{3(\kappa\delta)^2}{10}\Big)\frac{h_1^{(1)}(\kappa r)}{i\kappa r}\gamma_n\boldsymbol{E}^{inc}(0)\boldsymbol{e}_r\Big\} \\ + \underset{\delta\to0}{O}(\delta^5)$$

and

$$\boldsymbol{H}_\delta(\boldsymbol{x}) = (\kappa\delta)^3\Big\{\Big(1-\frac{3(\kappa\delta)^2}{10}\Big)h_1^{(1)}(\kappa r)\gamma_t\boldsymbol{E}^{inc}(0)\times\boldsymbol{e}_r \\ +\Big(\frac{1}{2}-\frac{3(\kappa\delta)^2}{10}\Big)\frac{h_1^{(1)}(\kappa r)+\kappa r h_1^{(1)'}(\kappa r)}{i\kappa r}\gamma_t\boldsymbol{H}^{inc}(0) + 2\Big(\frac{1}{2}-\frac{3(\kappa\delta)^2}{10}\Big)\frac{h_1^{(1)}(\kappa r)}{i\kappa r}\gamma_n\boldsymbol{H}^{inc}(0)\boldsymbol{e}_r\Big\} \\ + \underset{\delta\to0}{O}(\delta^5).$$

Proof. By inserting the expressions (D.9) and (D.5) into (D.6)-(D.7), we obtain

$$\mathbf{E}_\delta = -\frac{j_1(\kappa\delta)}{h_1^{(1)}(\kappa\delta)}\frac{i}{2\mathrm{j}_{1,1}}h_1^{(1)}(\kappa r)\gamma_t\mathbf{H}^{\text{inc}}(0)\times\mathbf{e}_r \\ -\frac{j_1(\kappa\delta)+\kappa\delta j_1'(\kappa\delta)}{h_1^{(1)}(\kappa\delta)+\kappa\delta h_1^{(1)'}(\kappa\delta)}\frac{i}{2\mathrm{j}_{1,1}}\Big[\frac{h_1^{(1)}(\kappa r)+\kappa r h_1^{(1)'}(\kappa r)}{i\kappa r}\gamma_t\mathbf{E}^{\text{inc}}(0)+2\frac{h_1^{(1)}(\kappa r)}{i\kappa r}\gamma_n\mathbf{E}^{\text{inc}}(0)\mathbf{e}_r\Big] + \mathfrak{E}_{\delta,2}(\mathbf{x})$$

and

$$\mathbf{H}_\delta = \frac{j_1(\kappa\delta)+\kappa\delta j_1'(\kappa\delta)}{h_1^{(1)}(\kappa\delta)+\kappa\delta h_1^{(1)'}(\kappa\delta)}\frac{i}{2\mathfrak{j}_{1,1}}h_1^{(1)}(\kappa r)\gamma_t\mathbf{E}^{\text{inc}}(0)\times\mathbf{e}_r$$
$$-\frac{j_1(\kappa\delta)}{h_1^{(1)}(\kappa\delta)}\frac{i}{2\mathfrak{j}_{1,1}}\left[\frac{h_1^{(1)}(\kappa r)+\kappa r h_1^{(1)'}(\kappa r)}{i\kappa r}\gamma_t\mathbf{H}^{\text{inc}}(0)+2\frac{h_1^{(1)}(\kappa r)}{i\kappa r}\gamma_n\mathbf{H}^{\text{inc}}(0)\mathbf{e}_r\right]+\mathfrak{H}_{\delta,2}(\mathbf{x}),$$

where the remainders $\mathfrak{E}_{\delta,2}$ and $\mathfrak{H}_{\delta,2}$ are of second order ($n\geq 2$) in the expansions (D.6)-(D.7). We remark that $\mathfrak{E}_{\delta,2}$ and $\mathfrak{H}_{\delta,2}$ are in $O(\delta^5)$ when δ tends to 0. Then, we expand the coefficients depending on δ

$$\frac{j_1(\kappa\delta)}{h_1^{(1)}(\kappa\delta)}=\frac{\mathfrak{j}_{1,1}}{\mathfrak{h}_{1,-2}}(\kappa\delta)^3+\Big[\frac{\mathfrak{j}_{1,3}}{\mathfrak{h}_{1,-2}}-\frac{\mathfrak{j}_{1,1}\mathfrak{h}_{1,0}}{(\mathfrak{h}_{1,-2})^2}\Big](\kappa\delta)^5+\underset{\delta\to 0}{O}(\delta^6),$$
$$\frac{j_1(\kappa\delta)+\kappa\delta j_1'(\kappa\delta)}{h_1^{(1)}(\kappa\delta)+\kappa\delta h_1^{(1)'}(\kappa\delta)}=-\frac{2\mathfrak{j}_{1,1}}{\mathfrak{h}_{1,-2}}(\kappa\delta)^3-\Big[\frac{2\mathfrak{j}_{1,1}\mathfrak{h}_{1,0}}{(\mathfrak{h}_{1,-2})^2}+\frac{4\mathfrak{j}_{1,3}}{\mathfrak{h}_{1,-2}}\Big](\kappa\delta)^5+\underset{\delta\to 0}{O}(\delta^6),$$

and we inject them into the previous expansions in order to obtain the result. □

The following proposition gives the Taylor expansion of the exact solution $(\mathbf{E}_\delta(\delta\,\cdot),\mathbf{H}_\delta(\delta\,\cdot))$ at the first order. That allows to find the first near-field term again, given by (2.8).

Proposition 6. *The analytical solution $(\boldsymbol{E}_\delta(\delta\,\cdot),\boldsymbol{H}_\delta(\delta\,\cdot))$ have the Taylor series expansion in fast variable, when δ tends to 0,*

$$\boldsymbol{E}_\delta(\delta\boldsymbol{X})=\frac{1}{\mathrm{R}^3}\Big[2\gamma_n\big(\boldsymbol{E}^{inc}(0)\big)\boldsymbol{e}_r-\gamma_t\big(\boldsymbol{E}^{inc}(0)\big)\Big]+\underset{\delta\to 0}{O}(\delta),$$
$$\boldsymbol{H}_\delta(\delta\boldsymbol{X})=-\frac{1}{2\mathrm{R}^3}\Big[2\gamma_n\big(\boldsymbol{H}^{inc}(0)\big)\boldsymbol{e}_r-\gamma_t\big(\boldsymbol{H}^{inc}(0)\big)\Big]+\underset{\delta\to 0}{O}(\delta).$$

Proof. Thanks to the Taylor series expansion of $(\mathbf{E}_\delta,\mathbf{H}_\delta)$ in Proposition 5, we have

$$\mathbf{E}_\delta(\delta\mathbf{X})=(\kappa\delta)^3\left[-\frac{h_1^{(1)}(\kappa\delta\mathrm{R})+\kappa\delta\mathrm{R}h_1^{(1)'}(\kappa\delta\mathrm{R})}{i\kappa\delta\mathrm{R}}\gamma_t\big(\mathbf{E}^{\text{inc}}(0)\big)-2\frac{h_1^{(1)}(\kappa\delta\mathrm{R})}{i\kappa\delta\mathrm{R}}\gamma_n\big(\mathbf{E}^{\text{inc}}(0)\big)\mathbf{e}_r\right]+\underset{\delta\to 0}{O}(\delta),$$
$$\mathbf{H}_\delta(\delta\mathbf{X})=(\kappa\delta)^3\left[\frac{h_1^{(1)}(\kappa\delta\mathrm{R})+\kappa\delta\mathrm{R}h_1^{(1)'}(\kappa\delta\mathrm{R})}{2i\kappa\delta\mathrm{R}}\gamma_t\big(\mathbf{H}^{\text{inc}}(0)\big)+\frac{h_1^{(1)}(\kappa\delta\mathrm{R})}{i\kappa\delta\mathrm{R}}\gamma_n\big(\mathbf{H}^{\text{inc}}(0)\big)\mathbf{e}_r\right]+\underset{\delta\to 0}{O}(\delta).$$

According to the Laurent series expansions of the spherical Hankel function of the first kind, we have

$$-\frac{h_1^{(1)}(\kappa\delta\mathrm{R})+\kappa\delta\mathrm{R}h_1^{(1)'}(\kappa\delta\mathrm{R})}{i\kappa\delta\mathrm{R}}=\frac{\mathfrak{h}_{1,-2}}{i}(\kappa\delta\mathrm{R})^{-3}+O(\delta^{-1}),$$
$$-2\frac{h_1^{(1)}(\kappa\delta\mathrm{R})}{i\kappa\delta\mathrm{R}}=-\frac{2\mathfrak{h}_{1,-2}}{i}(\kappa\delta\mathrm{R})^{-3}+O(\delta^{-1}).$$

Then, we obtain the result by substituting the previous expansions into that of $(\mathbf{E}_\delta(\delta\,\cdot),\mathbf{H}_\delta(\delta\,\cdot))$. □

References

[1] H. Ammari and H. Kang. *Reconstruction of small inhomogeneities from boundary measurements*. Springer, 2004.

[2] H. Ammari, S. Moskow, and M. S. Vogelius. Boundary integral formulae for the reconstruction of electric and electromagnetic inhomogeneities of small volume. *ESAIM: Control, Optimisation and Calculus of Variations*, 9:49–66, 2003.

[3] H. Ammari, M. S. Vogelius, and D. Volkov. Asymptotic formulas for perturbations in the electromagnetic fields due to the presence of inhomogeneities of small diameter ii. the full maxwell equations. *Journal de mathématiques pures et appliquées*, 80(8):769–814, 2001.

[4] H. Barucq, J. Chabassier, H. Pham, and S. Tordeux. Numerical robustness of single-layer method with Fourier basis for multiple obstacle acoustic scattering in homogeneous media. *Wave Motion*, 2017.

[5] A. Bendali. Numerical analysis of the exterior boundary value problem for the time-harmonic maxwell equations by a boundary finite element method. ii. the discrete problem. *Mathematics of Computation*, 43(167):47–68, 1984.

[6] A. Bendali, P.-H. Cocquet, and S. Tordeux. Approximation by multipoles of the multiple acoustic scattering by small obstacles in three dimensions and application to the foldy theory of isotropic scattering. *Archive for Rational Mechanics and Analysis*, 219(3):1017–1059, 2016.

[7] J. Blitz. *Electrical and magnetic methods of non-destructive testing*, volume 3. Springer Science & Business Media, 2012.

[8] V. Bonnaillie-Noël, D. Brancherie, M. Dambrine, F. Herau, S. Tordeux, and G. Vial. Multiscale expansion and numerical approximation for surface defects. In *ESAIM: Proceedings*, volume 33, pages 22–35. EDP Sciences, 2011.

[9] A. Buffa, M. Costabel, and D. Sheen. On traces for H(curl, Ω) in lipschitz domains. *Journal of Mathematical Analysis and Applications*, 276(2):845 – 867, 2002.

[10] M. Cassier and C. Hazard. Multiple scattering of acoustic waves by small sound-soft obstacles in two dimensions: mathematical justification of the foldy-lax model. *Wave Motion*, 50(1):18–28, 2013.

[11] D. P. Challa, G. Hu, and M. Sini. Multiple scattering of electromagnetic waves by finitely many point-like obstacles. *Mathematical Models and Methods in Applied Sciences*, 24(05):863–899, 2014.

[12] X. Claeys. *Analyse asymptotique et numérique de la diffraction d'ondes par des fils minces*. PhD thesis, Université de Versailles-Saint Quentin en Yvelines, 2008.

[13] P.-H. Cocquet. *Etude mathématique et numérique de modeles homogénéisés de métamatériaux*. PhD thesis, Université Paul Sabatier-Toulouse III, 2012.

[14] D. Colton and R. Kress. *Integral equation methods in scattering theory*, volume 72. SIAM, 2013.

[15] D. G. Crighton, A. P. Dowling, J. Ffowcs-Williams, M. Heckl, F. Leppington, and J. F. Bartram. Modern methods in analytical acoustics lecture notes, 1992.

[16] M. Dauge, S. Tordeux, and G. Vial. Selfsimilar perturbation near a corner: matching versus multiscale expansions for a model problem. In *Around the Research of Vladimir Maz'ya II*, pages 95–134. Springer, 2010.

[17] A. de La Bourdonnaye. Décomposition de $H^{-1/2}(\mathrm{div}_\Gamma,\Gamma)$ et nature de l'opérateur de Steklov-Poincaré du problème extérieur de l'électromagnétisme. *Comptes rendus de l'Académie des sciences. Série 1, Mathématique*, 316(4):369–372, 1993.

[18] M. Duruflé. *Intégration numérique et éléments finis d'ordre élevé appliqués aux équations de Maxwell en régime harmonique*. PhD thesis, 2006. Thèse de doctorat dirigée par Cohen, Gary Chalom Sciences. Mathématiques appliquées Paris 9 2006.

[19] W. Eckhaus. Matched asymptotic expansions and singular perturbations. 1973.

[20] L. L. Foldy. The multiple scattering of waves. I. General theory of isotropic scattering by randomly distributed scatterers. *Physical Review*, 67(3-4):107, 1945.

[21] L. Fraenkel. On the method of matched asymptotic expansions: Part I: A matching principle. In *Mathematical Proceedings of the Cambridge Philosophical Society*, volume 65, pages 209–231. Cambridge University Press, 1969.

[22] K. A. Fuller and D. W. Mackowski. Electromagnetic scattering by compounded spherical particles. *Light scattering by nonspherical particles: theory, measurements, and applications*, page 226, 2000.

[23] M. Ganesh and S. C. Hawkins. A high-order algorithm for multiple electromagnetic scattering in three dimensions. *Numerical Algorithms*, 50(4):469–510, 2009.

[24] A. M. Il'in. *Matching of asymptotic expansions of solutions of boundary value problems*, volume 102. American Mathematical Society Providence, RI, 1992.

[25] B. G. Korenev. *Bessel functions and their applications*. CRC Press, 2003.

[26] D. Korikov and B. A. Plamenevskii. Asymptotics of solutions for stationary and nonstationary maxwell systems in a domain with small holes. *Algebra i Analiz*, 28(4):102–170, 2016.

[27] J. Labat. Représentations modales pour la diffraction d'ondes électromagnétiques. Master's thesis, Université de Pau et des Pays de l'Adour, Sept. 2016.

[28] B. Laud. *Electromagnetics*. New Age International, 1987.

[29] E. B. Lindgren, A. J. Stace, E. Polack, Y. Maday, B. Stamm, and E. Besley. An integral equation approach to calculate electrostatic interactions in many-body dielectric systems. *Journal of Computational Physics*, 2018.

[30] V. Mattesi. *Propagation des ondes dans un domaine comportant des petites hétérogénéités: modélisation asymptotique et calcul numérique*. PhD thesis, Pau, 2014.

[31] V. Maz'Ya, S. Nazarov, and B. Plamenevskij. *Asymptotic theory of elliptic boundary value problems in singularly perturbed domains*, volume 1. Birkhäuser, 2012.

[32] P. Monk. *Finite element methods for Maxwell's equations*. Oxford University Press, 2003.

[33] J.-C. Nédélec. *Acoustic and electromagnetic equations: integral representations for harmonic problems*, volume 144. Springer Science & Business Media, 2001.

[34] V. Péron. *Modélisation mathématique de phénomènes électromagnétiques dans des matériaux à fort contraste*. PhD thesis, Université Rennes 1, 2009.

[35] R. E. Raab and O. L. De Lange. *Multipole theory in electromagnetism: classical, quantum, and symmetry aspects, with applications*, volume 128. Oxford University Press on Demand, 2005.

[36] C. Sheppard and S. Saghafi. Electromagnetic gaussian beams beyond the paraxial approximation. *JOSA A*, 16(6):1381–1386, 1999.

[37] B. Thierry. *Analysis and Numerical Simulations of Time Reversal and Multiple Scattering*. Theses, Université Henri Poincaré - Nancy I, Sept. 2011.

[38] S. Tordeux. *Méthodes Asymptotiques pour la Propagation des Ondes dans les Milieux comportant des Fentes*. Theses, Université de Versailles-Saint Quentin en Yvelines, Dec. 2004.

[39] M. Van Dyke. *Perturbation Methods in Fluid Mechanics*. Parabolic Press, 1975.

[40] B. Veihelmann, T. Nousiainen, M. Kahnert, and W. Van der Zande. Light scattering by small feldspar particles simulated using the gaussian random sphere geometry. *Journal of Quantitative Spectroscopy and Radiative Transfer*, 100(1-3):393–405, 2006.

[41] G. Vial. *Analyse multi-échelle et conditions aux limites approchées pour un probleme avec couche mince dans un domainea coin*. PhD thesis, 2003.

[42] D. Volkov. *An inverse problem for the time harmonic Maxwell's equations*. PhD thesis, 2003.

[43] T. Wriedt, J. Hellmers, E. Eremina, and R. Schuh. Light scattering by single erythrocyte: comparison of different methods. *Journal of Quantitative Spectroscopy and Radiative Transfer*, 100(1-3):444–456, 2006.

[44] Y.-l. Xu. Electromagnetic scattering by an aggregate of spheres. *Applied optics*, 34(21):4573–4588, 1995.

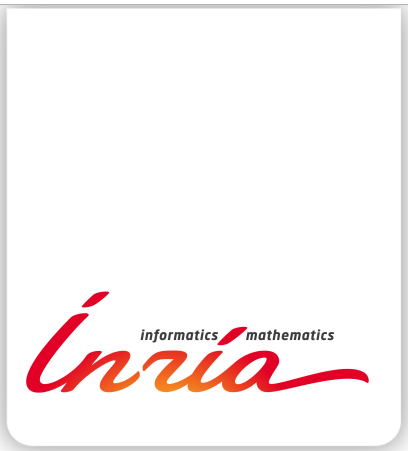

RESEARCH CENTRE
BORDEAUX – SUD-OUEST

200 avenue de la Vieille Tour
33405 Talence Cedex

Publisher
Inria
Domaine de Voluceau - Rocquencourt
BP 105 - 78153 Le Chesnay Cedex
inria.fr

ISSN 0249-6399